ORTA DOĞU TEKNİK ÜNİVERSİTESİ
FEN BİLİMLERİ ENSTİTÜSÜ MÜDÜRLÜĞÜ

TEZ ŞABLONU ONAY FORMU
THESIS TEMPLATE CONFIRMATION FORM

1. Şablonda verilen yerleşim ve boşluklar değiştirilmemelidir.
2. **Jüri tarihi** Başlık Sayfası, İmza Sayfası, Abstract ve Öz'de ilgili yerlere yazılmalıdır.
3. İmza sayfasında jüri üyelerinin unvanları doğru olarak yazılmalıdır. Tüm imzalar **mavi pilot kalemle** atılmalıdır.
4. **Disiplinlerarası** programlarda görevlendirilen öğretim üyeleri için jüri üyeleri kısmında tam zamanlı olarak çalıştıkları anabilim dalı başkanlığının ismi yazılmalıdır. Örneğin: bir öğretim üyesi Biyoteknoloji programında görev yapıyor ve biyoloji bölümünde tam zamanlı çalışıyorsa, İmza sayfasına biyoloji bölümü yazılmalıdır. İstisnai olarak, disiplinler arası program başkanı ve tez danışmanı için disiplinlerarası program adı yazılmalıdır.
5. Tezin **son sayfasının sayfa** numarası Abstract ve Öz'de ilgili yerlere yazılmalıdır.
6. Bütün chapterlar, referanslar, ekler ve CV sağ sayfada başlamalıdır. Bunun için **kesmeler** kullanılmıştır. **Kesmelerin kayması** fazladan boş sayfaların oluşmasına sebep olabilir. Bu gibi durumlarda paragraf (¶) işaretine tıklayarak kesmeleri görünür hale getirin ve yerlerini **kontrol edin**.
7. Figürler ve tablolar kenar boşluklarına taşmamalıdır.
8. Şablonda yorum olarak eklenen uyarılar dikkatle okunmalı ve uygulanmalıdır.
9. Tez yazdırılmadan önce PDF olarak kaydedilmelidir. Şablonda yorum olarak eklenen uyarılar PDF dokümanında yer almamalıdır.
10. **Bu form aracılığıyla oluşturulan PDF dosyası arkalı-önlü baskı alınarak tek bir spiralli cilt haline getirilmelidir.**
11. Spiralli hale getirilen tez taslağınızdaki ilgili alanları imzalandıktan sonra, Tez Juri Atama Formu ile birlikte bölüm sekreterliğine teslim edilmelidir.
12. Tez taslaklarının kontrol işlemleri tamamlandığında, bu durum öğrencilere METU uzantılı öğrenci e-posta adresleri aracılığıyla duyurulacaktır.
13. Tez yazım süreci ile ilgili herhangi bir sıkıntı yaşarsanız, **Sıkça Sorulan Sorular (SSS)** sayfamızı ziyaret ederek yaşadığınız sıkıntıyla ilgili bir çözüm bulabilirsiniz.

1. Do not change the spacing and placement in the template.
2. Write **defense date** to the related places given on Title page, Approval page, Abstract and Öz.
3. Write the titles of the examining committee members correctly on Approval Page. **Blue ink** must be used for all signatures.
4. For faculty members working in **interdisciplinary programs**, the name of the department that they work full-time should be written on the Approval page. For example, if a faculty member staffs in the biotechnology program and works full-time in the biology department, the department of biology should be written on the approval page. Exceptionally, for the interdisciplinary program chair and your thesis supervisor, the interdisciplinary program name should be written.
5. Write **the page number of the last page** in the related places given on Abstract and Öz pages.
6. All chapters, references, appendices and CV must be started on the right page. **Section Breaks** were used for this. **Change in the placement** of section breaks can result in extra blank pages. In such cases, make the section breaks visible by clicking paragraph (¶) mark and **check their position.**
7. All figures and tables must be given inside the page. Nothing must appear in the margins.
8. All the warnings given on the comments section through the thesis template must be read and applied.
9. Save your thesis as pdf and Disable all the comments before taking the printout.
10. **Print two-sided the PDF file that you have created through this form and make a single spiral bound.**
11. Once you have signed the relevant fields in your thesis draft that you spiraled, submit it to the department secretary together with your Thesis Jury Assignment Form.
12. This will be announced to the students via their METU students e-mail addresses when the control of the thesis drafts has been completed.
13. If you have any problems with the thesis writing process, you may visit our **Frequently Asked Questions (FAQ)** page and find a solution to your problem.

☒ **Yukarıda bulunan tüm maddeleri okudum, anladım ve kabul ediyorum. / I have read, understand and accept all of the items above.**

Name : **Niüfer**
Surname : **Kara**
E-Mail : **kara.nilufer@metu.edu.tr**
Date : **04.02.2021**
Signature : _____

APTAMER SELECTION AGAINST CADAVERINE/LYSINE ANTIPORTER (CadB) PURIFIED IN MILD DETERGENT

A THESIS SUBMITTED TO
THE GRADUATE SCHOOL OF NATURAL AND APPLIED SCIENCES
OF
MIDDLE EAST TECHNICAL UNIVERSITY

BY

NİLÜFER KARA

IN PARTIAL FULFILLMENT OF THE REQUIREMENTS
FOR
THE DEGREE OF MASTER OF SCIENCE
IN
BIOCHEMISTRY

FEBRUARY 2021

Approval of the thesis:

APTAMER SELECTION AGAINST CADAVERINE/LYSINE ANTIPORTER (CadB) PURIFIED IN MILD DETERGENT

submitted by **NİLÜFER KARA** in partial fulfillment of the requirements for the degree of **Master of Science** i**n Biochemistry, Middle East Technical University** by,

Prof. Dr. Halil Kalıpçılar
Dean, Graduate School of **Natural and Applied Sciences** _____

Assoc. Prof. Dr. Yeşim Soyer
Head of the Department, **Biochemistry** _____

Assoc. Prof. Dr. Çağdaş Devrim Son
Supervisor, **Biochemistry, METU** _____

Dr. Müslüm İlgü
Co-Supervisor, **Aptalogic Incorporated** _____

Examining Committee Members:

Prof. Dr. Ayşe Gül Gözen
Biological Sciences, METU _____

Assoc. Prof. Dr. Çağdaş Devrim Son
Biochemistry, METU _____

Assoc. Prof. Dr. Yeşim Soyer
Biochemistry, METU _____

Assoc. Prof. Dr. Özgül Persil Çetinkol
Chemistry, METU _____

Assoc. Prof. Dr. Eda Çelik Akdur
Chemical Engineering, Hacettepe University _____

Date: 15.02.2021

I hereby declare that all information in this document has been obtained and presented in accordance with academic rules and ethical conduct. I also declare that, as required by these rules and conduct, I have fully cited and referenced all material and results that are not original to this work.

Name Last name :Nilüfer Kara

Signature :

ABSTRACT

APTAMER SELECTION AGAINST CADAVERINE/LYSINE ANTIPORTER (CADB) PURIFIED IN MILD DETERGENT

Kara, Nilüfer
Master of Science, Biochemistry
Supervisor: Assoc. Prof. Dr. Çağdaş Devrim Son
Co-Supervisor: Dr. Müslüm İlgü

February 2021, 131 pages

Membrane Protein (MP) targeting remains a challenge because of their amphipathic nature. In the lipid bilayer, both hydrophobic and hydrophilic domains provide MPs their characteristic functions. Therefore *in vitro* studies require an environment for mimicking their natural membrane environment in order for MPs to fold into their native conformation to function properly. Here, treatment with a detergent is imperative for a MP solubilization to make it a stable individual protein without losing its functionality. In our studies, for aptamer selection we targeted Cadaverine/Lysine Antiporter (CadB) as a model protein for MPs, a secondary transporter on the inner membrane of *Escherichia Coli* with a critical role in acid stress adaptation.

Aptamers are short *in vitro*-selected RNA or DNA oligonucleotides. The selection of aptamer is engineered by the method known as Systematic Evolution of Ligands by EXponential Enrichment (SELEX). This process has iterative rounds to select the best aptamer/s with high affinity and selectivity for a given target. It consists of three main steps: incubation of the aptamer with the target, separation of bound oligo-protein complex, and oligo amplification. Interactions with the target lead to

conformational change on the aptamer structure. After aptamer development, these interactions may find potential uses in diagnostic or therapeutic applications. To date, many kinds of SELEX techniques have been carried out for aptamer selection. However, some are labor- and time- consuming and may give less specificity against MPs.

In this project, before selection, we achieved both solubilization and purification of CadB in a mild detergent, n-dodecyl-β-D-maltopyranoside (DDM). We performed eight rounds of protein-SELEX against CadB in DDM. After completing the final round, the RNA pool was sequenced, and we finally got 29 distinct sequences. We found three abundant sequences with double copies: CadB30, CadB35, and CadB39. Furthermore, we determined the potential binding motif by multiple sequence alignment analysis. After that, according to the predicted 2D secondary structures (done by RNAfold and KineFold), this motif was found on the loops of CadB35 and CadB39, while it was found on the stem of CadB30. Also, we randomly chose a proto-aptamer (CadB41), which is closed to CadB30 and CadB39, to show their structural similarity with their homology matrixes.

Overall, in this study, we successfully generated aptamers against CadB after eight rounds of protein-SELEX. This study shows that CadB, as an MP, can be targeted by protein-SELEX in a suitable mild detergent. In this way, targeting MPs may become more convenient for both diagnosis and therapeutic purposes in the near future. Protein-SELEX is suitable for all kinds of proteins, and it serves as an efficient, straightforward, time-saving, and cost-effective way for aptamer selection.

Keywords: Membrane Protein, CadB, Aptamer, protein-SELEX, DDM

ÖZ

HAFİF DETERJANDA SAFLAŞTIRILMIŞ KADAVERİN/LÖSİN ANTİPORTU (CadB) İÇİN APTAMER SEÇİLİMİ

Kara, Nilüfer
Yüksek Lisans, Biyokimya
Tez Yöneticisi: Doç. Dr. Çağdaş Devrim Son
Ortak Tez Yöneticisi: Dr. Müslüm İlgü

Şubat 2021, 131sayfa

Membran Proteinlerinin (MP) hedef molekülü olarak kullanımı, sahip oldukları amfipatik doğaları nedeniyle zordur. MP'lerin çift katlı lipit tabakasında bulunan hidrofilik ve hidrofobik kısımları, MP'lere karakteristik işlevlerini kazandırır. Bu sebeple, *in vitro* çalışmalarda, MP'lerin doğru bir şekilde işlevlerini yerine getirebilmeleri için protein katlanmasını sağlamak adına doğal çevrelerini taklit edebilecek bir ortama gereksinim duyulmaktadır. Bu noktada, deterjan ile muamele MP'lerinin işlevlerini yitirmeden çözünmesi ve stabil bir protein olarak kalması açısından çok önemlidir. Biz çalışmalarımızda, aptamer seçilimi için, *Escherichia Coli*'nin iç membranında yer alıp, ikincil bir antiport olan ve aynı zamanda asidik stres adaptasyonunda önemli rol oynayan Kadaverin/Lösin Antiportu (CadB) proteinini MP'lerine bir model olarak hedefledik.

Aptamerler, *in vitro* olarak seçilen DNA ya da RNA oligonükleotitlerinden oluşan kısa nükleik asit zincirleridir. Aptamerlerin seçilimi, Üstel Zenginleştirme ile Ligandların Sistematik Evrimi (SELEX) yöntemi ile gerçekleştirilir. Bu süreç, yüksek afinite ve seçilimle hedef molekülüne bağlanan aptamer/leri seçmek için tekrarlayan turlarla oluşmakta olup üç ana adımda bir tur tamamlanmaktadır: hedef

molekülü ile inkübasyon, oligo-bağlı protein yapılarının ayrılması, oligo çoğaltma. Hedef molekülü ile etkileşim, aptamerin yapısında konformasyonel bir değişiklik meydana getirir. Aptamer geliştirildikten sonra, bu etkileşim, ileriki çalışmalarda tedavi ve teşhis alanlarında potansiyel kullanıma sahiptir. Şimdiye dek, aptamer seçiliminde pek çok SELEX tekniği kullanılmıştır. Fakat bunlardan bazıları iş gücü gerektiren, zaman alıcı ve MP'lere karşı özgüllüğü düşük olan yöntemlerdir.

Bu projede, seçilimi gerçekleştirmeden önce, CadB'nin çözünürlüğünü ve saflaştırılmasını hafif bir deterjan olan n-dodesil-β-D-maltopiranosit (DDM)'te gerçekleştirdik. Son tur tamamlandıktan sonra, RNA havuzu sekanslaması yapıldı ve son olarak 29 farklı sekans elde ettik. En çok tekrarlanan sekansları (iki kez tekrarlanmış şekilde) belirledik: CadB30, CadB35 ve CadB39. Sonrasında, çoklu sekans hizalama analizi ile potansiyel bağlanma motifini bulduk. Sonra, tahmini ikincil yapılara (RNAfold ve KineFold tarafından yapıldı) göre, bu motif CadB35 ve CadB39'un ilmik (loop) yapısında bulunurken, CadB30'un sap (stem) yapısında bulundu. Ayrıca, biz bunların yapısal benzerliklerini homoloji matriksleriyle göstermek için, CadB30 ve CadB39'a yakın olacak şekilde rastgele bir proto-aptamer (CadB41) seçtik.

Biz bu çalışmada, sekiz tur protein-SELEX'inden sonra CadB'ye karşı aptamerleri başarıyla elde ettik. Bu çalışma, CadB bir MP olarak, uygun bir deterjanda protein-SELEX ile hedef molekülü olarak kullanılabileceğini göstermektedir. Bu şekilde, yakın gelecekte teşhis ve tedavi amaçlarında, MP'lerin hedef molekülü olarak kullanımı daha elverişli hale gelecektir. Protein-SELEX, bütün proteinler için uygun olduğundan daha basit, zaman kazandıran, uygun maliyetli aptamer seçilimi sağlar.

Anahtar Kelimeler: Membrane Protein, CadB, Aptamer, protein-SELEX, DDM

To my beautiful mother, Sebahat Kara

ACKNOWLEDGMENTS

First of all, I am deeply grateful to The Almighty Allah for allowing me to put a pinch of contribution to this field of science by completing this Master's thesis. Working with nucleic acids that I have been interested in since my childhood has made me really happy. I am also grateful for the combination of all beautiful paths to have this studying environment.

I want to express my sincere thanks to my supervisor Assist. Prof. Dr. Müslüm İlgü. I am incredibly indebted to him for his expert, sincere and valuable guidance throughout this study. The first day when we met in the Biology Department was a miracle day for me. I feel lucky that I met him and being his student. As a scientist, his behavior is exemplary with being hardworking, eager, and ambitious. Laboratory 210 became my second home with this group and him.

I would like to thank my co-supervisor Assoc. Prof. Dr. Çağdaş Devrim Son for his affable personality. I will never forget his contributions by helping me during difficult times in this program.

Besides, I would like to thank my other comittee members, Prof. Dr. Ayşegül Gözen, Assoc. Prof. Dr. Yeşim Soyer, Assoc. Prof. Dr. Özgül Persil Çetinkol and Assoc. Prof. Dr. Eda Çelik Akdur, for their valuable comments and precious time.

I also had the great pleasure of working with Dr. Hüseyin İlgü (from the Institute of Biochemistry and Molecular Medicine at the University of Bern) for his invaluable contribution, suggestion, and helpful in numerous ways for this study.

I want to express my heartfelt gratitude to my beautiful friend with a heart of gold, Nooraldeen Ayoub, for his helpful contribution, invaluable advice, and precious friendship throughout my Master's program. I am thoroughly grateful that I met him in this lab. I am very proud of his hardworking, determined, honest, helpful, and positive personality. His support by recommending me to be patient in difficult times has always made me motivated and happy. Together we overcame all

challenges to achieve this success. I have no doubt that he will make significant contributions to science with his future studies.

I would like to gratefully acknowledge the rest of the İlgü Research group members, Rezzan Fazlıoğlu, Meriç Öztürk, and Funda Ardıç, for their friendships and helps.

My sincere thanks also go to my high school biology instructor as my source of inspiration Tülay Erkan, who had supported me and changed my life by making me love biology.

I am also thankful for my dear friends Halime Serinçay and Tuğçe Yılmaz, especially for their invaluable support and help at the beginning of this Master's program and for their valuable friendship.

I want to thank my amazing friend, who is crazy physicist Merve Uslu (a.k.a. Mavi) from Hacettepe University, for her beautiful heart and for encouraging me to science since 2012. I will also never forget her help during my infection while I was writing this dissertation.

My special thanks go to my dear housemate Özge Güneş, and my old friends, Pınar Çalhan, Ayten Gözütok, Sebile Şahin, for their amazing friendships, prayers, and supports during my Master's program.

I would like to thank my spiritual sister Dilek Işık, who has sentimental value for me with her lovely family.

Last but not the least, I extend gratitude to my family members, dedicated to the memory of my mother, Sebahat Kara. She always believed me in my ability to be successful in the academic field as a scientist woman. Her prayers and belief in me have made this possible until today. I thank my father, Süleyman Kara, who has gone on the after-life, supporting me spiritually and made me prepared for these days. Finally, I thank my brother Ali Kara for his constant encouragement and patience.

TABLE OF CONTENTS

LIST OF TABLES

TABLES

LIST OF FIGURES

FIGURES

LIST OF ABBREVIATIONS

ABBREVIATIONS

ABC: ATP-binding cassette

ATP: Adenine triphosphate

CadB: Cadaverine/Lysine antiporter

CD: The human cluster of differentiation antigen

CTC: Circulating tumor cell

CNS: Central nervous system

DDM: n-dodecyl-β-D-maltopyranoside

DNA: Deoxyribonucleic acid

ds: Double-stranded

E.coli: Escherichia Coli

ELISA: Enzyme-linked immunosorbent assay

GPCR: G-coupled protein receptors

HCV: Hepatitis C virus

IVT: In vitro transcription

K_d: Dissociation constant

LDAR: Lysine-dependent acid resistance system

MFE: Minimum free energy

MPs: Membrane proteins

nt: Nucleotide

PBS: Phosphate-buffered saline

PCR: Polymerase chain reaction

RNA: Ribonucleic acid

RT: Reverse transcription

SDS-PAGE: Sodium dodecyl sulfate polyacrylamide gel electrophoresis

SELEX: Systematic evolution of ligands by exponential enrichment

ss: Single-standed

CHAPTER 1

INTRODUCTION

1.1 Plasma Membrane

All cell types, including non-living enveloped viruses, are surrounded by a lipid membrane. This structure provides the cell its shape with fluidity. In 1972, S. Jonathan Singer and Garth Nicolson proposed the idea of the membrane structure known as the fluid mosaic model (Singer & Nicolson, 1972). According to this model, the interaction of membrane proteins (MPs) and lipids creates critical physiological consequences. The vast majority of a membrane is made up of lipids and proteins in an approximate ratio of 60% and 40%, respectively. Their ratios, however, can vary by the cell and organism type. If we think of the cell as a living unit, the cell membrane plays a vital role in the sustainability of vital activities. Thousands of lipid and protein varieties along the cellular membrane give rise to a unique set of membrane functionality for each cell. For example, membrane-encapsulated compartmentalization is responsible for allowing a selectively permeable barrier, transporting solutes, providing a locus for biochemical activity, and signaling cell-to-cell communication (Casares, Escribá, & Rosselló, 2019; Siontorou, Nikoleli, Nikolelis, & Karapetis, 2017). Generally, MPs are described in three main topics regarding how the protein attaches to the membrane (Yeagle, 2016).

1.1.1 MPs

Integral MPs pass entirely through the lipid bilayer, and their intercellular domains interact with the hydrophobic inner space of the lipid bilayer, whereas other domains may extend into the aqueous milieu of the cytoplasm or extracellular

side of the membrane (Iwasa, 2016). Integral MPs are distinguished in terms of how many times the protein crosses the membrane. These can be either polytopic or monotopic proteins. Integral polytopic proteins are also known as "transmembrane protein" that fully spans the membrane either once (single-pass) or several times (multi-pass). However, integral monotopic proteins do not span the membrane entirely as polytopic ones do (Allen, Entova, Ray, & Imperiali, 2019) and thus can be removed from the membrane by applications of detergents (i.e., sodium dodecyl sulfate) or chaotropic agents (i.e., urea) (Yeagle, 2016). Transmembrane regions of integral proteins are composed of either α helices or β sheets. Numerous β barrels exist as porins in the outer membrane of gram-negative bacteria called "outer membrane proteins." Despite common β barrels scaffolds, outer MPs evolved as channel-performing proteins (Voet, Donald; Voet, 2011). β barrels exist in gram-negative bacteria and the outer membrane of mitochondria in eukaryotes and chloroplasts (Fairman, Noinaj, & Buchanan, 2012; Ravna, Sager, Dahl, & Sylte, 2008).

The system of membrane transporters has a number of critical roles for living organisms (Saier, 2000). Each cell requires transporters for highly polar ions and other molecules to selectively pass through the lipid bilayer. Polar molecules are unable to penetrate the cellular membrane and require transporter proteins with specific sites that can recognize a particular solute coming from an extracellular medium (Yang & Hinner, 2015). In this way, a variety of molecules are regulated by such proteins. For example, essential nutrients are allowed to pass through the membrane to access a particular organelle. The nutrients subsequently can undergo metabolism as exogenous sources of carbon, nitrogen, sulfur, and phosphorus. MPs take a role in the excretion of metabolic residues of substances taken into the cell to maintain the proper concentration (B. H. Kim & Gadd, 2019). Also, they regulate the drug metabolism and toxins which are coming from either cytoplasm or plasma membrane (Mayati et al., 2017). Another function of MPs is to allow ionic species mediation to efflux them properly to conserve the concentration difference between in and outside the plasma membrane (Gouaux & MacKinnon, 2005). To protect

against any threat beyond the membrane, they contribute to the secretion of macromolecules such as carbohydrates, lipids, and proteins, some of which provide cell communication between the same or different cell types and even with a pathogen. Transporter systems control the entrance of nucleic acids to enable cell communication and diversification (Lam et al., 2011). Uptake of signaling molecules, including neurotransmitters, hormones, and other molecules, is facilitated to have synergy in cell collaboration (I. Cho, Jackson, & Swift, 2016). Additionally, transporters allow the secretion of bacterial and antiviral agents (Tanaka, Song, Mason, & Pinkett, 2018). Finally, transporters enable biomolecules to remain at a certain level without disturbing their homeostatic balance (Savir, Martynov, & Springer, 2017).

Peripheral MPs can be located either outer (extracellular) or inner (cytoplasmic) leaflet of the lipid bilayer or bound to integral proteins by weak chemical interactions. They can be easily removed from where they are attached by detergent or alkaline pH treatment or ionic interaction (Smith, 2017). Different then peripheral ones, lipid-anchored MPs (lipoproteins) are bound to membrane lipids by covalent attachments. The lipid may also modify or activate the protein structure and regulate the protein-protein interactions in the cascade reactions. The interaction of lipid and protein comes up in three ways: prenylated proteins, fatty acylated proteins, and glycosyl phosphatidyl inositol-linked proteins. Similar to peripheral ones, lipid-anchored MPs have two different attachment sites to interact with either the membrane's outer or cytoplasmic sides (Iwasa, 2016).

1.1.2 Membrane Transport Process

All substances, vital molecules (i.e., nutrients) and chemicals (i.e., drugs) have to pass through the cell membrane. One of the plasma membrane's vital functions is to exchange the molecules or atoms depending on their size and polarity. The density of substances on either side of the membrane affects their exchange rate. In general, there are two ways for the movement through the

membrane: passively or actively by energy-coupled transport processes (Laterra, Keep, Betz, & Goldstein, 1999).

Passive diffusion, facilitated diffusion, osmosis, and filtration belong to passive transport types (Lord, 1999). In a passive transport system, non-polar molecules like O_2, CO_2, and non-polar lipids can easily penetrate through the membrane as a result of non-polar lipid tails in the membrane. Here, gradient level flowing is vital for the molecule to pass through the membrane through which the molecules move from high to low concentration (Pignatello, 2013).

In the case of the active transport process, ions or polar molecules move against their electrochemical gradient, and the process requires the expenditure of energy and contribution of specialized integral proteins called "carrier protein" (Alberts et al., 2002). This process occurs in two ways as primary and secondary active transporters, depending on energy consumption. The former operates by ATPases along the membrane to utilize metal ions like sodium, potassium, magnesium, and calcium through ion pumps/channels. P-type ATPase, F-ATPase, V-ATPase, and ABC transporter belong to this group (I. Chen & Lui, 2019). Unlike primary active transport, the secondary transport system does not require direct use of ATP; it employs the pumps using the electrochemical gradient difference. Entropy increases during molecular movement from more concentrated to less concentrated medium. This system uses the entropy difference as an energy source for pumping ions by the porter systems like uniporter, symporter, and antiporter (Yang & Hinner, 2015). In the human body, the secondary active transport system mainly exists in the small intestine, kidney proximal tubules, and central nervous system (CNS) (Wright, Hirayama, & Loo, 2007). The absorption of nutrients like amino acids and sugars is carried out by the secondary transport in the small intestine and returned to the body after passing across the glomerular filter in the kidney via the same system (Slack, 2020). Examples of CNS transporters include serotonin (5-HT) transporter (SERT), noradrenaline transporter (NET), dopamine transporter (DAT), GABA transporter (GAT), and an excitatory amino acid (glutamate) transporter (EAAT). These transporters help maintain the

balance of neurotransmitter levels by taking back into the presynaptic nerve terminals via pumps (Ravna et al., 2008).

1.1.3 Lysine-dependent Acid Resistance System (LDAR) and Cadaverine/Lysine Antiporter (CadB)

The enterobacterium *Escherichia coli* are colonized naturally in the mammalian digestive tracts (Kanjee & Houry, 2013). Due to the low pH of the environment in which *E. coli* live, they must counteract acid stress to survive. Having an acid resistance system protects these cells under acid stress. Their acid resistance systems start to operate in case of acidic medium (e.g., stomach, which has a pH range of 1.5 to 3.0). Even in the intestine, bacterial cells are exposed to acid stress due to nutrient metabolism products such as lactic, acetic, and formic acids. This system serves as a physiological adaptation against extreme (the pH range of 2.0 to 3.0) and mild (the pH range of 4.0 to 5.0) acidic conditions. Acid damage starts with the outer membrane of *E. coli* and the periplasm, where *E.coli* change the composition of both membranes to reduce membrane fluidity and to have decreased the influx of protons. It can also be achieved by preventing the outer membrane porins since cadaverine or phosphate to outer membrane porins blocks protein influx.

E.coli has four different acid resistance systems, each consisting of two components. One of the components is a cytoplasmic pyridoxal-5'-phosphate (PLP)-dependent decarboxylase, which serves as an electronic sink yielding a product and CO_2 (Aquino et al., 2017). The second component is substrate/product antiporter located on the inner membrane, which facilitates the external substrate and internal product exchange. LDAR system performs effectively under mild acid conditions. One of its components is CadA, a decarboxylase that converts lysine to cadaverine and produces CO_2 in the cytoplasm. Under acidic conditions, cadaverine can be used to block the outer membrane porins. CadB is another component of the LDAR system that serves as a membrane-integrated

lysine/cadaverine antiporter on the inner membrane and catalyzes cadaverine and lysine transport in the opposite directions.

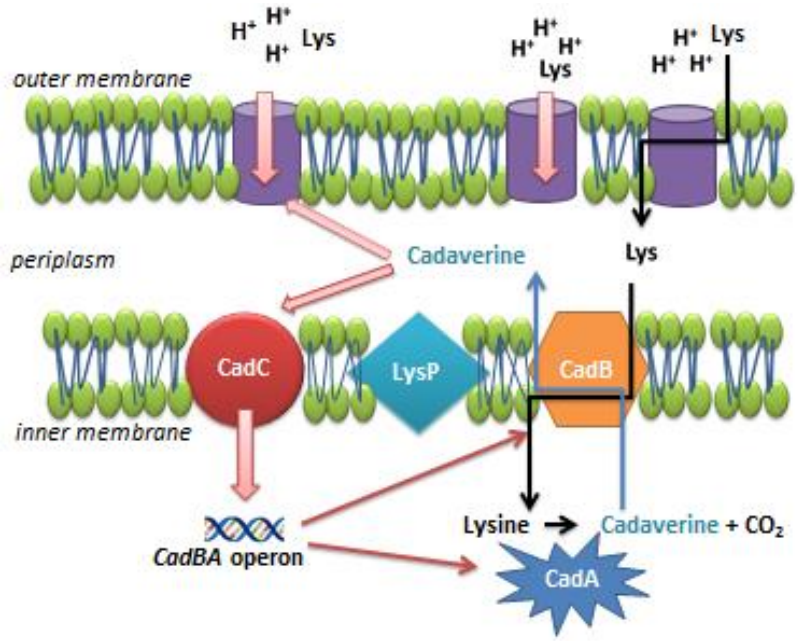

Figure 1.1. Representation of CadB Function in *E.coli* at low pH.

The CadABC module is another inducible amino acid-specific decarboxylase system in *E. coli* species (Jung, Fabiani, Hoyer, & Jung, 2018). CadC belongs to a homodimeric one-component system (ToxR-like receptors) and is a regulator of cadBA operon. The cadBA function together to maintain pH homeostasis by increasing external and internal pH, which is vital for *E. coli* under acid stress situations.

Under non-induced conditions, CadC is inhibited by the lysine-specific transporter LysP (Aquino et al., 2017; Jung et al., 2018). Two different ways to activate CadC: low pH (less than 6.8) and lysine presence (greater than 0.5 mM). A patch of amino acids directly senses a decrease in pH where placed on the periplasmic domain of CadC. A drop in the external pH stimulates the protonation of these amino acid residues. This protonation causes receptor activation. An

incoming signal must be transduced via the transmembrane helix to the DNA-binding domain for expression of the operon by interacting with the target promoter of cadBA. The secondary transporter LysP inhibits CadC under non-induced conditions. At low pH and in the presence of lysine, the interaction is weak and thereby rendering CadC susceptible for protonation and transcriptional activation. Moreover, the end of the products of the cadaverine and CO_2 act as feedback inhibitors on CadC. Cadaverine binding to the periplasmic domain of CadC leads cadBA transcription to switch off.

The functionality of CadB has been tested and proven (Soksawatmaekhin, Kuraishi, Sakata, Kashiwagi, & Igarashi, 2004). CadB protein carries out two primary functions, each of which is to participate in neutral pH as a "cadaverine uptake activity" by consuming a proton motive force as an energy source, and the second one is to decarboxylate lysine in acidic pH as a "cadaverine-lysine antiporter activity" by generating a membrane potential (Soksawatmaekhin, Kuraishi, Sakata, Kashiwagi, & Igarashi, 2004). CadA consumes a cytoplasmic proton and generates a pH gradient **(Figure 1.2)**. This proton motive metabolic cycle leads to the neutralization of acidic conditions and ATP increase in the cells. These physiological functions of CadB are highly beneficial for the growth of bacterial cell.

1.1.4 Expression and Purification of MPs

MPs make up about 20-30% of synthesized proteins in whole organisms (Mathieu et al., 2019). Native MPs are usually insufficiently isolated for biological studies. However, MPs can possibly be expressed in bacteria, mammalian cell lines, yeast, or insect. For *in vitro* MP expression, *E. coli* is the most preferred cell type due to its low cost and simplicity among all cell types. Using *E.coli* facilitates short-expression time for recombinant protein by its rapid growth kinetics and easy genetic manipulations (e.g., DNA transformation) to yield genetically modified strains for specific purposes. For example, *E. coli* C43_(DE3) and C41_(DE3)

strains were generated for MP overexpression (Pandey, Shin, Patterson, Liu, & Rainey, 2016). *E. coli* has an extensive collection of expression vectors (Martínez-Espinosa, 2020). However, this cell type has some restractions for eukaryotic MP expression. Due to a lack of post-translational modification, molecular chaperons, and some essential lipids in their plasma membrane, expressed MPs may not function and fold into correct 3D structures.

Another step of MP preparation for *in vitro* studies involves their purification (Lin & Guidotti, 2009). MPs are embedded in the lipid bilayer with low abundance; therefore, they generally need extra steps to be isolated from the membrane. The first step in the purification is the isolation of plasma membranes from cells or tissues, and the second step is to solubilize these isolated MPs using a detergent. Detergents used as solubilizing agents are indispensable for the isolation and purification of MPs to conduct biochemical and biophysical studies with them.

Detergents can be categorized into three groups: ionic, nonionic, and zwitterionic (Yu, Zhao, & Bayly, 2008). Their amphipathic nature, similar to the plasma membrane, makes them suitable for solubilizing integral proteins. After treatment with detergent, protein shifts into a "solubilized" form by the high detergent amount, disrupting the plasma membrane. As solubilization progresses, it forms a lipid/detergent/protein ternary complex. Based on the experiment, the ratio of these components has to be determined in advance. Here the critical point is to keep the protein in its active form in the detergent. After the first and second steps, the purification of MPs can be followed by conventional chromatography techniques such as gel filtration, affinity, ion exchange, and chromatofocusing (He, Wang, & Yan, 2014).

1.1.5 MPs in Therapeutics

The vast majority of drug targets consist of proteins, while only non-proteins such as lipids and nucleic acids represent a small percentage of drug targets (Freyhult, Gustafsson, & Strömbergsson, 2015). Due to accessibility on the cell surface, MPs make up the most well-recognized targets (~60% of the current drugs) (Yin & Flynn, 2016). These drug targets have been broadly classified, such as enzymes, receptors, transporters, and ion channels (Arinaminpathy, Khurana, Engelman, & Gerstein, 2009).

Any functional impairment, such as misfolding and protein degradation in MPs results in cellular impairments and, thus, many diseases (Marinko et al., 2019). Mutations that disrupt even only a single hydrogen bond, ion pair, or hydrophobic interactions may decrease the yield of protein folding. As misfolded proteins accumulate in the medium, toxicity arises and damages the cells due to decreased functional proteins. A list of diseases that MPs are involved is given in **Table 1.1** with their mutated gene or protein.

Table 1.1 The table of diseases caused by MP dysfunction (Várady, Cserepes, Németh, Szabó, & Sarkadi, 2013).

MPs	Mutated genes/proteins	Diseases
Membrane Receptors **(Traxler, 2003)**	• FGF receptors: FGFR1, FGRF2 • FGFR3 • Calcium-sensing receptor • Growth hormone receptor • INSR • Bone morphologic protein receptor • Cytokine receptor: IL2Rγ • G-protein-coupled receptor • Cannabinoid receptor	Pfeiffer syndrome (early osteocalcification) Kallman syndrome (delayed or absent puberty and an impaired sense of smell) Muenke syndrome (complex developmental disease) Neonatal severe hyperparathyroidism Laron-type dwarfism Donohue syndrome, leprechaunism (nonfunctional INSR) Mendenhall syndrome (less severe for insulin-resistant diabetes) Primary pulmonary hypertension type 2 X-linked severe combined immunodeficiency Color vision deficiency Neurodegenerative diseases
Ion Channels **(Bagal et al., 2013)**	• KCNE1, KCNQ1 • KCNE1, KCNE2, KCNH2, KCNQ1 • SCN5A • CACNA1C	Jervell and Lange–Nielsen syndrome Romano–Ward syndrome (long QT syndrome) Cardiac arrhythmia, idiopathic ventricular fibrillation Thimoty syndrome (cardiac long QT syndrome)
ATP-dependent Membrane Transporters **(Dean, 2005)**	• Mg transporter: ATP1G1 • Na–K transporter: ATP1A2 • Calcium transporter: ATP2B2 • Copper transporter: ATP7A • Calcium transporter: ATP2A2	Autosomal dominant Mg-loss syndrome Familial hemiplegic migraine Nonsyndromic deafness Menkes disease (copper metabolism) Darier disease (desmosome–keratin filament complex abnormality)

Table 1.1 (Cont'd)

ABC transporters (Gottesman & Ambudkar, 2001)	• ABCA1	Tangier disease (familial a-lipoprotein deficiency)
	• ABCA3	Surfactant metabolism dysfunction
	• ABCA4	Stargardt syndrome, retinitis pigmentosa
	• ABCB3	Bare lymphocyte syndrome, immunodeficiency
	• ABCB4	Intrahepatic cholestasis type 3
	• ABCB7	Syderoblastic anemia with ataxia
	• ABCB11	Intrahepatic cholestasis type 2
	• ABCC2	Dubin–Johnson syndrome (direct bilirubin accumulation)
	• ABCC6	Pseudoxanthoma elasticum (fragmentation and mineralization of elastic fibers in some tissues)
	• ABCC7	Cystic fibrosis, male sterility
	• ABCC8	Persistent hyperinsulinemia of infancy
	• ABCD1	Adrenoleukodystrophy (a disorder of peroxisomal fatty acid b-oxidation)
	• ABCG5, ABCG7	Sitosterolemia
SLC transporters (Hediger, Clémençon, Burrier, & Bruford, 2013)	• SLC2A1	Glut-1 deficiency syndrome (De Vivo disease)
	• SLC2A2	Fanconi–Biskel syndrome (uncontrolled glucose levels)
	• SLC2A9	Renal hypouricemia
	• SLC12A1	Type I Bartter syndrome (Na, K and Cl cotransporter deficiency)
	• SLC12A3	Gitelman syndrome (kidney-based cation imbalance)
	• SLC16A1	Hyperinsulinemic hypoglycemia type 7
	• SLC16A2	Allan–Herndon–Dudley syndrome
	• SLC26A2	Diastorphic dysplasia
	• SLC26A4	Pendred syndrome
	• SLC40A1	Hemochromatosis
	• SLC34A2	Pulmonary alveolar microlithiasis

Table 1.1 (Cont'd)

Structural MPs	• PMM2 (CDG-Ia)	Carbohydrate-deficient glycoprotein syndrome
	• PIG-A	Paroxismal nocturnal hemoglobinuria
	• DMD	Duchenne and Becke-type muscular dystrophy
	• Functional cell surface integrins in neutrophils and macrophages	Leukocyte adhesion deficiency type 1
	• GPIIb–IIIa complex	Glanzmann thrombasthenia
	• Cytokeratins: KRT5, KRT14	Epidermolysis bullosa
	• Connexin: GJB1	Charcot–Marie–Tooth disease
	• Connexin: GJB2	Nonsyndromic deafness
	• Proteolipid protein: PLP1	Pelizaeus–Merzbacher disease
	• Glypican: GPC3	Simpson–Golabi–Behmel-type growth disorder

ABC: ATP-binding cassette; SLC: Solute carrier.

GPCRs (G-protein coupled receptors) represent the most drug-targetted MPs (Arinaminpathy et al., 2009; Schfneberg et al., 2004). They are dynamic receptors and play critical roles in major signaling pathways, such as those related to the actions of drugs, toxins, hormones, and neurotransmitters, sensing light and odors, water reabsorption, and blood calcium levels. The malfunction of the GPCRs causes severe disorders such as hypertension, congestive heart failure, stroke, and cancer (Arinaminpathy et al., 2009). Channelopathies such as long QT syndrome and cystic fibrosis are another group of diseases that can arise from defects in transmembrane proteins involving ligand- and voltage-activated ion channels, known to regulate ion and water balance, membrane potentials, and information transfer.

In the human body, many MPs either as receptors or transporters such as ATP binding cassette (ABC) and solute carrier (SLC) found in CNS (CNS; the brain and spinal cord). ABC proteins are another group of transporters with various functions related to the transport of peptides, phospholipids, and bile materials (e.g., salts, cholesterol) and surfactants, and the presentation of antigens (Hediger et al., 2013).

On the other hand, SLC proteins transport a wide variety of endogenous substrates, such as inorganic ions, amino acids, neurotransmitters, and sugars, vital for normal physiological functioning (Pillai, 2019). They govern the movement of endogenous substrates, xenobiotics, and therapeutic drugs. Any change in the structures of these transporters in CNS leads to the onset and progress of neurodegenerative diseases. For example, Alzheimer's disease (AD) is characterized by a hallmark called amyloid-β, which is the substrate of ABCB1 (P-glycoprotein) in ABC transporters (Chai, Leung, Callaghan, & Gelissen, 2020). Like ABCB1, ABCG2 (breast cancer resistance protein, PCRP), and ABCCs (multidrug resistance-associated proteins, MRPs) are found in endothelial cells, astrocytes, and neurons (Hartz & Bauer, 2011). P-gp (P-glycoprotein) acts as an efflux pump overexpressed in tumor cells and targeted by approximately % 50 anticancer drugs. Low-molecular-weight drugs frequently target ABC transporters

due to their overexpression in several cancer types, and they significantly decrease the chemoresistance of cancer drugs (Qosa et al., 2016).

1.1.6 MPs in Diagnostic Applications

For disease detection, MPs have been one of the most targeted molecules. Such MPs include N-cadherin, CD47, Human epidermal growth factor receptor 2 (HER2), membrane-associated metalloproteases, and members of GPCR (Rucevic, Hixson, & Josic, 2011). They serve as significant diagnostic biomarkers because of their localization on cell surface and organelles. CD antigens, also known as CD markers, allow the cells to be distinguished from other cells and have been used for phenotyping the immune cells (Cibiel, Dupont, & Ducongé, 2011). Almost all hematopoietic disease detection targets MPs by molecular imaging agents and antibody-based panels to target CD specificities and examine the expression profiles of the receptors (Batool et al., 2017). However, these antibody-based detection systems have the challenge to identify MPs in their native state. Besides, even though the number of MPs is estimated at a thousand, only about 400 CD antigens have been recognized by identified antibodies (Kalina et al., 2019).

As a hematopoietic disease biomarker, human erythrocytes (RBCs) express many MPs in their plasma membrane. Owing to their availability in the blood sample and the potential reflection of tissue-specific expression in the RBC membrane, MPs are suitable for rapid and straightforward quantitative biomarker assays using flow cytometry and mass spectroscopy-based technologies (Várady et al., 2013). Flow cytometry is the most widely used and accessible antibody-based diagnostic method to evaluate cell surface biomarkers; other frequently used antibody-based technologies include western blotting (Gwozdz & Dorey, 2017), ELISA (Vashist & Luong, 2018), and tissue immunostaining techniques (Souf, 2016; Várady et al., 2013). Although immunoassays can be highly efficient and sensitive in the detection of cell surface biomarkers, they may have a variety of limitations such as high costs, risks of interferences, the need for quality controls,

labor-intensiveness, the requirement for particular expertise and instrumentation, difficulties in MPs quantification and the inaccessibility to MPs as possible targets. Antibodies are used to detect circulating tumor cells (CTCs) based on the expression of epithelial markers such as EpCAM (J. Zhang et al., 2015). However, this antibody-based approach can be limited as CTCs can lose their epithelial characteristics (e.g., EpCAM downregulation) due to epithelial-mesenchymal transition (EMT) and may end up the similar antigen expression profiles that are shared with normal cells. Consequently, antibodies cannot effectively detect CTCs and cannot discriminate between malignant and benign cells.

1.2 Aptamers

As an alternative to antibodies, aptamers have recently been developed. The oligonucleotide libraries are based on laboratory evolution, which typically contains 10^{15} synthesized random nucleotide sequences for *in vitro* selection (Parashar, 2016a). A high number of sequences increases the chance of having active folds in the oligo pool. Therefore, oligonucleotide sequences can be selected for any target from nearly 10^{15} different sequence combinations. In 1990, three different research groups had contributed to the "nucleic acid selection" against the chosen target using a random sequence pool of RNA. These *in vitro* selected nucleic acids were called aptamers. Ellington and colleagues (Ellington & Szostak, 1990) established a process of RNA binding to organic dye; meanwhile, Robertson and Joyce (Robertson & Joyce, 1990) identified a generation of RNA capable of cleaving the DNA at the specific sites, and finally, Tuerk and Gold (Tuerk & Gold, 1990) developed RNA ligands which are specific for a bacteriophage T4 DNA polymerase (Klussmann, 2006).

All of these processes come together to create the SELEX method, by which aptamers were isolated against a specific target. SELEX consists of three parts: Incubation, separation, amplification **(Figure 1.2)**

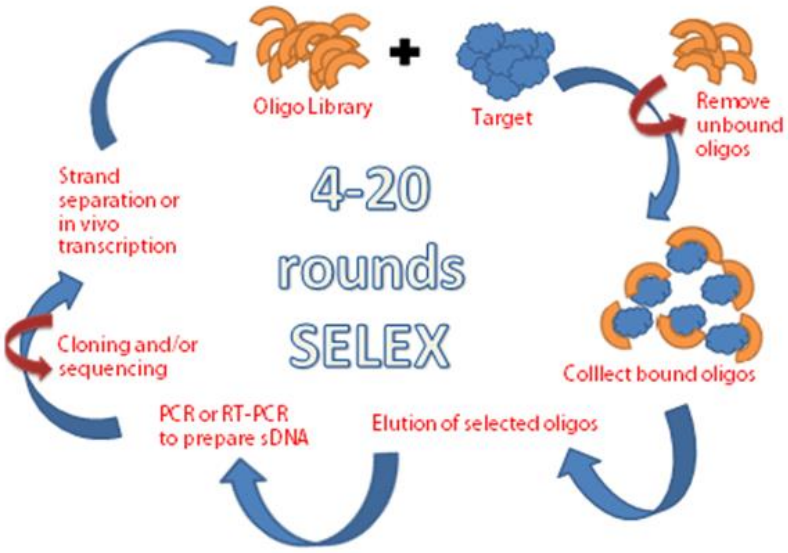

Figure 1.2. The schematic overview of the SELEX process.

Each SELEX method involves a pool of RNA or DNA, consisting of a randomized sequence region in the middle strands (Ilgu, Fazlioglu, Ozturk, Ozsurekci, & Nilsen-Hamilton, 2019). Depending on the type of oligonucleotide in the pool, the process starts with incubating the target with DNA or RNA pool. In DNA SELEX, single-stranded DNAs are converted to dsDNA by PCR, whereas, in RNA SELEX, RNA strands are converted to cDNA by RT-PCR for amplification followed by RNA production.

After binding the oligonucleotide with the target molecule, the second step involves the removal of unbound oligonucleotides. There are several different methods for partitioning step in SELEX: capillary electrophoresis, electrophoresis on the polyacrylamide gel, affinity chromatography, flow cytometry, size fraction on columns, surface plasmon resonance, and the nitro-cellulose filter binding. Each method can be used to collect bound oligonucleotide-target complex and (Nilsen-hamilton, Miller, & Huiatt, 2012), thereby aptamer candidates would be ready for the next step. This step is critical to increase the number of aptamer candidates that

bind to the target molecule with high specificity and affinity. The last step includes amplification of separated oligonucleotides either by PCR (for DNA) or RT-PCR (for RNA). These steps can be completed up to 10 iterative rounds. In the end, selected oligonucleotides become ready for cloning and sequencing for aptamer identification in conventional SELEX.

The developed aptamers are small-sized RNA or DNA nucleic acid structures made up of 20–100 nucleotides. These oligonucleotides are flexible and capable of binding to various targets such as small molecules, proteins, viruses, and whole cells, in a specific manner and with high affinity. ATP, GTP, B12, malachite green and caffeine, HIV-1 Rev peptide, MS2 coat protein, and thrombin are examples of targets for aptamer selection (Pfeiffer & Mayer, 2016). The specific binding region of the aptamer is critical to make it unique for target recognition. The base pairing and stacking in DNA and RNA interactions help forming secondary structures as the stem, loop, bulge, pseudoknot, G-quadruplex and kissing hairpin (J. Zhou & Rossi, 2017). These structures then form unique three-dimensional shapes that characterize the aptamers and increase their affinity and specificity to their cognate targets. With hydroxyl (-OH) in their ribose sugar, RNA aptamers can utilize more biochemical activities and perform reactions including phosphodiester bond formation and cleavage, carbon-carbon bond formation, alkylation, a Diels-Alder condensation, acyl-transfer reactions like amide bond formation. However, the absence of a hydroxyl group in the deoxyribose sugar allows DNA to be more stable than RNA (Klussmann, 2006; J. Zhou & Rossi, 2017).

Aptamer binding affinities to their targets are often represented by the dissociation constant (K_d), which ranges from picomolar (pM) to micromolar (μM) values (Kalra, Dhiman, Cho, Bruno, & Sharma, 2018); the types of interactions that characterize this binding include hydrophobic and electrostatic interactions, hydrogen bonds, van der Waals forces, shape complementarity (Cai et al., 2018; Ilgu et al., 2019).

1.2.1 2D Secondary Structure Prediction of Aptamers

After cloning of the pool, sequencing and structural prediction are the next procedures for downstream selection (Bing, Yang, Mei, Cao, & Shangguan, 2010). In an organism, the RNA function is basically determined by its 3D structure (H. Zhang et al., 2019). Many methods can build either 2D or 3D structural models for nucleic acid determination: bio-crystallography, nuclear magnetic resonance (NMR) spectroscopy, and chemical modification. Nevertheless, they are experimentally tedious, expensive, and time-consuming techniques (Magnus, Kappel, Das, & Bujnicki, 2019; H. Zhang et al., 2019). 2D secondary structure prediction is alternatively used for nucleic acid structure determination due to its easier process to access a model than the tertiary structure, and it allows valuable structural information. Besides, it is more thermodynamically stable than RNA 3D structure due to having robust base-stacking and base-pairing interactions (Shi, Wu, Wang, & Tan, 2014). Basically, a secondary structure is defined by which nucleotides are present in the loop and which has a Watson-Crick base pairs pattern (Afanasyeva, Nagao, & Mizuguchi, 2019).

RNAs can be grouped into families based on their sequence alignments as a representation at the level of individual residues to detect regions as active sites, ligand binding sites, or regions involved in a function. The sequence alignment can also be used to predict secondary structures (Magnus et al., 2019). Some known secondary structures of the RNA motifs, such as multi-helical motifs, internal loops, and bulges, are reliably predictable from sequences (Capriotti & Marti-Renom, 2008).

Many computational methods for 2D secondary structure prediction of nucleic acids can serve as an important and easy way of generating hypotheses about aptamer structure and binding ability (Bing et al., 2010). The RNAfold is one of the 2D prediction algorithms that make use of optimized structures and generates a minimum energy solution. Herein, the optimized structure provides the best representation of native structure via its thermodynamically minimum free

energy (MFE, ΔG), which is produced during the formation of a secondary structure (Andrews & Moss, 2019). Because, in the organism, the equilibrium energy status for the RNA folding is near to MFE status (H. Zhang et al., 2019). Moreover, RNAfold is capable of estimating G-quadruplex formation in DNA structures (Afanasyeva et al., 2019).

On the other hand, KineFold is another algorithm that allow the secondary structure prediction with their pseudoknots. During RNA folding stimulation with a long-time-scale, this algorithm calculates the stochastic opening and closing of an RNA helix in a structure with geometrical and topological constraints (Shi et al., 2014). However, due to the inexact scoring function in MFE-based algorithms, these algorithms may not profess that the predicted final structure will be a native structure that corresponds to a near-native conformation (Capriotti & Marti-Renom, 2008). ΔG is not necessarily important for corresponding with a correct target-binding structure because target-induced refolding of the aptamer focuses on aptamer-target interactions commonly (Shangguan, Tang, Mallikaratchy, Xiao, & Tan, 2007).

2D secondary structure estimation tools may be crucial for aptamer-based drug design for further studies (Afanasyeva et al., 2019). The sequences coming from the same family with their same/similar secondary structures are generally assumed to bind the same target but different with K_d (Bing et al., 2010; Shangguan et al., 2007). Identifying a minimal binding motif that lacks unnecessary nucleotides is important for further aptamer applications with high yield and low cost. Because not all nucleotides directly interact with a target or contribute aptamer folding through the target (Bing et al., 2010). The standard methods are used to identify the binding motif and binding site in aptamers, such as *in vitro* transcription truncated DNA, enzymatic footprinting, and partial hydrolysis. However, such complicated techniques require extensive time and money. In this case, comparing the aptamers' secondary structures can provide a successful way to deduce binding motifs. Briefly, after comparing the secondary structure similarities, a unique secondary structure binding motif and conservative

nucleotides in the loop and bulge can be found. Additionally, Shangguan and his group implied that the stem-loop structures might have importance for target binding while the stem stabilizes the structure's conformation for target binding (Shangguan et al., 2007).

1.2.2 Comparison with Antibodies

Antibodies have been the most used probes in diagnostics as they can bind a broad range of targets with high affinities (Fernandes et al., 2017). However, studies have proven that aptamers are worthy candidates to provide new opportunities and overcome issues related to using antibodies as diagnostic and therapeutic tools **(Table 1.2)** (Y. Zhang, Lai, & Juhas, 2019). Aptamers, like antibodies, recognize and bind their targets with high affinity and specificity. However, unlike antibodies, aptamers have little immunogenicity. Their toxicity is also low, and they are selected against a broader range of targets, including non-immunogenic and toxic targets. In terms of size, aptamers are relatively small molecules; this makes them versatile molecules that bind small epitopes inaccessible to the relatively larger antibodies (W. Zhou, Jimmy Huang, Ding, & Liu, 2014). Due to their large size, only a few antibodies are able to achieve to penetrate the blood-brain barriers by binding more than one target (Heidi Ledford, 2011).

Regarding the production of antibodies, the process is done *in vivo*, often involves animals' suffering. Process yields batch-to-batch variations and requires expensive and time-consuming downstream processes (Ilgu et al., 2019; Molefe et al., 2018; W. Zhou et al., 2014). On the other hand, the production of aptamers is quick, easier, and cost-effective. Moreover, unlike antibodies, chemical synthesis is highly reproducible and yields aptamers with high purity. SELEX processes are also continuously being optimized to produce aptamers more efficiently. Also, antibodies are prone to denaturation (especially at high temperatures), frequently

lose their functionality after use once or a few times, and are difficult to label at specific sites.

Assays involving antibodies often require immobilization, extensive washing, and can be challenging to perform with homogeneity (Shen, Rusling, & Dixit, 2017). On the other hand, aptamers are highly thermostable and renature easily after repetitive denaturation, can be stored for more extended periods (years), and can be repeatedly used without any loss of binding capacity (Ospina-Villa, Zamorano-Carrillo, Castañón-Sánchez, Ramírez-Moreno, & Marchat, 2016). Furthermore, their small size provides them higher densities for immobilization (Balamurugan, Obubuafo, Soper, & Spivak, 2008). Moreover, they can be more sensitive than antibodies; thus, they can differentiate target isoforms (Marshall & Wagstaff, 2020).

Table 1.2 The comparison of aptamer and antibody.

	Aptamer	Antibody
Production	Chemical Synthesis • Inexpensive • Easy	Cell culture and animal need • Expensive • Labour expensive
Discovery time	SELEX takes approximately eight weeks	About six months
Stability	Stable in harsh condition • No loss of activity	Difficult to apply to harsh condition • Storage is problem with a potential loss of functions
Assays	No secondary region is needed • Simple, no cross-reactivity in western blotting	The secondary antibody is needed • Cross-reactivity in western blotting
Modification	Easy for chemical modification	Difficult for chemical modification
Size	Small size (<30 KDa) • Easy membrane penetration	Large size (~150 KDa) • Difficult penetration
Immunogenicity	Non-immunogenic	Immunogenic

1.2.3 Improvement of Aptamers

Although aptamers have several advantages over antibodies, they have faced some limitations. Their inherent physicochemical characteristics can affect pharmacokinetic properties resulting in rapid excretion through renal filtration, metabolic instability, elimination of non-protein-bound, non-specific immune activation, polyanionic effects, and rapid biodistribution from the plasma compartment into the tissues. For example, rapid excretion through renal filtration is one of the challenges that decrease the circulation time in the human body. However, aptamer's ability to undergo conjugations has been contributed to the improvement of pharmacokinetic properties as aptamer-based therapeutics. In this way, aptamers can be functionalized with bulky moieties such as polyethylene glycol (PEG), liposomes, proteins, cholesterol, organic or inorganic nanomaterials (Ho Lee et al., 2015; Parashar, 2016b; J. Zhou & Rossi, 2017).

In vitro selected aptamers have to be optimized for the reaction conditions and chemical alteration before they are ready to be used for *in vivo* applications. Making nuclease resistance increases the aptamer stability during targeted drug delivery in the circulatory system or cells. Both natural DNA and RNA species have a short half-life in human serum due to nucleases exposure. These chemical modifications are possible on the terminal of nucleic acids, phosphodiester linkage, or sugar ring. Naturally, the 2’-hydroxyl group influences the conformation of ribose and allows RNA binding to proteins via hydrogen bonds, and such a binding can be prevented by substituting the 2’-position of the ribose. The 2' substitutions of the ribose, such as 2’-fluoro (2’-F),), 2’-Omethyl (2’-OCH_3), and 2’-amino (2’-NH_2), are the most common aptamer modifications (Kratschmer & Levy, 2017; Ni et al., 2017; Shigdar et al., 2013).

An aptamer truncation is another approach to improve aptamer functionality (Le, Chumphukam, & Cass, 2014). It is known that the unnecessary nucleotides of the full-length aptamers may affect the binding affinity. In such cases, eliminating non-essential nucleotides from the whole sequence leads to a smaller aptamer size

and increases the binding affinity. Final aptamer with a shorter length has advantages in the cost of chemical synthesis and modification. In addition, the small-sized aptamer with high binding affinity has powerful performance as therapeutic or an analytic agent. For example, such aptamers can be easily modified or encapsulated for new nanomaterial and nanostructure development (Quang Vu, Tantirungrotechai, Soontornworajit, & Rotkrua, 2016).

1.2.4 Applications of Aptamers

Due to their easy modification, simple preparation besides high binding affinity and specificity through the targets, aptamers can be used in therapeutic and diagnostic applications (Y. Zhang et al., 2019).

1.2.4.1 Application of Aptamers in Diagnostics

The small size, low cost, and easy preparation make aptamers suitable to recognize agents in many platforms where they can be used alone or in combination with antibodies (Vivekananda & Kiel, 2006). For example, the ALISA (aptamer linked immobilized sorbent assay) method is similar to the ELISA technique, but it uses only a single aptamer as a recognition element. In 2006, Vivekananda and Kiel used this method to detect tularemia antigen, and they claimed that ALISA was more sensitive than the antibody-based method. Similarly, aptamer-based lateral flow assays are also useful for target detection, simply based on capillary action. Aptamer application areas can be classified depending on the intended purpose (Parashar, 2016a).

1.2.4.1.1 Aptamer-based Biosensors

Aptamers offer significant advantages as recognition elements in biosensing technologies due to their chemical stability, small size, cost-effective, and potential diagnostic agents to replace conventional antibodies for clinical diagnosis, including cancer recognition and pathogen recognition or monitoring toxic molecules to prevent food or environmental contamination. Moreover, aptamers offer flexibility, reusability, and high affinity upon target binding compared to antibody based-biosensors. Unlike antibody-based ELISA assays, aptamer based-biosensors (aptasensors) can be readily multiplexed to achieve many biomarkers' simultaneous measurements for a more confident diagnosis. After target binding, the 3D structure of aptamers is subjected to conformational changes that are utilized in signal enhancement in aptasensors. Aptasensors are basically grouped as electrochemical, optical (as fluorescence-based and colorimetric-based), mass-sensitive (e.g., surface plasmon resonance-based, microcantilever-based), depending on their signal-harvesting method. Some MP targeting aptasensor detections are given in **Table 1.3** (Song, Wang, Li, Zhao, & Fan, 2008).

Table 1.3 The MP targeting with aptasensor-based detection.

Aptasensor Type	Aptamer Backbone	Target	LOD	Reference
Electrochemical	DNA	MUC1	16 fg mL^{-1} (from 100 fg mL^{-1} to 1 ng mL^{-1})	(Zhao et al., 2019)
Electrochemical	DNA	CD63	$1x10^6$ particles/mL	(Q. Zhou et al., 2016)
Optical	DNA	Outer MP of *S. typhimurium*	11 cfu/mL (from 11 to 1.10 x 10^5 cfu/mL)	(S. Wu, Duan, Qiu, Li, & Wang, 2017)
Mass-Sensitive	DNA	HER2	550 cells/mL, 1574 cells/mL (unless amplification)	(Poturnayová, Dzubinová, Buríková, Bízik, & Hianik, 2019)
Mass-Sensitive	-	MUC1 on the surface of breast cancer cells MCF-7	0.9 nM (5-500 nM) for MUC1, 213 cells/mL for MCF-7 cells (from 2.0x103 to 5.4x104 cells/mL)	(C. Li, Zhang, Zhang, Tang, & Zhang, 2019)

1.2.4.1.2 Aptamers in Detection of Pathogen and Parasite

In 2010, Bruno *et al.* developed the fluorescence resonance energy transfer (FRET)-aptamers against *E. coli* outer MPs to detect enterotoxaemia *E. coli* (ETEC) K88 as a novel high-throughput screening tool. Moreover, aptamers generated against bacterial surface proteins can be used to detect *Campylobacter jejuni. T*he whole bacterium-based SELEX procedures have been contributed to the detection of other pathogens such as Lactobacillus acidophilus, Staphylococcus aureus, and the virulent strain of *Mycobacterium tuberculosis*, *Vibrio parahemolyticus*, *Shigella sonnei*. Furthermore, these molecular probes can be used for detecting viral infections such as vaccinia virus, herpes simplex virus, hepatitis C virus (HCV), hepatitis B virus, human immunodeficiency virus, influenza virus, and severe acute respiratory syndrome coronavirus (SARS-CoV). Aptamers also can be used for the detection of parasites such as *Trypanosoma spp*., *Leishmania spp*., *Plasmodium spp*., *Cryptosporidium parvum*, *Entamoeba histolytica* (Bruno, Carrillo, Phillips, & Andrews, 2010; Y. Zhang et al., 2019).

1.2.4.1.3 Aptamers in Cancer Diagnosis

Cancer cells are used as a biomarker with critical roles to continue their vital activities, including cell proliferation, cell migration, cell-cell interaction, and signal transduction. Cancer biomarkers can indicate abnormal states of cancers. The MPs are endogenously overexpressed on the surface of tumors in case of abnormal states of cancers. These overexpressed MPs on the tumors are potential targets for cancers in therapeutic and diagnostic use. Aptamers against tumor-related biomarkers have been developed successfully and extensively studied for therapeutic applications to various cancers such as breast cancer, colorectal adenocarcinoma, lung cancer, and prostate cancer. Mucin 1 (MUC1), human epidermal growth factor receptor 2 and 3 (HER2 and HER3), epithelial cell adhesion molecule (EpCAM), nuclear factor kappa-light-chain-enhancer of

activated B cells (NF-kB), prostate-specific membrane antigen (PSMA), CD44, programmed death-1 (PD-1), CD137 (4-1BB), CD134 (OX40), platelet-derived growth factor (PDGF), vascular endothelial growth factor (VEGF), nucleolin (NCL) are aptamer targeting cancer-related biomarkers. Moreover, aptamers can be used for the detection of cancer stem cells (CSCs), which targets EpCAM, CD133, CD117, and CD44. Besides, many aptamers have been selected against tumor cells for diagnosis and prognosis. *In vivo* imaging of cancer types such as lymphoma, adenocarcinoma, glioblastoma, leukemia was achieved by fluorescently labeled aptamers (M. Kim, Kim, Kim, Jung, & Kim, 2018).

1.2.4.1.4 Aptamers in Detection of Small Molecules

Aptamers also have been selected that specific to small molecules such as ofloxacin, ochratoxin A, bisphenol A, cocaine, bacterial endotoxins, and heavy metals (e.g., mercury, arsenic, copper, and lead) (Y. Zhang et al., 2019). These small molecules can lead to food and drinking water contamination and environmental pollutants and thus; can be toxic to humans and animals. Aptamer based-biosensor systems have been developed to detect pollution and toxins (M. Kim et al., 2018; Pfeiffer & Mayer, 2016).

1.2.4.2 Applications of Aptamers in Therapeutics

The nucleic acid-based therapeutic drug must be stable against nuclease degradation, metabolism in the circulatory system, and a specific and high binding affinity to its cognate target (Roberts, Langer, & Wood, 2020). Also, depending on the target localization, drugs may require modification for undergoing the internalization of the cells to reach targets in the cells (Wan et al., 2019).

For therapeutic uses, aptamers have some advantages: the lack of immunogenicity, low toxicity, small-size, cell internalization, easy modification and synthesis, and rapid tissue penetration (Parashar, 2016b). Such advantages

enable the aptamer to be used for medical purposes. Macugen (pegaptanib sodium) was commercialized as the first US Food and Drug Administration (FDA) approved aptamer-based drug in 2004. This PEGylated drug has been used for the treatment of macular degeneracy disease. Many aptamers are currently undergoing clinical trials for the treatment of diseases such as clot bluster (thrombotic thrombocytopenic purpura, intravascular thrombus), diabetes, obesity, allergies, cancers (e.g., renal cell carcinoma, non-small cell lung cancer), acute myeloid leukemia, Willebrand factor-related disorders, von Hippel–Lindau syndrome (VHL), macular degeneration, acute coronary syndrome, and choroidal neovascularization (W. Zhou et al., 2014).

Table 1.4 Some therapeutic features of aptamers for therapeutic purposes (Klussmann, 2006).

Features of aptamers	Advantages of drug discovery
Specific inhibition of target function	Small molecule hits are likely to be inhibitors as well
High-binding affinity binding to most proteins	Almost unlimited target space including orphan and genomic targets
Binding mode different from the natural binding partner	Small molecules potentially exhibit a novel mode of action
Directed against specific epitopes	Targeting of functional domains, active sites, specific conformations, allosteric sites
Selected *in vitro*	The fast development of screening assays
Production by chemical synthesis	Consistently high batch quality and low cost of reagents when produced in small scale
Site-specific labeling by phosphoramidite chemistry	Integration of all common assay formats

1.2.4.2.1 Aptamers as Agonist and Antagonist

Aptamers have functions that serve as an agonist or antagonist to inhibit or stimulate the interaction of tumor-related targets, including the receptors on cancer progression (M. Kim et al., 2018; Parashar, 2016b). Aptamers for clinical trials are extensively used based on their antagonistic effects. Pigpen, Platelet-Derived Growth Factor Receptor (PDGF-r), Tenascin-C, Cytotoxic T cell antigen-4 (CTLA-4), tetrasaccharide carbohydrate (Sialyl Lewis X), NCL, and PMSA are among the aptamer targets developed successfully for cancer treatment. For example, the epidermal growth factor receptor (VEGFR) is overexpressed in the case of cancers such as pancreatic, bladder, breast, and colon. Therefore, modulating these molecules can help alleviate the impact of cancer cells.

Another example of the aptamers' inhibitory effect is used for an allergic response. Mendonsa *et al.*(Mendonsa & Bowser, 2004) developed a DNA aptamer to prevent allergic responses caused by antibody and mast cell interaction. The aptamer was specific to the Immunoglobulin E antibody and inhibited its effect.

Aptamers are also able to activate the functions of the target receptors. However, only a few aptamers have been generated as an agonist for improved cancer immunotherapy. These cancer-associated targets include HER3, OX40 (also known as CD134), 4-1BB (also known as CD137), CD40, CD28, VEGFR2, and they act as receptor agonist (M. Kim et al., 2018).

1.2.4.2.2 Aptamers as Antiviral Agents

Aptamers can be used for viral agents as well (M. Kim et al., 2018). The infection starts as viral particle fusion into host cells through viruses' surface proteins interacting with the host cell receptor. For example, HCV has specific glycoproteins (E2) on their surface for binding to liver cell receptors (CD81) to begin the viral fusion through the cells (Flint et al., 1999). In 2009, a DNA aptamer was selected against E2 glycoprotein to prevent HCV infection (F. Chen, Hu, Li,

Chen, & Zhang, 2009). As the antiviral agents, many aptamers have been selected against viral polymerase enzymes (Bellecave et al., 2003), proteins associated with the viral replication process (Nishikawa et al., 2003), and viral processing inside the host cell (H.-M. Kwon et al., 2014). Similar to an approach for cancer therapy, aptamers are conjugated to small interfering RNA (siRNA) also can be used for viral infection treatment (M. Kim et al., 2018).

1.2.4.2.3 Conjugated Aptamers as Targeted Drug Delivery Agents

The targeted therapy aims to specifically boost the toxicity in tumor tissues while decreasing toxicity in healthy tissues (Wan et al., 2019). Aptamers are able to utilize the internalization through cells by transporting agents for therapeutic delivery purposes, and this property makes use of aptamers as a delivery agent for therapeutic fields such as chemotherapy, gene therapy, and immunotherapy. This is achieve by conjugating aptamers with cholesterols, dialkyl lipids, drugs, chemotherapeutic agents, protein or peptides, photosensitizers, and photothermal agents (Zhu, Niu, & Chen, 2015).

Moreover, aptamer-based oligonucleotide chimeras can be used for disease treatment as new approaches include the use of RNAi agents (e.g., small interfering RNAs (siRNAs), shRNAs, microRNAs, antimiRs, antisense oligonucleotides (ASOs), CRISPR/Cas9) (Zhu et al., 2015). As an example, Wang *et al.* (R. Wang et al., 2014) constructed an aptamer-drug-conjugated module to carry multiple copies of anticancer drug moieties (increases the drug loading) using phosphoramidite, which was site-specifically linked to each aptamer via photocleavable linkers, a widely prescribed medicine for the treatment of colon and pancreatic cancers. Another example for conjugated aptamers, RNAi-based gene therapy, is that 2'-fluoropyrimidine-modified PSMA aptamer has been successfully conjugated to therapeutic oligonucleotides and PSMA aptamer–siRNA chimera constructions, which are internalized into PSMA-expressing cells and effectively suppressed the target tumor genes (Chu et al., 2006). Also, this study demonstrated that

conjugation of aptamer with cholesterol increases the aptamers half-life in the body. Aptamer conjugation is not used only in cancer therapeutics but also in virus-based drug development (Chandola & Neerathilingam, 2020). In 2015, Lee *et al*. generated cholesterol conjugated aptamer to NS5B protein (a non-structural protein located inside the virus) for inhibition of HCV replication in liver cells without induction of cytotoxicity *in vitro* and *in vivo* (Ho Lee et al., 2015).

1.3 MP Targetting in Aptamer Selection

Cancer cell hallmarks are defined by the deregulation of cell-surface MP expressions and activities (Mercier, Dontenwill, & Choulier, 2017). Uniquely expressed, overexpressed, and mutated receptors (tyrosine kinase receptors, cell adhesion receptors, cell death receptors) in tumors are primary pharmaceutical targets (Jacobi, Seeboeck, Hofmann, & Eger, 2017; Lemech & Arkenau, 2011). A large number of drugs have been focused on such proteins/receptors to impede their activities. The latest data from the Mercier group emphasized that histologically similar tumors have high inter-and intra-tumoral heterogeneity at genomic as well as protein levels of relevant targets (Mercier et al., 2017). The reason is that the failure of clinical trials for targeted therapies could be related to underappreciated tumor heterogeneity. As particular tools, aptamers may represent molecular probes for labeling the targets. Moreover, the accessibility of the cell surface receptors allows the use of aptamer in molecular imaging and drug delivery for cancer cell treatment or detection. The list of aptamers generated against MPs is given with their potent application areas in **Appendix A**.

Several SELEX methods have been developed in order to shorten the selection time and increase hit rates (Cibiel et al., 2011; Zhuo et al., 2017). These different SELEX methods are protein SELEX (Ellington & Szostak, 1990; Robertson & Joyce, 1990; Tuerk & Gold, 1990), negative SELEX (Ellington & Szostak, 1992), counter SELEX (Jenison, Gill, Pardi, & Polisky, 1994), capillary electrophoresis SELEX (Mendonsa & Bowser, 2004), microfluidic SELEX (M-

SELEX) (Hybarger, Bynum, Williams, Valdes, & Chambers, 2006), cell SELEX (S. Ohuchi, 2012) (other cell SELEX-based SELEX methods: Fluorescence-activated cell sorting SELEX (FACS-SELEX) (Raddatz et al., 2008), 3D cell SELEX (Souza et al., 2016), cell-internalization SELEX (Thiel et al., 2015; Yan & Levy, 2014), TECS-SELEX (S. P. Ohuchi, Ohtsu, & Nakamura, 2006), hybrid-SELEX (Soldevilla et al., 2016)), *in vivo* SELEX (Mi et al., 2010), high-throughput sequencing SELEX (HTS-SELEX) (M. Cho et al., 2010), cross-over SELEX (Hicke et al., 2001), tissue slide-based SELEX (S. Li et al., 2009), virus-based SELEX (viro-SELEX) (J. Kwon et al., 2019).

1.3.1 Protein Based-Selection of Aptamers

As mentioned earlier, a conventional SELEX procedure **(Figure 1.2)** is followed for protein based-SELEX, and the target is a protein (Szeitner, András, Gyurcsányi, & Mészáros, 2014). In this case, a critical part for the traditional SELEX, high purity of the target protein is required for aptamer isolation. Using various fusion tags (e.g., polyhistidine) simplifies *in vitro* translation system and the purification method from the protein overexpressing cell culture. Therefore, the cognate epitope of the protein could become ready for aptamer selection.

Protein based-SELEX provides quick, cheap, and time-saving advantages for targetting the proteins **(Figure 1.6)**.

1.3.2 Cell Based-Selection of Aptamers "Cell-SELEX"

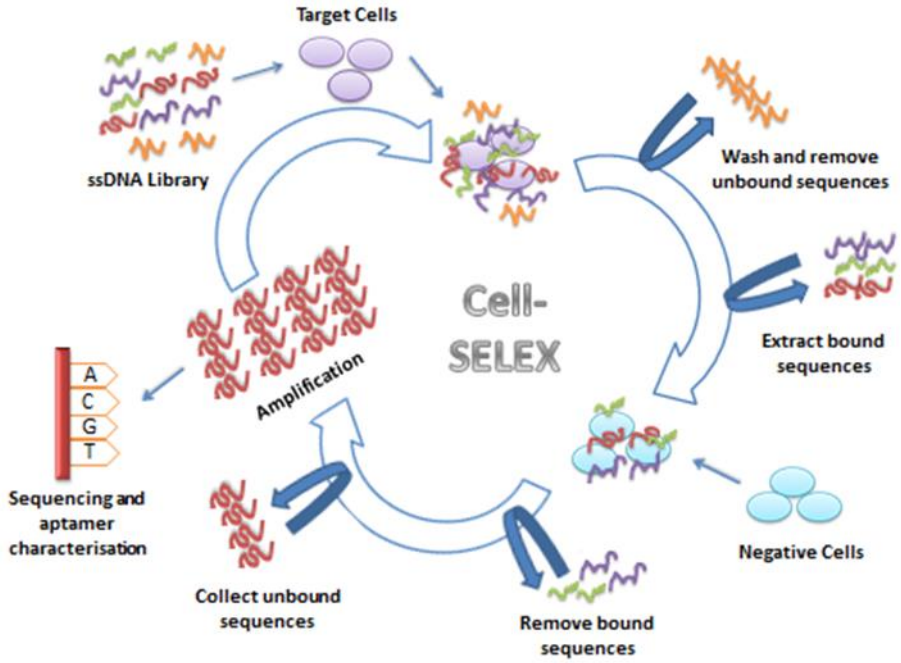

Figure 1.3. A basic representation of the Cell-SELEX process.

Cell-SELEX is a type of SELEX targeting the whole cells by sharing similar main steps **(Figure 1.3)** as the protein SELEX: incubation, partitioning, and amplification (S. Ohuchi, 2012). In addition, it includes positive and negative (counter) selections. Cell-SELEX is used to select aptamers for pathogenic organisms, virus-infected cells, and cancer cells (Lyu et al., 2016). The first step is DNA or RNA pool incubation with the cell targets. At this point, there are two crucial factors: the first one is the choice of cell-line and the second one is to have proper cell culture maintenance (Sefah, Shangguan, Xiong, O'Donoghue, & Tan, 2010). The determination of cell-line depends on which types of cells or surface protein is targeted. Human hepatocellular carcinoma cells, prostate cancer cells, and cancer stem cells have been used as cultured cancer cell lines and using these cell-lines, aptamers have been generated to differentiate them between two different cancer cells or between healthy and cancer cells. Nevertheless, cell

overgrowth increases the dead cell numbers altering cell morphology and protein expression that may affect the aptamer functions.

The second step is partitioning as a counter-selection to remove the oligonucleotides that bind to similar cell targets (e.g., mock cells, non-cancer cells). In this case, cell lines are used to increase aptamer selectivity. This step is the final step for one round and should be repeated to remove non-targeted cells. After the counter selection round, the SELEX continues with positive selection rounds to enrich the aptamer pool against the specific cell lines (M. Chen et al., 2016).

In the cell-SELEX, oligonucleotides are commonly labeled with a fluorescent tag, and this tag provides aptamers to be monitored by microscopy or flow cytometry during the selection. At the end of the process, potential aptamers are cloned into bacteria, and then positive clones are collected for sequencing. After sequencing analysis, aptamer candidate's identification is completed (M. Chen et al., 2016; S. Ohuchi, 2012; Sefah et al., 2010).

Table 1.5 The MP targeting by SELEX over the years (Takahashi, 2018).

Year	SELEX methods targeting cell surface proteins	References
1990	Invention of SELEX	(Tuerk & Gold, 1990) (Ellington & Szostak, 1990) (Robertson & Joyce, 1990)
1996	Purified cell surface protein, L-Selectin	(O'Connell et al., 1996)
1998	Purified plasma membrane (human red blood cell ghosts)	(Morris, Jensen, Julin, Weil, & Gold, 1998)
1999	Whole living parasites (Trypanosoma brucei)	(Homann & Göringer, 2001)
	Bacteria spore (Bacillus anthracis)	(Bruno & Kiel, 1999)
2000	Whole virus (human cytomegalovirus)	(J. Wang, Jiang, & Liu, 2000)
2001	Whole living mammalian cells (rat YPEN-1 cells)	(Blank, Weinschenk, Priemer, & Schluesener, 2001)
2002	Specific protein stabilized by detergent micelle **(NTS-1)**	(Daniels, Sohal, Rees, & Grisshammer, 2002)
2006	A specific protein expressed on the cell surface **(TbRIII)**	(S. P. Ohuchi et al., 2006)

1.3.3 Applications of Cell-SELEX to Enrich Aptamers

Cell-SELEX aptamers can be used in cancer research for imaging, cell profiling, and rare cancer cell detection (Takahashi, 2018). As explained in the previous section, aptamer-based probes using the cell-SELEX method have been developed for many cancer cell detections, including cervical, ovarian, liver, prostate, breast cancers, glioma, colorectal carcinoma, and lung carcinoma (Y. Zhang et al., 2019). For example, ssDNA aptamers were selected that functioned as a histological marker to detect microvessels in the experimental glioma of rats (Blank et al., 2001). Another example is those 2'-F RNA aptamers that have successfully generated against mouse embryonic stem cells (ESC), making a significant contribution to developmental biology, medicine, and novel molecular probes. Monitoring of differentiation is quite tricky for stem cells. Fluorescent labeled Cell-SELEX aptamers can bind stem cells to overcome this difficulty (Iwagawa, Ohuchi, Watanabe, & Nakamura, 2012). As another example, Tang *et al.* used a medium that contains both vaccinia virus-infected and uninfected lung cancer cells together for developing DNA aptamer probes by cell-SELEX. Their results demonstrate that aptamers bind the vaccinia virus-infected cells by most likely targeting a cell surface protein (Tang, Zhiwen; Parekh, Parag; Turner, Pete; Moyer, Richard P.; Tan, 2009).

Aptamers selected through the cell-SELEX were further developed as intracellular transportation of oligonucleotides for therapeutic purposes (C. C. N. Wu et al., 2003). In this strategy, aptamers enter the cell membrane by endocytosis as an intracellular targeting agent. This study can be utilized for intracellular drug delivery (S. Ohuchi, 2012). As previously mentioned before, 2'-fluoropyrimidine-modified PSMA aptamer was successfully developed as aptamer–siRNA chimera constructions to suppress the target tumor genes (Chu et al., 2006).

1.3.4 Advantages of Cell-SELEX

In conventional protein-SELEX, if recombinant proteins do not fold into the correct 3D structure due to the requirement of post-translational modifications, and if the target protein is not at high purity to enrich aptamers specifically, SELEX may fail. However, prior knowledge of protein target is not necessary in the first place in cell-SELEX (Sefah et al., 2010). As mentioned before, the ability of selection against unknown surface molecules provides cell-SELEX an excellent potential for aptamer development. Aptamers are selected to surface proteins in their native states; therefore, they can represent these surface proteins' natural folding structures and their distribution. Even many different molecules located on the cell surface can be a target. The surface complexity for targeting remains a problem for any surface molecule. To overcome these problems, the cell-SELEX has been an alternative method (M. Chen et al., 2016; Sefah et al., 2010).

Table 1.6 The comparison of protein-SELEX and cell-SELEX.

Methods	Key Aspects	Advantages	Disadvantages
Protein-SELEX	Target to protein specifically	• Suitable for whole proteins, including surface proteins to target. • Aptamers bind to a target with high specificity and selectivity. • Cost-effective, straightforward process. • Suitable for either bacterial or cell cultures.	• Prior knowledge of the target is required. • Aptamers are selected against molecules recombinant proteins that may lack post-translational modifications or cannot fold correctly. • Recombinant protein concentration may need far higher than cell would typically have. • Protein purification is required.
Cell-SELEX	Target to whole live cell	• Prior knowledge of the target is not required. • Aptamers are selected against molecules in their native state. • Many potential targets are available on the cell surface. • Protein purification is not required.	• Suitable for cell surface targets. • Requires high level of technical expertise. • Costly. • Time-consuming • Post SELEX identification of the target required.

1.3.5 Limitations of Cell-SELEX

Even though cell-SELEX can be employed extensively for many applications, several technical limitations must be overcome during selection (M. Chen et al., 2016; Sefah et al., 2010; Takahashi, 2018). Firstly, in the course of selection, the presence of dead cells in the suspension would lead to non-specific uptake and binding of oligonucleotides that negatively affect the whole selection and enrichment process. Some methods are required to remove dead cells to eliminate the non-specific oligonucleotides. For example, a novel method was developed to discard many cells by centrifuging after EDTA treatment to dead cells in the suspension Meltem *et al.* (Avci-Adali, Metzger, Perle, Ziemer, & Wendel, 2010).

Due to the high complexity of cell surface components, cell-SELEX requires additional counter-selection rounds to eliminate other non-target cells (M. Chen et al., 2016; Sefah et al., 2010). However, this can add more time to process and require more labor-intensive experimentation. Different cell-SELEX-based methods have been developed to improve the success rate and shorten the selection period, such as automated high-throughput selection (Zhuo et al., 2017).

Target identification can be quite tricky since cells are complex targets and their components on the surface are also complex (M. Chen et al., 2016). Besides, some aptamers are capable of internalizing into the target cells. In these cases, new procedures need to be developed to identify target proteins. Biomarker discovery is one of the approaches to identify the membrane targets in molecular medicine. In 2010, several proteins have been identified as novel membrane targets based on this method. Fang *et al.* made use of aptamers to discover the new cancer biomarkers through the MP targets (Fang & Tan, 2010).

Surface charges can create problems during cell-SELEX. It is known that cell surface has a net negative charge due to the presence of a high number of anionic phospholipid phosphatidylserine on cell membranes (Takahashi, 2018).

Similarly, nucleic acids (either DNA or RNA as an aptamer) have a negative charge as a result of their phosphate component. Some charge distribution can prevent aptamers from getting closer to the cell surface. So far, no successful technique has yet been developed to overcome this problem. To overcome the polarity problems of the binding site or the target molecule, modified aptamers (e.g., SOMAmer, Ds-base, AEGIS-DNA, or 2' position of ribose modifications) have been utilized. Therefore, similar modified aptamer development strategies can be developed to overcome surface charge repulsion issues during cell-SELEX.

1.4 Aim of This Study

1.4.1 Importance of Targeting CadB as a MP using protein-SELEX

CadB protein is a bacterial cadaverine/lysine antiporter located on the inner membrane of *E. coli*. Herein, we focused on enriching aptamers against a recombinant CadB protein as a model MP. Targeting MPs has occasionally faced problems due to their need for native lipidic environments to properly perform their functions. To overcome this problem, the use of a detergent is essential for *in vitro* studies. In our study, we used DDM as a detergent to mimick the cell membrane. CadB was successfully solubilized and purified in DDM. After that, the selection of aptamers was carried out by the protein-SELEX method using the 2'F-modified RNA pool. Even though cell-SELEX is commonly used for MP targeting, this process has some restrictions, such as lack of target identification and specific binding. Besides, this process is time-consuming and requires expensive materials as well as more labor-intensive compared to protein-SELEX. We aimed to perform the protein-SELEX method for aptamer selection against CadB in DDM. In this way, using a proper lipidic environment, studies with MPs would be more effortless, fast, and cost-effective for *in vitro* selection.

As aptamers can bind with high binding and specificity, they can be used for diagnostic and therapeutic approaches. This project's outcome has the potential uses for drug development targeting CadB function, and it would also be used for bacterial detection by aptamer-based biosensors.

Furthermore, this report can serve as an economical, fast, and easy way to use MP targeting *in vitro* studies. Serious health problems such as cardiovascular disorder, cancer, and depression are increasing day by day. Since it is known that many MP-related dysfunctions (e.g., mutation or overexpression) can cause such widespread diseases, MPs are mostly studied in current therapeutics and diagnostic approaches.

CHAPTER 2

MATERIALS AND METHODS

2.1 Reagents

All chemicals used in the experiment are summarized in **Appendix B** with their suppliers.

2.2 Cloning and Overexpression of CadB

Preparation of CadB (cloning into the vector, overexpression, and purification) was performed by Zöhre Uçurum (Fotiadis Laboratory, University of Bern, Switzerland). According to the protocol, after the extraction of *E. coli* strain DH5α, the gene of CadB was cloned from genomic DNA of *E.coli* XL-1 Blue by PCR using the forward primer 5' AAA AAA GCT TAT GAG TTC TGC CAA GAA GAT C 3' and the reverse primer 5' AAA ACT CGA GAT GTG CGT TAG ACG CGG TGT GG 3'. The PCR products were digested with the restriction enzymes HindIII and Xhol and ligated into the pZUDF21 vector (Ilgü et al., 2014). The DNA constructs were verified by sequencing. The pZUDF21-CadB construct results in recombinant CadB protein with a human rhinovirus 3C (HRVC3) protease cleavage site followed by a deca-His tag at the C terminus. This constructed DNA was eventually certified and successfully transformed into BL21_(DE3) pLysS.

For overexpression of CadB, the bacteria were grown in Luria Bertani (LB) with 0.1 mg/mL ampicillin at 37˚C by putting onto an orbital shaker at 180 rpm. After OD_{600} reached to the range of 0.5-0.6, 0.3 mM isopropyl β-d-1-thiogalactopyranoside (IPTG) was added to induce the protein expression, and incubation was extended for 4 hours at 37˚C. Then cells were centrifuged at

10,000xg for 10 minutes at 4˚C, and pellets were resuspended in lysis buffer (20 mM Tris-HCI pH 8.0, 300 mM NaCI, and 10 % (v/v) glycerol). This cell suspension can be stored at -20˚C for use when required.

In the course of membrane preparation step, the resuspended cells were lysed by Microfluidizer M-110P (Microfluidic, Newton, MA) at 16,000 psi in five passages. Resuspended cells were centrifuged at 12,000xg with low-spin centrifugation for 20 minutes at 4˚C to prevent cell debris separation and avoid high molecular weight aggregation. The supernatant was then put in ultracentrifugation at 150,000xg for 1.5 hours at 4˚C to collect cell membranes into the pellet. After this step, the pellet was homogenized and resuspended in a lysis buffer with a small volume. Eventually, this membrane solution was separated into 1.85 mL fractions, and kept for storage at -80˚C until required for later use.

2.3 Purification of CadB

Two frozen membrane homogenate aliquots were brought by Dr. Hüseyin İlgü (University of Bern, Switzerland) for the purification of CadB. These aliquots in 50 mL tubes were then thawed by hands, vortexed, and placed suddenly in an ice bath. The samples were then solubilized in 0.1 mL of 20 mM Tris-HCI pH 8.0, 1.55 mL of 300 mM NaCl, 1.05 mL of 1.5 % (w/v) DDM, and 1.59 mL of dH_2O for 2 hours at 4˚C and put on a slow rotational shaker. DDM was added at last. These solutions were added consecutively to the membrane samples, and the total volume of the solubilization reaction mixture reached up to 7 mL. After solubilization, the samples were transferred to centrifugation tubes for centrifugation at 34,000 rpm for 20 minutes at 4˚C. After centrifugation, both supernatants were taken from centrifugation tubes to a corresponding 50 mL falcon. The pellet, which contains cell debris, was rereleased into the solution. 10 µL of supernatant and the pellet were then resuspended into the 7 mL of water. This solution was stored for later use in SDS-PAGE analysis.

The volumes of the supernatants in both falcons were completed up to 15 mL (twofold dilution) by adding purification buffer-5 (PB-5, containing 20 mM Tris-HCI pH 8.0, 300 mM NaCI, 10% (v/v) glycerol, 5 mM L-histidine, 0.04% (w/v) DDM).

For the resin preparation, 1 mL of TALON® Metal Affinity Resin (Takara, CA, USA) pre-equilibrated with PB-5 was added into new a 50 mL falcon, and then each sample was added in them. The samples with resin beads were incubated overnight at 4˚C with a slow rotating shaker.

For the affinity chromatography, the CadB-bound beads were transferred into a corresponding column (Promega) fitted with a plunging syringe to manually control gravity flow in the column-based setups. Flow rates can be slow in the course of washing; however, it can be increased during the pre-washing step as flow-through (FT). 100 µL was collected from columns as FT_A and FT_B. 3 mL of PB-5 was added to wash, then poured into the columns, and collected as Pre-wash A and Pre-wash B. The beads were washed with 5 mL of PB-5, and they were labeled as wash IA and wash IB. After that, the beads were washed with 5 mL of PB-6.5 (PB-6.5, containing 20 mM Tris-HCl pH 8.0, 300 mM NaCl, 10% (v/v) glycerol, 6.5 mM L-histidine, %0.04 (w/v) DDM) and the sample were collected as wash IIA and WashIIB. The beads were then washed by 1 mL of PB-10 (PB-10, containing 20 mM Tris-HCl pH 8.0, 300 mM NaCl, 10% (v/v) glycerol, 10 mM L-histidine, %0.04 (w/v) DDM) and they were collected as wash IIIA and wash IIIB. For the post-wash step, the beads were washed with 3 mL of wash buffer (WB, containing 20 mM Tris-HCl pH 8.0, 300 mM NaCl, 10% (v/v) glycerol, 0.04% (w/v) DDM), and they were collected as Post-wash A and Post-wash B.

During the incubation of beads with PB-5, PB-6, PB-10, and WB, each washing step took 10, 10, 10, and 5 minutes, respectively, to recover pure CadB protein before filtration. Here, it is essential that the beads do not dry out during filtration. For later use in SDS-PAGE, 1 mL samples can be collected at each filtration, including 10 µL from FT. After filtration, elution buffer (EB, containing

20 mM Tris-HCl pH 8.0, 300 mM NaCl, 10 % (v/v) glycerol, 400 mM imidazole, 0.04% (w/v) DDM) was added to retrieve the bound CadB, and the beads then were incubated for 10 minutes at 4˚C on a rotating shaker. Elution buffer has imidazole, which detaches the protein from the beads. The protein sample was eluted from each duplicate (E_A and E_B). Elution of CadB was performed using the lower segment of the column, fitting into a 2 mL Eppendorf tube and performing centrifugation at 1000 rpm for 1 minute. Finally, CadB was obtained in pure form in the Eppendorf tubes and stored at 4˚C until later use. Preparation of SDS-PAGE is explained in **Appendix C**.

2.4 Concentration CadB and Buffer Exchange

Buffer exchange was carried out into the buffer containing 10 mL of 2X PBS, 80 µL of DDM, and 20 mL of dH_2O. Since CadB concentration in the PBS with DDM solution was low, a concentrator was used after buffer exchanging.

To concentrate CadB, Amicon® Ultra-4 Centrifugal Filter Unit (Merck, Germany) was used. Before adding protein, this centrifugal filter unit was kept in 20% ethanol solution, and thus the filter was centrifuged for 15 minutes to get rid of alcohol. CadB was added to it and then centrifuged again. Centrifugation time was arranged depending on the volume of CadB. The volume should be controlled every 5 minutes until the protein reaches to low concentration as little as possible by avoiding the protein drying.

After concentrating CadB, its temperature was controlled down to 4˚C and then centrifuged at 1,000 rpm. Here, a 2 mL buffer exchange column (Zeba™ Spin Desalting Columns, 7K MWCO, Thermo Scientific™) was used. Therefore, the beads were collected in imidazole, while CadB was eluted. After that step, beads were centrifuged and stored into 2 mL of 20% ethanol for later use. The beads were washed three times, with 1 mL of water and 1 mL of PBS, consecutively. CadB was then added, and the whole solution was collected into a new 15 mL-falcon;

finally, this falcon was washed by water three times to discard unwanted components. The concentration was measured via BioDrop µLite (Cambridge, UK).

2.5 Quantification of CadB

For quantification of CadB, we carried out the Bradford assay (Bradford, 1976). This assay is suitable for the microplate measurement of the protein concentration. This method is based on an absorbance measurement of the amount of the light at 595 nm wavelength that the protein-dye complex absorbs. A detector reads the intensity of transmitted light through the protein sample. According to Beer's law, absorbance can be calculated as the following equation.

$$A = \varepsilon . c . p$$

In this equation, ε is the molar extinction coefficient, in L mol^{-1} cm^{-1}, c is the solute concentration in solution, in mol L^{-1}, and p is the sample's path length (He, 2011).

Bradford contains bovine serum albumin (BSA) as standard, and Coomassie® Brilliant Blue G 250 dye as the colorimetric reagent. This reagent maximally absorbs the light at a wavelength of 595 nm under acidic conditions. The reagent binds to protein and results in altering the intensity of light absorbance, which can also be seen by the naked eye. The color of the sample changes to brown-reddish to blue depending on the concentration of protein in the sample as the color intensity increases proportionally to the amount of protein. After incubation of dye with protein, the reader creates a graph of absorbance versus BSA concentration, and then we can easily find the unknown concentration of the protein with a linear equation and knowing the absorbance of the sample. The x-axis represents BSA concentration, while the y-axis shows the absorbance at 595 nm (Bradford, 1976).

2 mg/mL of BSA was prepared as the stock. For the dilution, the BSA volumes were added into the tubes according to **Table 2.1**, and the volumes were completed with PBS up to 40 µL as the total volume. 7th tube was blank and had no BSA. 5 µL of CadB was added into the well without any dilution. BSA and CadB were prepared as duplicates. The linear range was 1-1400 µg/mL for the reader. As a final step, 250 µL of Bradford Reagent was added into all wells, and the plate was kept for 10 minutes at room temperature. The microplate reader Multiskan GO (Thermo Scientific™, MA, USA) and Skanlt software were used; the program was set for shake 1 for 30 seconds. The software created a graph after measuring absorbance at 595 nm.

Table 2.1 Preparation of tubes for Bradford assay.

Tube Number	Standard's volume (µL)	Standard's source	Diluent's volume (µL)	Final [standard] in µg/mL
1	30	2 mg/mL stock	10	1,500
2	20	2 mg/mL stock	20	1,000
3	30	Tube 2	10	750
4	20	Tube 3	10	500
5	20	Tube 4	20	250
6	20	Tube 5	20	125
7 (blank)	-	-	20	0

2.6 RNA Library and Primers for SELEX

Oligo sequences in the pool are divided into three parts: forward primer, random sequence (53 nucleotides), and reverse primer. In **Table 2.2**, Oligo 484 is the forward, Oligo 485 is the reverse primer, and Oligo 487 is a DNA pool with 100 nucleotides. The ssDNA pool and the primers used in the SELEX were synthesized by Integrated DNA Technologies (IDT; IA, USA). N represents that the same molar mixture of A, C, G, and T was used during the synthesis of the pool. The underlined red sequences show that T7 promoter in the forward primer.

Table 2.2 ssDNA pool sequence and forward and reverse primers for PCR.

Oligonucleotides used in SELEX	Sequences (5'→3')
ssDNA Library (Oligo487)	GCC TGT TGT GAG CCT CCT GTC GAA **(53 N)** TTG AGC GTT TAT TCT TGT CTC CC
Forward Primer (Oligo484)	TAA TAC GAC TCA CTA TAG GGA GAC AAG AAT AAA CGC TCA A
Reverse Primer (Oligo485)	GCC TGT TGT GAG CCT CCT GTC GAA

Oligonucleotides in the pool have a random sequence with 53 nt and two constant regions. Primers, either of two ends must have a T7 RNA polymerase promoter to select RNA aptamers from the ssDNA pool **(Figure 2.1)**.

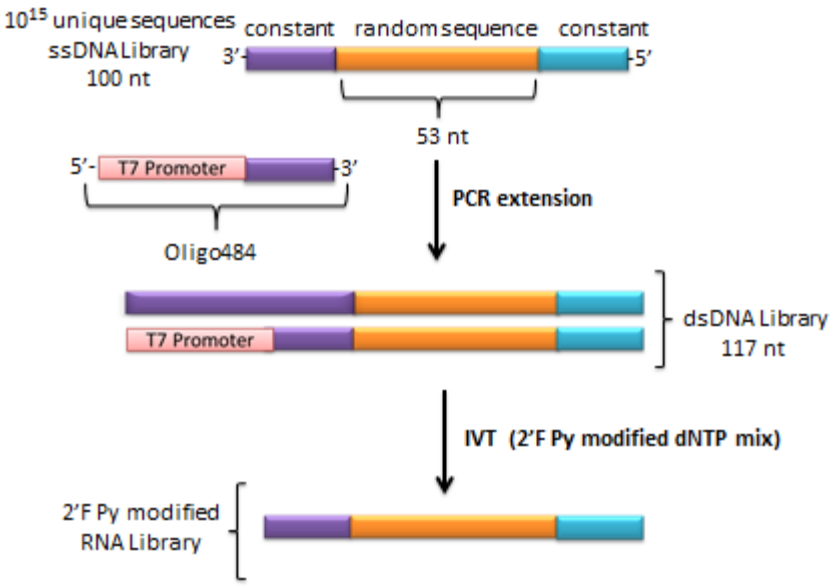

Figure 2.1. The schematic diagram of the RNA synthesis from the ssDNA pool.

2.7 SELEX

Before the selection of RNA aptamers, the DNA extension was done. We started with the DNA pool (Oligo 487), and we added components **(Table 2.3)** into a tube.

Table 2.3 Components for DNA extension.

Component	**Volume (µL)**
dH_2O	32.5
10X PCR buffer	5
0.5 mM dNTP (from 2.5 mM stock)	10
3.33 µM Oligo 484 (from 100 µM stock)	1.67
1.67 µM Oligo 487 (from 100 µM stock)	0.835
DNA Taq polymerase	1

After that extension program was started, as shown in **Table 2.4**, the DNA pool was spun down and vortexed. 15 µL was taken from the pool for agarose gel.

Table 2.4 The extension of the DNA program.

Degree (℃)	**Time (min)**
95	5
65	10
72	90
4	∞

After the DNA extension, we did *in vitro* transcription (IVT) using a kit (Apt-Get 2'-F T7 Transkription Kit, Roboklon, Germany). 2'Fluoro Pyrimidine NTP mix contains 2'-deoxy-2'-fluorocytodine 5'-triphosphate, 2'-deoxy-2'-fluorouridine 5'-triphosphate and non-modified ATP and GTP. The NTP mix does not contain any non-modified CTP or UTP.

Table 2.5 The components for *in vitro* transcription.

Component	**Volume (µL)**
RNase-free water	25-(all volumes)
DNA template (our sample)	1-2 µg (the volume depends on the concentration of the sample)
5X T7 Reaction buffer	5
2'F Py NTP mix	1.5
Apt-Get 2'F T7 RNA polymerase	0.5
Total volume	25

After adding, all the components, tubes were spun down and vortexed. They were placed into the water bath at 42.5˚C for 4-15 hours depending on the concentration. After IVT, 0.5 µL of DNase I was added and then incubated in the water bath at 37˚C for 30 minutes to remove the dsDNA template. Two PCR tubes were combined into a new Eppendorf and the volume was completed to 150 µL with autoclaved water. We now have the RNA pool for round of next selection.

Table 2.6 The parameters used in SELEX for IVT and RNA pool concentrations after IVT.

	IVT		
Rounds	**cDNA quantity (µg)**	**Reaction Time (h)**	**RNA pool (µg/mL)**
1	No Record	4	2644
2	0.36	13	2469
3	0.24	12	2162
4	0.22	12	2087
5	2.88	15	1437
6	1.4	12	1725
7		15	1368
8	3.19	15	1731

For the RNA precipitation, 15 µL of 2.86 M sodium acetate (NaOAc) at pH: 5.3 (1/10 of total sample volume) was added, then tubes were vortexed and spun down then they were left for 2 minutes. 150 µL of isopropanol was added (1:1of total sample). Tubes were spun down and vortexed again and then left for incubation at -80˚C o/n. After that, tubes were centrifuged at 13.000 rpm for 30 minutes, and supernatant was discarded gently. Tubes were then washed with 500 µL of 70% cold ethanol and vortexed and centrifuged at 13.000 rpm for additional 15 minutes. Ethanol was discarded gently and the pellet was allowed to air dry on the bench for 2 hours.

For RNA resuspension, the dried pellets were spun down. Two Eppendorf tubes of 2'F Py RNA pool were resuspended with 50 µL of RNase free water, and tubes were vortexed and spun down. Then the tubes were placed into heat-block at 42˚C for 2 minutes and vortexed and spun again. Samples were transferred to the next 2 Eppendorf tubes, and these tubes were vortexed and spun down. This process was iteratively repeated until the samples combined in a single tube. All tubes were washed with 25 µL of RNase-free water and transferred into the rest of the RNA sample. Pool concentrations were measured as summarized in **Table 2.6**.

For the incubation with protein, the volumes of RNA and CadB were calculated according to the RNA: protein ratio then the desired total reaction volume was calculated (50 µL was the total volume for CadB). The volumes of 2X PBS and water were calculated according to rest of the reaction components. Calculations for each round are given in **Appendix D**. For the RNA refolding, after adding RNA samples, PBS and water were added. After the samples were vortexed and spun down, tubes were placed into heat-block at 95˚C for 2 minutes, and the block was left on the bench at room temperature for 1 hour. After the refolding step, CadB (it must be warmed by hands) was added into the tubes for incubation at room temperature for 60 minutes (this interval of time decreases 15 minutes for each round of SELEX). The tube was tapped in every 15 minutes during incubating.

Table 2.7 The parameters used in SELEX for incubation.

Selection						
Rounds	**[CadB] (mg/mL)**	**Oligo:Target (µM:µM)**	**Oligo/ Target**	**Reaction Volume (mL)**	**Incubation Time (min)**	**1X PBS wash (mL)**
1	0.36	10.00:2.00	5	50	60	5
2	0.36	9.00:1.70	5.29	50	50	5
3	0.36	8.10:1.45	5.59	50	40	6
4	0.36	7.29:1.23	5.93	50	30	5
5	0.36	6.56:1.04	6.31	50	20	7
6	0.36	5.90:0.89	6.63	50	15	10
7	0.36	5.31:0.75	7.08	50	15	15
8	0.36	4.78:0.64	7.47	50	15	15

After placing the nitro-cellulose membrane, a vacuum had started to run for the washing unbound oligos, and the membrane was soaked with 1 mL of 1X PBS. The sample was added slowly to the membrane to collect the protein-bound RNA complexes on the membrane. The membrane was washed with 10-15 mL of 1X PBS again. After this step, extra sides of the membrane, which were unnecessary, were cut to discard, and only the center of the membrane was taken. It was then placed into a 15 mL conical tube (falcon). 1 mL of 6 M urea was added to the sample on the membrane, vortexed, diluted with 5 mL of autoclaved water and vortexed again. Now, the bound RNA sample is expected to be removed from the membrane by urea (now we had 6 mL of the sample). The sample was left in the water bath at 40-45˚C for 30 minutes. It was vortexed every 5 minutes.

For the second RNA precipitation, 60 µL of 2.86 M NaOAc was added into each of the Eppendorf tubes, and 600 µL RNA samples were added. Each of the tubes was vortexed and spun down. The membrane in the falcon was washed with

300 µL of 6 M urea, vortexed and spun down, 1.5 mL of water was added afterwards. All samples were collected in one or two tubes after they were vortexed and spun down. After collecting, the sample was vortexed and spun down again, and it was left for 2 minutes. Finally, 600 µL of isopropanol was added, and then it was vortexed and spun down. Finally the tubes were left at -80˚C for o/n. After incubation, tubes were immediately centrifuged at 13.000 rpm for 30 minutes. Supernatants were discarded gently, pellets were washed, centrifuged and the tubes were left for air-drying on the bench for 2 hours.

For resuspension of protein bound-oligos, two Eppendorf tubes which had dried pellet and each of which was washed with 50 µL of RNase free water, vortexed and spun down. Tubes were placed into 42˚C in the water bath for 2 minutes to loosen the pellet and were vortexed and spun again. Samples were transferred to the next 2 Eppendorf tubes, and tubes were vortexed and spun down. This process was repeated for all the samples to collect all in one tube. All the tubes from which samples were already collected were washed with 25 µL of RNase-free water and transferred into the rest of the RNA sample.

For cDNA production, the components were added as given in **Table 2.8**. This step is essential for the amplification of the pool. We used RNA pool for protein incubation; however, we had to convert them to DNA for PCR amplification. During cDNA production, we used a trail to ensure positive results, and then continued with the rest of the RNA sample.

Table 2.8 Components of the reaction mixture for cDNA production.

Component	**Volume (µL)**
RNase-free water	4
Collected RNA sample	5
200 µM Oligo485	1
Total volume	10

For annealing, the PCR machine was arranged accordingly to **Table 2.9**.

Table 2.9 Arrangement of the PCR machine for annealing, RT, and PCR.

Degree (°C)	Time (sec/min)	
65	5 min	Annealing
4	5 min	
65	60 min	RT
85	5 min	
4	∞	
93	5 min	PCR
93	30 sec	
65	1 min	
72	1 min	
72	10 min	
4	∞	

After annealing, 9.5 µL of 2X RT MasterMix (containing 2 µL of 10X Reaction Buffer, 1 µL of 20X dNTP mix, 0.5 µL of RNase inhibitor, 6 µL of RNase free water) and 0.5 µL of RTase were added, and volume was completed to 20 µL. RTase should be added at last.

After RT, 5 µL of 100 µM Oligo 484, 2.5 µL of 200 µM Oligo 485, and 27.5 µL of 2X PCR MasterMix (containing Taq DNA Polymerase, $MgCI_2$, dNTPs, enhancer, and stabilizer) were added, respectively, and PCR was started as **Table 2.9**. The number of PCR cycles can be arranged depending on the intensity of the bands. We generally did PCR between 13-16 cycles. The numbers of PCR cycles performed in each round are given in **Appendix E**.

After PCR was finished, the sample was run in agarose gel. The parameters that we used for agarose gel electrophoresis are given in **Appendix E**. If the results were meaningful, we continued with PCR purification.

For the PCR purification, we followed the QlAquick PCR Purification Kit Protocol (QIAGEN Science, Maryland, USA). This protocol is designed to purify single- or double-stranded DNA fragments from PCR. According to the procedure, 5 volumes of Buffer PB to 1 volume PCR sample was added and mixed. pH indicator I was added to Buffer PB. The expected color of the solution was yellow. A QlAquick spin column was placed into a provided 2 mL collection tube. The

sample was then put into the QlAquick column to bind DNA and was then centrifuged at 13.000 rpm for 30-60 seconds. After the flow-through was discarded, the QlAquick was placed back into the same tube. 0.70 mL of Buffer PE was added to the QlAquick column to wash and centrifuged for 120 seconds. After the flow-through was discarded, the QlAquick column was placed back into the same tube again. The column was centrifuged for an additional 1 minute. QlAquick column was placed in a clean 1.5 mL microcentrifuge tube. 35 µL of water (pH 7.0-8.5) was added to the center of the QlAquick membrane to elute DNA and then centrifuged the column for 1 minute. Alternatively, 30 µL of elution buffer can be added to the center of the QlAquick membrane, let the column stand for 1 minute, and then centrifuge. After that, concentration was measured via BioDrop µLite, and in case of low concentration, vacuum-centrifuge (Heto Maxi Dry Lyo Freeze-dryer, The Netherlands) was done to increase the concentration.

2.8 Aptamer Cloning and Bacterial Transformation

After the 8th round of SELEX, CloneJET™ PCR Kit (Thermo Scientific™) was used for DNA cloning. The blunting reaction was started on ice, and the components which are given in **Table 2.10** were added into an Eppendorf tube.

Table 2.10 The reaction components for DNA cloning.

Component	**Volume (µL)**
2X Reaction Buffer	10
DNA (as PCR product)	1
Nuclease-free water	6
Blunting Enzyme	1
Total volume	18

Eppendorf tube was briefly vortexed and spun down, and it was then incubated at 70˚C in the water-bath for 5 minutes; after that, it was left to chill on ice.

The ligation reaction was set up on ice, and the following components were added to the blunting reaction mixture.

Table 2.11 The reaction components for ligation.

Component	**Volume (µL)**
pJET1.2/blunt Cloning Vector (50 ng/µL)	1
T4 DNA Ligase	1
Total volume	2

The mixture was briefly vortexed and centrifuged for 3-5 seconds to collect drops, and for the incubation, the ligation mixture was left at 22˚ (room temperature) for 5 minutes. Here, the ligation mixture should be kept in the icebox until transformation.

For transformation, 20 µL of the ligation product was added to 120 µL of previously prepared BL21 competent cells **(Appendix F)**, and incubated in ice for 40 minutes. After that, the tube was placed in the water bath at 42˚C for 30-45 seconds, and put in the ice again for 10 minutes. 880 µL of LB (or SOC medium also can be added) was added into the tube and incubated at 37˚C for 1.5 hours. 250 µL of the sample was taken from the tube and spread on four agar plates containing 4 mL of LB with ampicillin. These plates should be kept o/n in the incubator. After o/n incubation, 100 colonies were picked out.

2.9 Plasmid DNA Purification

In order to achieve the isolation of high-copy plasmid DNA from *E.coli*, NucleoSpin® Plasmid/Plasmid (NoLid) protocols (Macherey-Nagel, Germany). 1-

5 mL of a saturated *E.coli* LB culture was used to cultivate and harvest bacterial cells, and pellet cells were centrifuged for 30 s at 11,000xg using a microcentrifuge; the supernatant was discarded.

For cell lysis, 250 µL of Buffer A1 was added. The cell pellet was entirely resuspended by vortexing or pipetting up and down. 250 µL of Buffer A2 was added and mixed gently by inverting the tube 6-8 times; the tube then was incubated at room temperature for up to 5 minutes. After that, 300 µL of Buffer A3 was added into the tube, and it was mixed thoroughly by inverting 6-8 times until blue samples turn colorless.

For clarification of lysate, the tube was centrifuged at 11,000xg at room temperature.

To collect the bound DNA on the membrane, a Nucleospin® Plasmid/Plasmid (NoLid) Column was placed in a 2 mL-Collection Tube, and the supernatant was decanted from the clarification step. It was centrifuged for 1 minute at 11,000xg. The flow-through was discarded, and the column was placed back into the collection tube. This step was repeated to load the remaining lysate.

600 µL of Buffer A4 was added, and the tube was centrifuged for 1 minute at 11,000xg. Flow-through was discarded, and the column was placed back into the vacant collection tube.

Then it was centrifuged for 2 minutes at 11,000xg to dry the silica membrane, and the collection tube was discarded. Finally, the column was placed in a 1.5 mL microcentrifuge tube to elute the DNA with 50 µL of Buffer AE incubating for 1 minute at room temperature, it was centrifuged it for 1 minute at 11,000xg. The collected samples were determined by BioDrop spectrophotometer.

2.10 Prediction of Aptamer Structures

For the 2D prediction of these proto-aptamers, we used RNAfold (Hofacker, 2003) and KineFold (Xayaphoummine, Bucher, & Isambert, 2005) webservers. RNAfold web server can predict not only the MFE structure of a single structure, but also; equilibrium base-pairing probabilities can be calculated by this server (Hofacker, 2003). On the other hand, the KineFold web server provides stochastic folding simulations of both DNA and RNA structures on second to minute molecular time scales. In addition to simulations, KineFold can show the pseudoknots and helices with entangled topologies (Xayaphoummine et al., 2005).

Table 2.12 List of the web servers used for 2D prediction.

Web Server	**URL**
RNAfold	http://rna.tbi.univie.ac.at/cgi-bin/RNAWebSuite/RNAfold.cgi
Kinefold	http://kinefold.curie.fr/cgi-bin/form.pl)

CHAPTER 3

RESULTS AND DISCUSSION

3.1 Protein Solubilization and Purification

Membrane's amphipathic nature serves a unique environment for MPs to function properly. *In vitro* studies with MPs can be challenging due to the hydrophobic surface of MPs. To overcome this problem, DDM was used as the detergent during solubilization and purification. DDM was chosen for CadB based on the study of AdiC stability in DDM at the University of Bern (Ilgü et al., 2014).

After solubilization and purification, we run the gel to see CadB protein. 10 µL of sample and 2.5 µL of dye were added. We used 5 mL of PB-5 for wash I, 5 mL of PB-6.5 for wash II, and 1 mL of PB-10 for wash III.

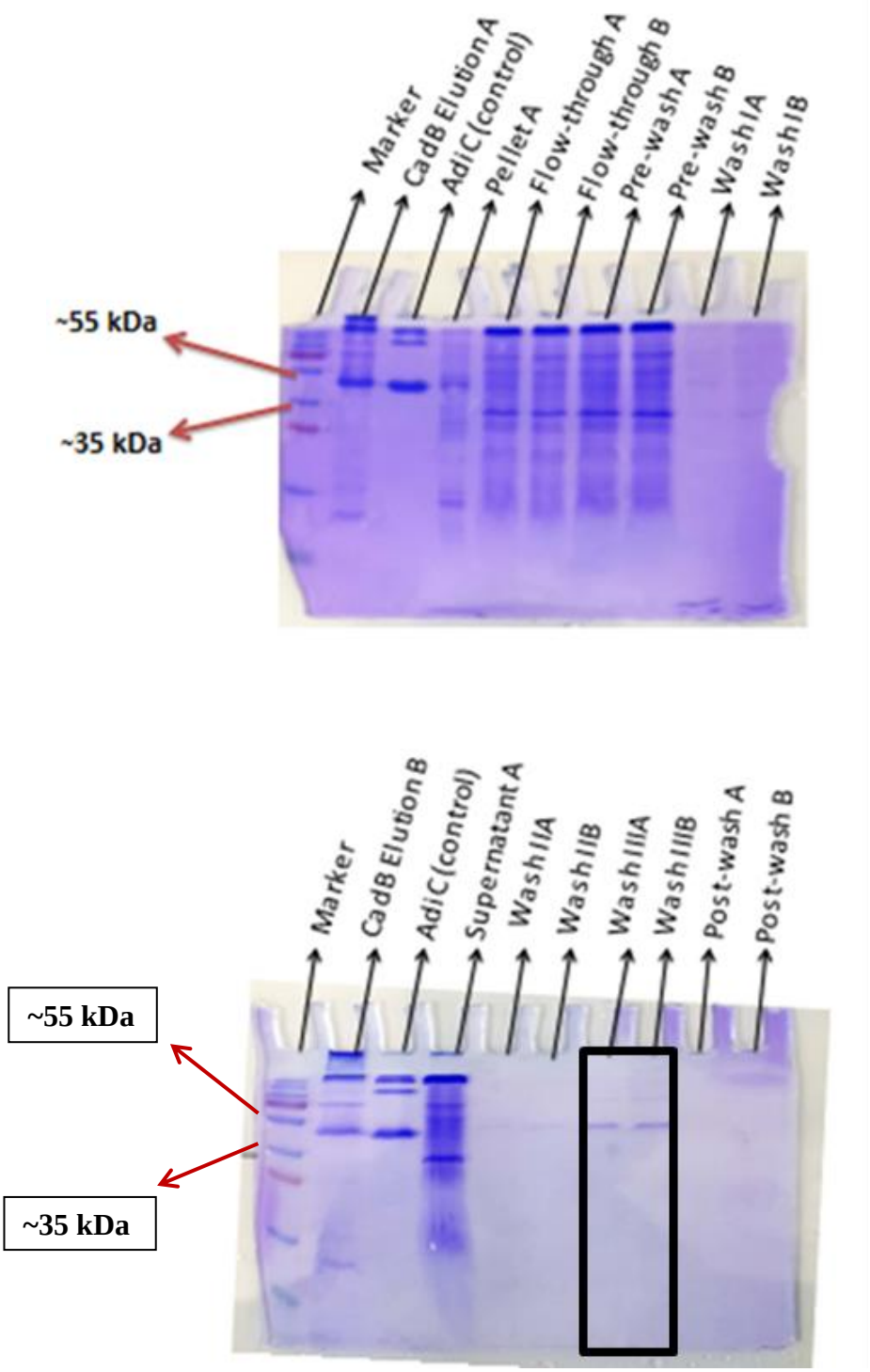

Figure 3.1. SDS-PAGE gel bands for CadB purification.

In these gels **(Figure 3.1)**, AdiC (another secondary transporter in *E.Coli*, 50.9 kDa) was used as control. The molecular weight of a recombinant CadB is approximately 50.77 kDa. According to the marker's profile, the elution A and B bands between 55 and 35 kDa bands show that we had CadB. However, multimerization of CadB protein might have lead to higher molecular weight bands at the top of the elution A and B lanes. On the other hand, we do not see these probable aggregation bands at the wash IIIA and IIIB lanes. Thus, we chose these samples to continue to experiment based on the assumption that CadB was pure in wash IIIA and IIIB.

Herein, we lowered the concentration using PB-10 in order to have the monomeric form of CadB (wash IIIA and IIIB). Because continuing with the monomeric form of the protein is better for SELEX. In this case, we preferred a more dilute concentration, which probably has the monomeric form of CadB.

The details of the SDS-PAGE band profile for the marker were given in **Appendix B**.

3.2 CadB Concentration and Buffer Exchanging

Wash III A and B were chosen instead of EB due to their purer bands of CadB in the SDS-PAGE gel results **(Figure 3.1)**. CadB had been kept in PB-10 before buffer exchanging. After purification, CadB's buffer has to be changed with phosphate-buffered saline (PBS) to continue to SELEX. PBS mimics the human blood serum that consists of NaCI, KCl, and phosphate with pH 7.4.

After buffer exchanging with 10 mL of 2X PBS, 80 µL of DDM, and 20 mL of dH_2O and then CadB concentration, we measured the CadB concentration in wash IIIA & wash IIIB mixed form via BioDrop µLite.

Table 3.1 The concentration of CadB before & after buffer exchanging and protein concentration.

Before	**Concentration (µg/mL)**
Wash IIIA	0.933
Wash IIIB	1.200
After	
Wash IIIA & Wash IIIB mixed form	1.200

3.3 Quantification of CadB

The reader measured the absorbance for each duplicate of BSA and CadB as **Table 3.2**. It is important to mention that due to the low amount of DDM in which CadB is purified, BSA interaction with the detergent can be negligible. The linear equation of the absorbance graph versus BSA concentration was used to find the concentration of CadB **(Figure 3.2)**. The absorbance values were absorbance average of duplicate 1, 2, and blank was subtracted to reach correct absorbance. The average absorbance of CadB was 0.2135 (blank subtracted). According to the y = 0.0007x equation, y is the absorbance value while x is the concentration, and 0.0007 is the line's slope. When 0.2135 was substituted for y, x could be find as 305 µg/mL = 0.305 mg/mL.

Table 3.2 Absorbance duplicates 1 and 2 and absorbance averages (ABS, Absorbance).

Tube	ABS Duplicates 1	ABS Duplicates 2	ABS Average	ABS Average (Blank subtracted)
1	1.523	1.502	1.5125	1.0120
2	1.260	1.291	1.2755	0.7750
3	1.069	1.124	1.0965	0.5960
4	0.883	0.877	0.8800	0.3795
5	0.631	0.628	0.6295	0.1290
6	0.578	0.583	0.5805	0.0800
7	0.507	0.494	**0.5005**	0.0000
CadB (wash IIIA & wash IIIB)	0.733	0.695	0.7140	**0.2135**

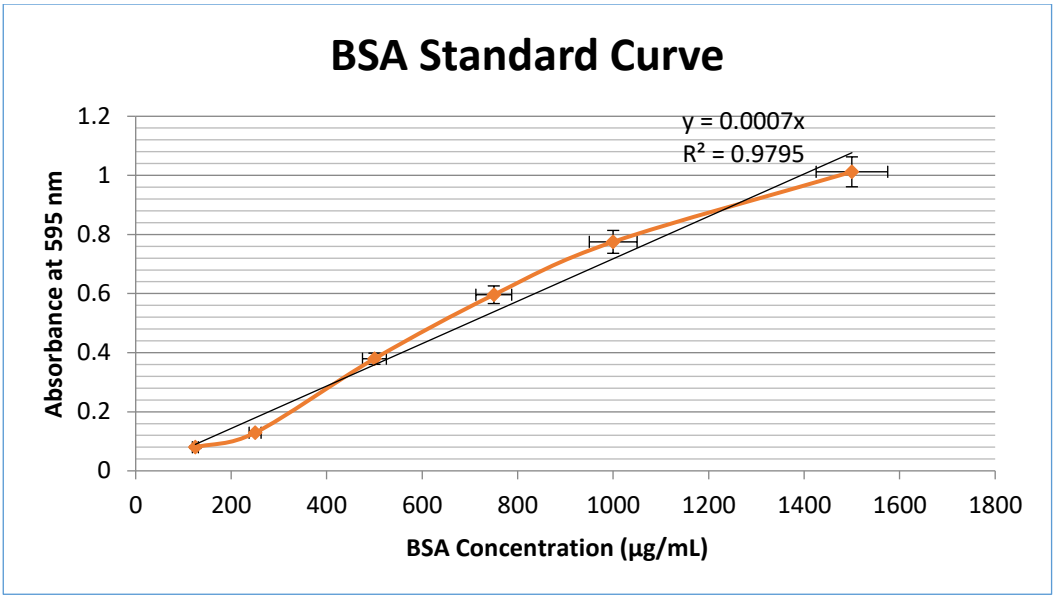

Figure 3.2. The graph of absorbance versus BSA concentration.

According to the BSA standard curve **(Figure 3.2)**, R^2 is very close to 1.0.

- [CadB] $= \frac{0,2135}{0,0007}$ = 305 µg/mL = 0.305 mg/mL.

Based on the assumption that Bradford measured the protein with a good approximation, we continued with SELEX.

3.4 SELEX for CadB

We performed SELEX against CadB with eight rounds. We aimed to select RNA aptamer against CadB. We started with the ssDNA pool, and we have done DNA extension, and then we converted the DNA pool to the RNA pool using an *in vitro* transcription (IVT) kit. The RNA pool concentrations were given in **Table 3.3** for each round. During transcription, we used a 2'F Py dNTP mix, which is mostly used to get modified RNA aptamers. Here, 2'F displays with 2'OH of the ribose ring structure, which serves long-termed half-life by resisting against nucleases in the bloodstream. After IVT, we added DNase I, and this enzyme degrades single- or double-stranded DNA into small fragments. Then we added NaOAc to

precipitate the RNA fragments; in this way, Na^+ interacts with PO^{3-}. Then, we added isopropanol to prevent dissolubility of RNA by allowing Na^+ interaction. While the RNA molecule is soluble in the water due to its anionic structure, it is not soluble in isopropanol. After cleaning with cold ethanol, we incubated the RNA pool with CadB. Oligo: CadB ratio was arranged according to **Table 2.6**. We measured the concentration of the RNA pool via BioDrop µLite, and it was 2.64 µg /µL. Calculation of component volumes (RNA, CadB, 2X PBS, and H_2O) for each SELEX round is given in **Appendix E**. According to these volumes, we got results as below. Each round RNA and CadB volumes were reduced by %10 and %15, respectively. This decrease was done to select high-affinity binders. For high affinity, the incubation duration was reduced by 10 minutes each round, and the last three rounds were kept constant for 15 minutes. For the separation part, it is highly crucial to choose a suitable separation method for successful SELEX. We preferred the nitro-cellulose filter binding method, and this membrane allows collecting protein-oligo complexes so that unbound-oligos can be separated. We washed the membrane with urea to collect the oligos, which bound with protein. Because urea separates the protein-oligo complex from each other by breaking the hydrogen bonds between oligo and protein. Urea should not be kept for more than one hour; otherwise, RNA could be damaged. Now, we got the RNA molecules that could bind to CadB. After the partitioning part, RNA precipitation and RNA resuspension was followed. We converted these RNA oligos to cDNA to increase the number of RNA molecules that can bind to CadB. We started with the annealing part, and we used a reverse primer (Oligo 485). We converted RNA to DNA by reverse transcriptase (an RNA-dependent DNA polymerase). DNA amplification had carried out with 13-16 PCR cycles **(Appendix D)**. After cDNA production, we used a kit for PCR purification to discard unwanted things in the pool. We then converted the DNA to RNA again by IVT and continued with incubation. After completed eight rounds, we have obtained a pool enriched with RNAs that can bind CadB.

Table 3.3 Each round of RNA pool concentrations after IVT.

RNA Pool After IVT

Rounds	**RNA Pool (µg/mL)**
1	2644
2	2469
3	2162
4	2087
5	1437
6	1725
7	1368
8	1731

Table 3.4 The DNA pool concentrations before-after vacuum-centrifuge and their volumes after vacuum-centrifuge.

DNA pool (µg/mL)

ds-Oligo 487 pool (ug/mL) : 65			
Rounds	**Before vacuum-centrifuge**	**After vacuum-centrifuge**	**Volume (after vacuum-centrifuge) (µL)**
1	5	66	45
2	7	57	33
3	9	55	28
4	8	96	
5		22	65
6		39	45
7		58	55
8			

The vacuum centrifuge concentrates nucleotide samples from a liquid state into a dry or wet pellet state. After vacuum centrifuge, the DNA pool concentration was increased according to **Table 3.4**.

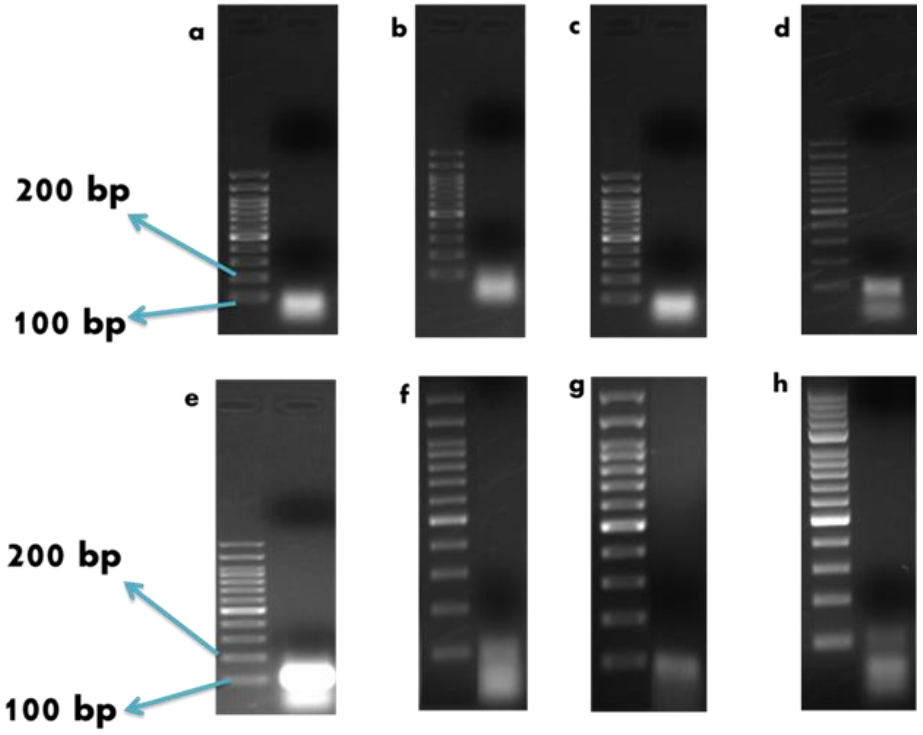

Figure 3.3. The PCR gels for 8 rounds SELEX against CadB. *a)* Round 1, *b)* Round 2, *c)* Round 3, *d)* Round 4, *e)* Round 5, *f)* Round 6, *g)* Round 7, and *h)* Round 8. The agarose gel band profile is in Appendix B. %1 of agarose gel was prepared in 40 mL of TAE (Appendix D). Each PCR cycle number was given in Appendix D.

Our beginning ssDNA pool was 100 nt. When we made PCR extension of the pool, it became 117 bp dsDNA. After each round, we converted RNA to DNA by reverse transcription; therefore, we performed agarose gels to make sure if we have DNA with 117 nt or not. As seen in **Figure 3.3** we successfully obtained DNA with 117 bp after every round of SELEX.

3.5 Identification of Aptamer Candidates

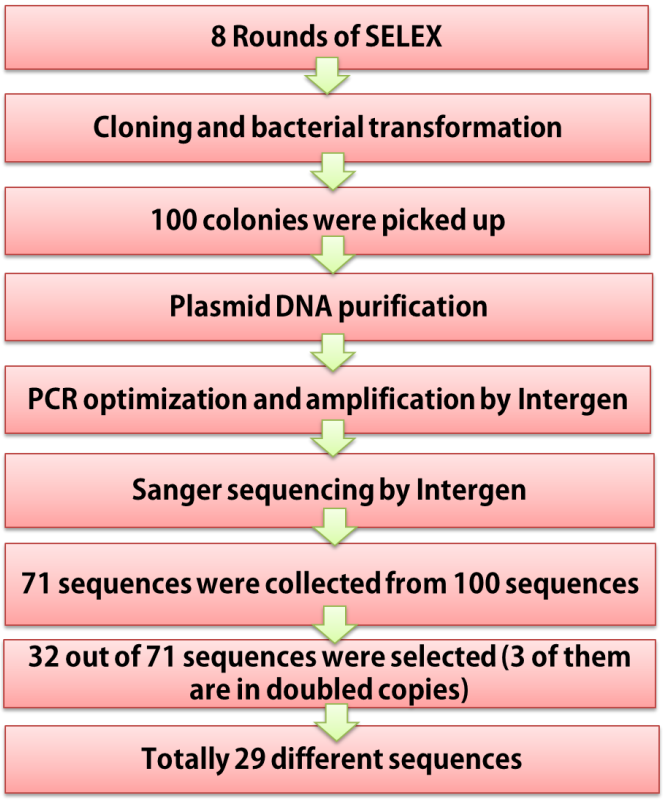

Figure 3.4. Post-SELEX methods and procedures.

The DNA pool from round 8 of SELEX had enriched oligos that potentially bind to CadB. Methods that we used after SELEX are summarized in **Figure 3.4**. For sequencing the pool, Sanger sequencing was carried out by Intergen (Ankara, Turkey). After our enriched pool was sequenced, we got 71 sequences out of 100 colonies. We then chose 32 sequences out of 71 for further analysis. The eliminated sequences had a low signal, had no insert, had altered constant regions, or had sequences shorter than 100 nt (random region together with two constant regions) as we did SELEX using 100 nt RNA pool. Additionally, some sequences included repeated nucleotides (just Uracils) with 10 and more of them in a row.

Generally, not all nucleotides must exist for direct interaction with the target or folding into the target-binding structural motif (Shangguan, Tang,

Mallikaratchy, Xiao, & Tan, 2007). These unnecessary nucleotides have a high probability of contributing to the destabilization of target-binding conformation by forming various secondary structures. After filtering sequences, we got 29 distinct sequences **(Table 3.6)** that could be an aptamer candidate (we call these proto-aptamers) for CadB. Three of those sequences were in double-copies: CadB30 and CadB53, CadB39 and CadB40, and CadB35 and CadB67. Thus, a total of 32 sequences were analyzed.

Table 3.5 Constant regions of selected aptamer sequences.

Constant Region	Sequence
5'	GGGAGACAAGAAUAAACGCUCAA
3'	UUCGACAGGAGGCUCACAACAGGC

Table 3.6 29 aptamer sequences selected after eight rounds of SELEX against CadB. Only the random regions (~53 nt) of the sequences are listed. Aptamer names sharing the same highlight color share the same sequence.

Name	Sequence (random region) 5'→3'
CadB2	UUUCCUUUUCUCUUUUCCAUUUUCUUUCCUUUGUGGCAUUUUAGUACUUUUA
CadB7	CUUUCUUCCAUUUCUUUUCUUACCACUCUUAUUUUCCAACACCUUUGUGCUUC
CadB8	UUCCUGUUCUUUCCUUUUAUUUUUUGUUUUUGUGAUU
CadB17	CGUUUGUGAUGCCUCUUGUUUAUUUUAUUUGUGUUUUUUAUAUUGGGAUUUUA
CadB20	UCUUUUCUUUCCCUUUAUUAGUUGCACUCACCAUUUUCUAUUUCCCUUGUGAC
CadB22	CCUUAAUUGUUCUCUACUUUUACAACUUUUGGCUU
CadB28	ACCGUUAUUGUUCUCCUUCCUUCUUGUUCUUUGUAUUCCUUGCCUUGUGUUUC
CadB30*	UUUUCUAAUCUUCUUUUUUCUUUCAGGCUUGU
CadB31	UCUUUAUUCUAUUUCUCUUUUUCCCUCUUUUUUCAUGUUUCCUUGUGGUGCU
CadB32	UUUUUCCUUCCUUUUUUUCUUAUCAUUUUUCU
CadB35*	CUUUCUUCCAUUUCUUUUCUUACCAUUCUUAUUUUCCAACACCUUUGUGCUUC
CadB36	CUCCUCUUCCAUUUCUUUUCUUACCAUUCUUAUUUUCCAACACCUUUGUGCUUC
CadB37	CCUCAUAUCAACAAUUAUUAACACUUUUUUAAUUAUACUUUAUAACAUAUUUA
CadB39*	AUUCCUACUUUAUUACUCUUAAUACCAUUUAUUUUCUUCUCUUUUAUCUCUUUUU

Table 3.6 (Cont'd)

CadB40*	Same with CadB39
CadB41	UUUCUUCUUCUUUUCUAUUCCUAUCUACCAUAAUCCUUC UUUCUAACCUUCUU
CadB43	CCUUGAUUUUCCAAUUCAUCAUUUUUUCUAUUU
CadB44	UUAUCUCUUUCUUCUUAUUUUUCUUUAUUUUUUCC
CadB53*	Same with CadB30
CadB54	CUCUUGUUUUCGUUGUUAUCCACAUUUUCAUCUAGCGUU CUUUUUAUGUUUA
CadB59	CUAAUCUUUUUUCUCUCUUUUCUUUUCCUUUUU
CadB60	UUUAUUCAUUUUUUAUAAUUUUUAUUUAAUAU
CadB67*	Same with CadB35
CadB68	UCUCGAUUUAAGCCUCCAACUAUUUAUUGCUUUGCAACU UCGUUCUUGUUGCU
CadB72	UAUUCUUUCAUUCGAUGUUCUUUCCCUUCUUUUUUU
CadB73	UUUCGAUUCAUUUUCUUAUUUUCUUUUACCCUUCUA
CadB78	UUUUGUCAUUAUUUUUUCGGUCUAUCCUGUCUUUUUUUU AUCGCAUUUUAUCCUC
CadB84	ACUAUUUGUUGAGCCUCACACAUUAUAAUUUACAUUUUU UUGAAUGCCUUGCA
CadB85	UUCUUCUCUUUCUUUUUCUUUUUAACCUAUUUCUCUCUA ACUCA
CadB88	UUCCUGCUUCCUUAUUUUAAAUAUUAGUGCGAGCUUUUU GAUCCUGUUCAGUU

Table 3.6 (Cont')

CadB97	CUUCCUUUUUUCAUUUCUCUUAGAUUUUUUAUU
CadB99	CGAUUGUGAUGCCUCUUUUUUAUUUUAUUUGUGUUGUUUAUAUUGGGAUUUUA

Both RNAfold and KineFold algorithms help to predict the near-native secondary structures of RNA aptamers. The secondary structure prediction has a critical role for binding motif identification in the whole structure. As mentioned earlier, these two algorithms are capable of estimating the secondary structure based on different perspectives (for example, KineFold allows the pseudoknots while RNAfold can predict G-quadruplex). Because these two algorithms are complementary to each other in order to assess the secondary structures, thus we can use both.

Table 3.7 The MFE values prediction for abundant sequences by RNAfold and KineFold serves.

Name	RNAfold (kcal/mol)	KineFold (kcal/mol)
CadB30	-12.30	-12.50
CadB35	-19.47	-18.3
CadB39	-8.87	-10.6

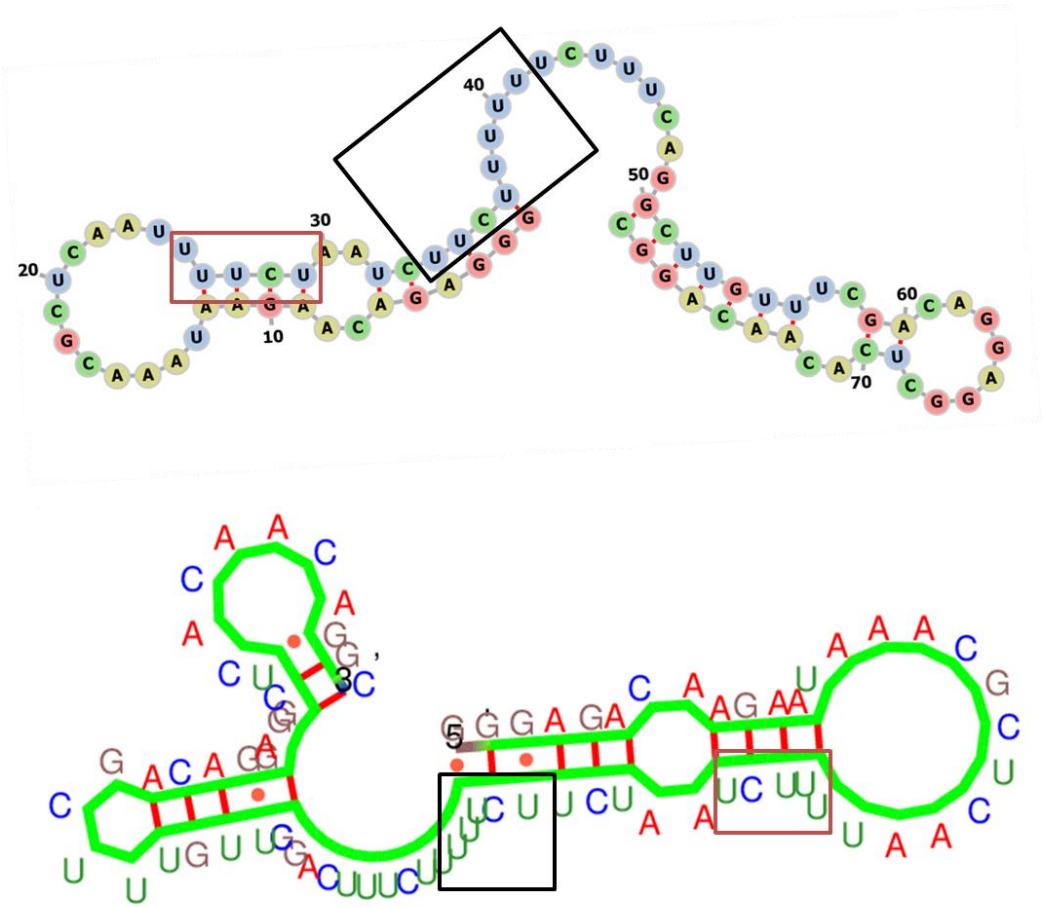

Figure 3.5. CadB30 2D secondary prediction by RNAfold (above) and KineFold (below).

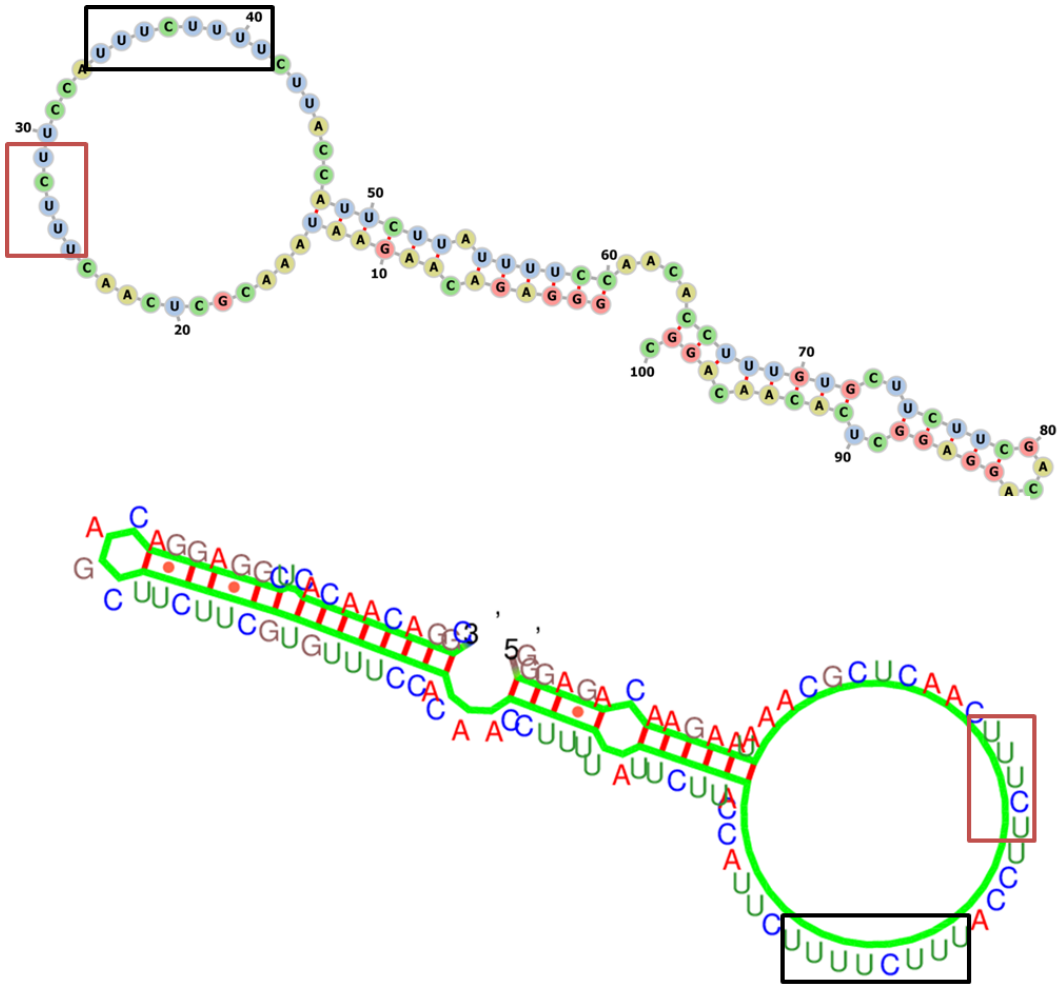

Figure 3.6. CadB35 2D secondary prediction by RNAfold (above) and KineFold (below).

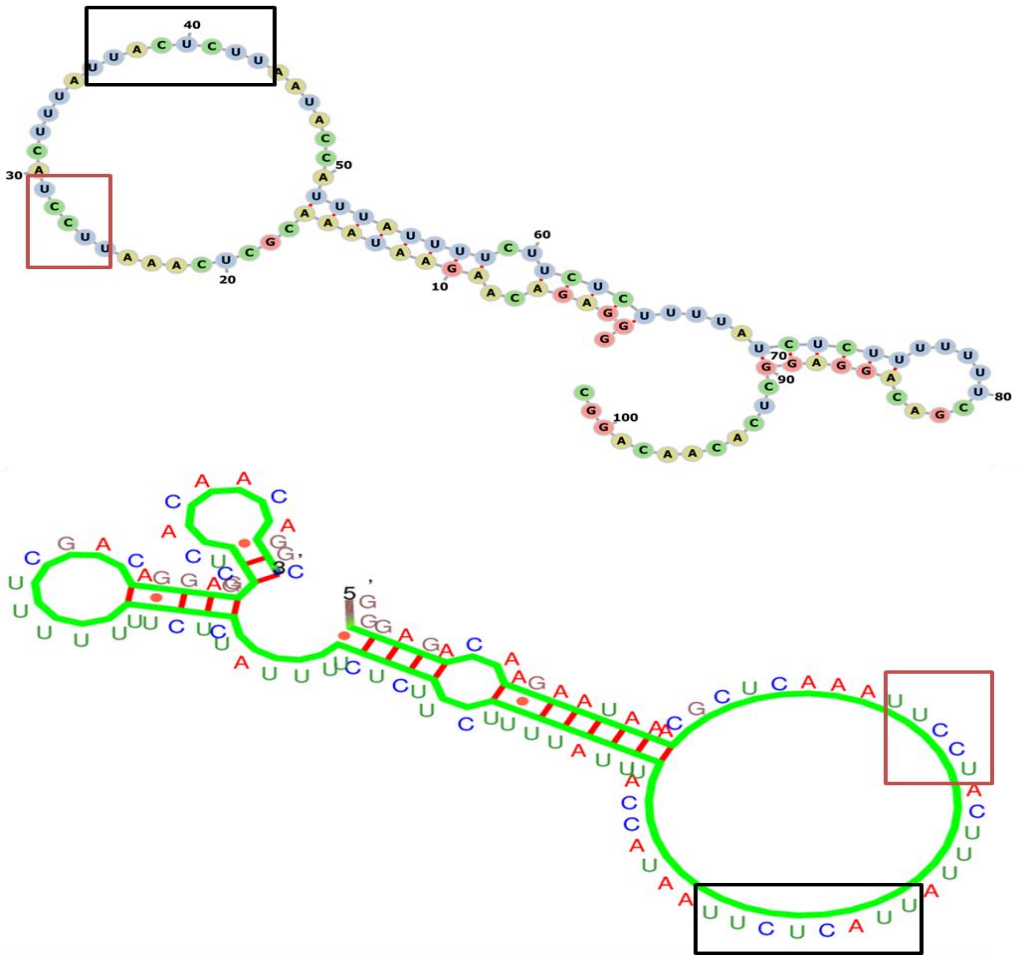

Figure 3.7. CadB39 2D secondary prediction by RNAfold (above) and KineFold (below).

```
cadb39      GGGAGACAAGAAUAAACGCUCAAAUUCCUACUUUAUUACUCUUAAUACCAUUUAUUUUCU    60
cadb30      GGGAGACAAGAAUAAACGCUCAAUUUUCUAAU--CUUCUUUUU-----------------    41
cadb35      GGGAGACAAGAAUAAACGCUCAACUUUCUUCC--AUUUCUUUUCUUACCAUUCUUAU---    55
********************** ** **      **  * **
Consensus sequences:               UUYCU      UUHYUYUU

cadb39      UCUCUUUUAUCUCU---UUUUUUCGACAGGAGGCUCACAACAGGC102
cadb30      --UCUUUCAGGCU-----UGUUUCGACAGGAGGCUCACAACAGGC 79
cadb35      UUUCCAACACCUUUGUGCUUCUUCGACAGGAGGCUCACAACAGGC100
**    *         *  ************************
```

Figure 3.8. The multiple sequence alignment result of three abundant sequences (CadB30, CadB35, and CadB39) by Clustal Omega. Motifs are shown by red and black-bold letters, and the consensus sequences are highlighted with yellow.

Binding motif identification is an important step for aptamer applications such as drug design or aptamer-based biosensors developments. Determining binding motifs can be achieved by comparing the predicted secondary structure of the aptamer candidates, assessing conserved motif sequences and overall percent homologies among the candidate sequences. In other words, looking at secondary structures enhances the efficiency of finding binding motifs compared to mere primary sequence comparisons.

When we look at the sequences in **Table 3.6**, we can see that three of the sequences are repeated, which means that our SELEX has potentially enriched these sequences for target binding. According to multiple sequence alignment of the three abundant sequences, we found two locations where seems the sequence was conserved. These locations are indicated in the alignment above with the consensus sequence for each location (the motifs are shown as red and black in the alignment). Due to their conservation, these locations may constitute aptamer binding motifs and thus, we define both of them to be potentially as such. However, it can be hypothesized that the smaller motif may be a stronger binding domain than the larger one as its nucleotides are more defined and tolerate less variation. However, interestingly, the smaller (and more defined) conserved motif is in fact a part of the larger (and less defined) motif. According to CadB35 and CadB39 structures, the two potential binding motifs are located on a relatively

large loop in a stem-loop structure (**Figure 3.6** and **Figure 3.7**). On the other hand, for CadB30, the smaller motif is located at the connection of the stem and loop substructures that form the hairpin **(Figure 3.5)** and the larger one is located along the stem and an open-loop structure. This may further support the possibility that the smaller and more defined binding motif is the stronger one.

The homology percentage between CadB30 and CadB35, CadB30 and CadB39, and CadB35 and CadB39 were 76.62%, 84.81%, and 72.00%, respectively, as shown by the percent identity matrix in the result summary of the Clustal Omega alignment. Both the abundance and the homology results of these three proto-aptamers support the overall sequence and structure conservation observed, and also they support their SELEX enrichment and the occurrence of binding motifs.

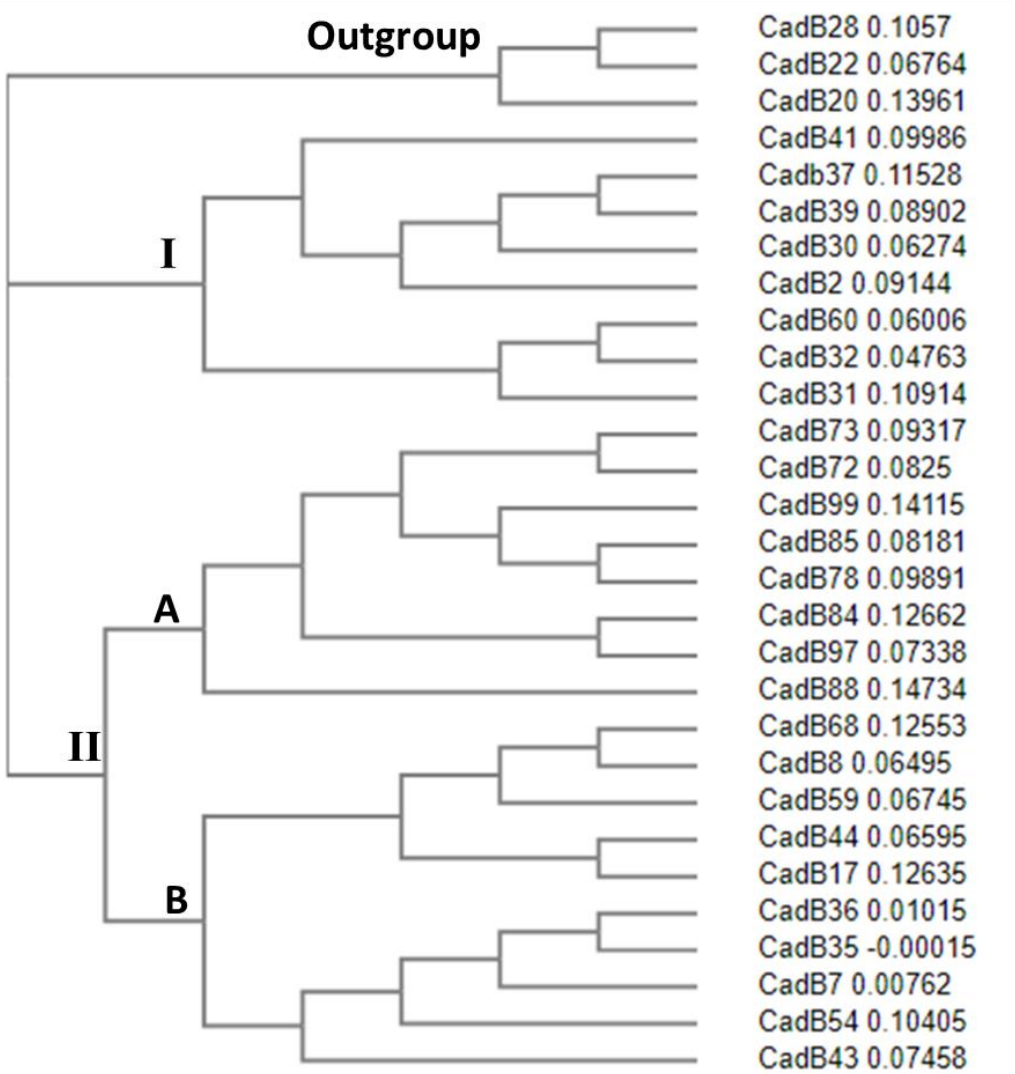

Figure 3.9. The phylogenetic tree of 29 aptamer candidate sequences.

As mentioned earlier, similar secondary structures from the same aptamer family should commonly bind the same target. Therefore, their structures are expected to have highly homologous primary sequences. Indeed, this was seen from the percent identity of CadB30, CadB35, and CadB39. The phylogenetic tree in **Figure 3.9** was built for the 29 aptamer candidate sequences based on their sequence similarity and can be used to estimate the evolutionary relationship between its nucleic acid sequences for a comparative study. Here, we grouped the

sequences into families according to their clustering in the tree. To validate the assumption that proto-aptamers in a given family are likely to conserve a common secondary structure (thereby, helping us find more candidate aptamers with similar properties), we randomly chose two sequences one of which is phylogenetically close to the abundant sequences (CadB30 and CadB39 in particular) and the other one distant from them. According to the phylogenetic tree in **Figure 3.9**, CadB41 is a closely related candidate (found in the same family; I), while CadB85 is a distantly related candidate (found in a different family; IIA). The percent homologies of CadB30:CadB41 and CadB39:CadB41 are 82.05% and 81.32%, respectively, while those for CadB30:CadB85 and CadB39:CadB85 are, 52.35%, and 56.76%, respectively. Certainly, a significant homology difference is seen between candidates from the same family and a different family and we expect this difference to show in the secondary structures as well. Indeed, when looking at the predicted structures of the randomly chosen sequences (but still referenced to the abundant ones) we see that the difference between CadB41 and CadB85 in their homology to the abundant sequences is carried to the level of the secondary structures. Although each of CadB41 and CadB85 conserve a sequence that fits the less defined consensus binding motif, for CadB41 the motif is found in a hairpin substructure that highly resembles that of CadB30. Furthermore, its overall secondary structure resembles those of the abundant sequences (including CadB35). On the other hand, the motif in CadB85 is found in an internal loop and stem (RNAfold) or in a bulged loop and stem (KineFold), localizations that had not been observed in any of the abundant proto-aptamers.

Although we have shown by two example sequences (CadB41 and CadB85) that sequences that are in the same and in different phylogenetic families can, respectively, have the same and different structures and binding motifs. We do not expect to see this trend especially when the minimum percent similarity between any pair of sequences is still considered to be high. For example, although, CadB35 is located in a family (family IIB) different from that of CadB30 and CadB39 (family I), we have already seen its high similarity with CadB30 and CadB39 at both the primary and secondary structure levels in addition to being one of the three sequences isolated twice after cloning.

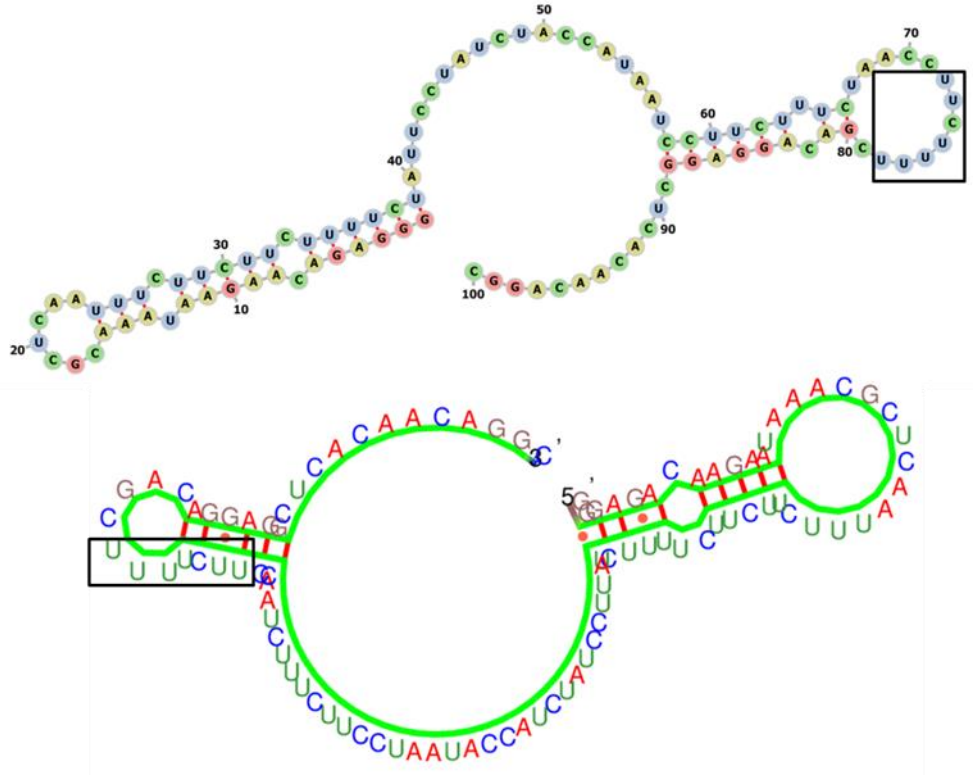

Figure 3.10. CadB41 structures. Above is RNAfold and below is KineFold.

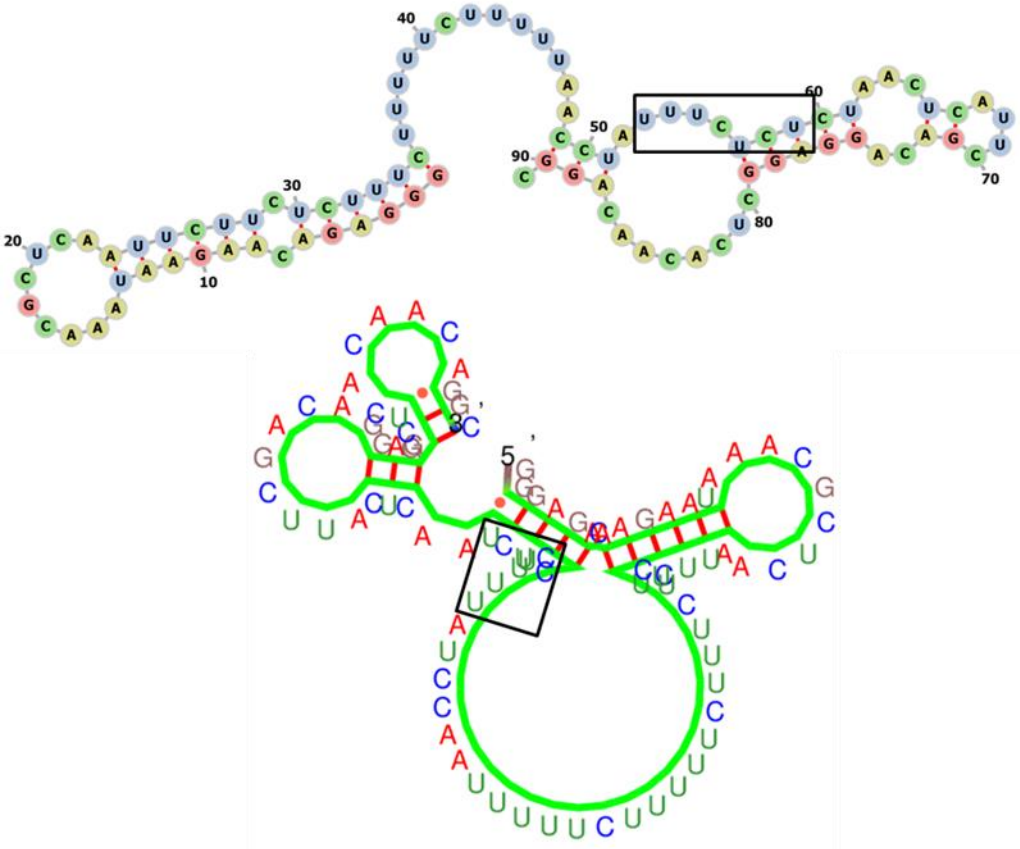

Figure 3.11. CadB85 structure. Above is RNAfold and below is KineFold.

CHAPTER 4

CONCLUSION

In this study, we successfully applied the protein-SELEX with eight rounds for CadB targeting (as a model protein for MPs) in a membrane-mimicking environment. As a bacterial MP, CadB utilizes cadaverine/lysine antiporter activity in *E.coli* under acidic conditions to survive. According to studies that have done at Bern University, we followed the same detergent for solubilizing and purification methods. The recombinant CadB was solubilized in a buffer including 1.5 % (w/v) DDM and purified.

We started SELEX with the ssDNA pool extension. We converted this pool to RNA using an *in vitro* transcription kit, including a 2'F Py NTP mix for aptamer improvement against nuclease resistance. Incubation time was decreased each round to increase high-affinity binders because only high-affinity binders can bind the target with fast interaction in a short time. PCR cycles were arranged based on cDNA concentration.

After sequencing, we chose 29 different proto-aptamer sequences, and we observed 3 of them were in doubled copies. Then, we determined potential binding motifs in these abundant ones (CadB30, CadB35, and CadB39) by analyzing multiple sequence alignment (determining their conserved sequence) and compared our aptamer candidates based on their predicted secondary structures by RNAfold and KineFold webservers.

Determining the binding motif can be helpful for therapeutic and diagnostic developments. Additionally, cutting off non-essential nucleotides from the aptamer may increase the binding affinity and decrease chemical synthesis costs. Besides, small-sized aptamers have the potential to use together with nanostructures and then can be easily encapsulated for drug design. Hence, structural estimation,

binding motif analysis, and homology studies are invaluable procedures after aptamer selection.

We observed for CadB35 and CadB39 potential binding motifs placed on the loops. At the same time, for CadB30, it is located on the stem-loop region of the identified structure. The 29 distinct sequences were classified into different families based on their sequence homologies. In addition, we randomly picked another aptamer candidate (CadB41) from the phylogenetic tree and base homology data, which is near to CadB39 and CadB30, to prove its structural similarity with our abundant ones. Like CadB30 and CadB39, the potent binding motif was found on the loop (a hairpin structure) of CadB41.

For future work, the capability of binding to CadB would be achieved by binding assay studies. After their improvement and optimization, these aptamer candidates would be used in drug development by stimulating or inhibiting the CadB function (against *E.coli*, instead of using any antibiotic) or diagnostic applications by detecting CadB (*E.coli* detection). Herein, in order for aptamers to pass through the outer membrane to reach the inner membrane, they can be conjugated. As mention earlier, aptamer conjugation allows cell internalization.

This study also set an example for mammalian MP targeting. One-third of the drugs on the market target MPs. Because any structural defect in MPs may lead to severe diseases such as cancers, neurological disorders, and cardiovascular problems. Besides, MPs are overexpressed on the surface of cancer cells, especially in breast and prostate cancers. Accumulation of MPs on the surface allows MPs to use as a marker in cancer diagnosis. Since they are embedded in the lipid bilayer with a low abundance level, they still remain a challenge for MP targeting. Creating an amphipathic nature for MPs using a detergent can overcome this challenge. For both therapeutic and diagnostic purposes, after MP solubilized in a suitable detergent, the protein-SELEX can provide great convenience during any MP targeting.

REFERENCES

Ababneh, N., Alshaer, W., Allozi, O., Mahafzah, A., El-Khateeb, M., Hillaireau, H., … Ismail, S. (2013). In vitro selection of modified RNA aptamers against CD44 cancer stem cell marker. *Nucleic Acid Therapeutics*, *23*(6), 401–407. https://doi.org/10.1089/nat.2013.0423

Afanasyeva, A., Nagao, C., & Mizuguchi, K. (2019). Prediction of the secondary structure of short DNA aptamers. *Biophysics and Physicobiology*, *16*(0), 287–294. https://doi.org/10.2142/biophysico.16.0_287

Alberts, B., Johnson, A., Lewis, J., Raff, M., Roberts, K., & Walter, P. (2002). Carrier Proteins and Active Membrane Transport.

Allen, K. N., Entova, S., Ray, L. C., & Imperiali, B. (2019). Monotopic Membrane Proteins Join the Fold. *Trends in Biochemical Sciences*. Elsevier Ltd. https://doi.org/10.1016/j.tibs.2018.09.013

Andrews, R. J., & Moss, W. N. (2019). Computational approaches for the discovery of splicing regulatory RNA structures. *Biochimica et Biophysica Acta - Gene Regulatory Mechanisms*. Elsevier B.V. https://doi.org/10.1016/j.bbagrm.2019.04.007

Aquino, P., Honda, B., Jaini, S., Lyubetskaya, A., Hosur, K., Chiu, J. G., … Galagan, J. E. (2017). Coordinated regulation of acid resistance in Escherichia coli. *BMC Systems Biology*, *11*(1). https://doi.org/10.1186/s12918-016-0376-y

Arinaminpathy, Y., Khurana, E., Engelman, D. M., & Gerstein, M. B. (2009). Computational analysis of membrane proteins: the largest class of drug targets. *Drug Discovery Today*. https://doi.org/10.1016/j.drudis.2009.08.006

Avci-Adali, M., Metzger, M., Perle, N., Ziemer, G., & Wendel, H. P. (2010). Pitfalls of cell-systematic evolution of ligands by exponential enrichment (SELEX): Existing dead cells during in vitro selection anticipate the enrichment of specific aptamers. *Oligonucleotides*, *20*(6), 317–323. https://doi.org/10.1089/oli.2010.0253

Bagal, S. K., Brown, A. D., Cox, P. J., Omoto, K., Owen, R. M., Pryde, D. C., … Swain, N. A. (2013). Ion channels as therapeutic targets: A drug discovery perspective. *Journal of Medicinal Chemistry*. https://doi.org/10.1021/jm3011433

Balamurugan, S., Obubuafo, A., Soper, S. A., & Spivak, D. A. (2008). Surface immobilization methods for aptamer diagnostic applications. *Analytical and Bioanalytical Chemistry*, *390*(4), 1009–1021. https://doi.org/10.1007/s00216-007-1587-2

Bates, P. J., Laber, D. A., Miller, D. M., Thomas, S. D., & Trent, J. O. (2009).

Discovery and development of the G-rich oligonucleotide AS1411 as a novel treatment for cancer. *Experimental and Molecular Pathology*. https://doi.org/10.1016/j.yexmp.2009.01.004

Bates, P. J., Reyes-Reyes, E. M., Malik, M. T., Murphy, E. M., O'Toole, M. G., & Trent, J. O. (2017). G-quadruplex oligonucleotide AS1411 as a cancer-targeting agent: Uses and mechanisms. *Biochimica et Biophysica Acta - General Subjects*. Elsevier B.V. https://doi.org/10.1016/j.bbagen.2016.12.015

Batool, S., Bhandari, S., George, S., Okeoma, P., Van, N., Zümrüt, H. E., & Mallikaratchy, P. (2017). Engineered aptamers to probe molecular interactions on the cell surface. *Biomedicines*. MDPI AG. https://doi.org/10.3390/biomedicines5030054

Bellecave, P., Andreola, M. L., Ventura, M., Tarrago-Litvak, L., Litvak, S., & Astier-Gin, T. (2003). Selection of DNA Aptamers That Bind the RNA-Dependent RNA Polymerase of Hepatitis C Virus and Inhibit Viral RNA Synthesis In Vitro. *Oligonucleotides*, *13*(6), 455–463. https://doi.org/10.1089/154545703322860771

Berg, K., Lange, T., Mittelberger, F., Schumacher, U., & Hahn, U. (2016). Selection and Characterization of an α6β4 Integrin blocking DNA Aptamer. *Molecular Therapy - Nucleic Acids*, *5*, e294. https://doi.org/10.1038/mtna.2016.10

Bing, T., Shangguan, D., & Wang, Y. (2015). Facile discovery of cell-surface protein targets of cancer cell aptamers. *Molecular and Cellular Proteomics*, *14*(10), 2692–2700. https://doi.org/10.1074/mcp.M115.051243

Bing, T., Yang, X., Mei, H., Cao, Z., & Shangguan, D. (2010). Conservative secondary structure motif of streptavidin-binding aptamers generated by different laboratories. *Bioorganic and Medicinal Chemistry*, *18*(5), 1798–1805. https://doi.org/10.1016/j.bmc.2010.01.054

Blank, M., Weinschenk, T., Priemer, M., & Schluesener, H. (2001). Systematic evolution of a DNA aptamer binding to rat brain tumor microvessels: Selective targeting of endothelial regulatory protein pigpen. *Journal of Biological Chemistry*, *276*(19), 16464–16468. https://doi.org/10.1074/jbc.M100347200

Boltz, A., Piater, B., Toleikis, L., Guenther, R., Kolmar, H., & Hock, B. (2011). Bi-specific aptamers mediating tumor cell lysis. *Journal of Biological Chemistry*, *286*(24), 21896–21905. https://doi.org/10.1074/jbc.M111.238261

Bradford, M. M. (1976). A rapid and sensitive method for the quantitation of microgram quantities of protein utilizing the principle of protein-dye binding. *Analytical Biochemistry*, *72*(1–2), 248–254. https://doi.org/10.1016/0003-2697(76)90527-3

Bruno, J. G., Carrillo, M. P., Phillips, T., & Andrews, C. J. (2010). A novel screening method for competitive FRET-aptamers applied to E. coli assay development. *Journal of Fluorescence*, *20*(6), 1211–1223. https://doi.org/10.1007/s10895-010-0670-9

Bruno, J. G., & Kiel, J. L. (1999). In vitro selection of DNA aptamers to anthrax spores with electrochemiluminescence detection. *Biosensors and Bioelectronics*. https://doi.org/10.1016/S0956-5663(99)00028-7

Cai, S., Yan, J., Xiong, H., Liu, Y., Peng, D., & Liu, Z. (2018). Investigations on the interface of nucleic acid aptamers and binding targets. *Analyst*. Royal Society of Chemistry. https://doi.org/10.1039/c8an01467a

Camorani, S., Esposito, C. L., Rienzo, A., Catuogno, S., Iaboni, M., Condorelli, G., … Cerchia, L. (2014). Inhibition of receptor signaling and of glioblastoma-derived tumor growth by a novel PDGFRβ aptamer. *Molecular Therapy*, *22*(4), 828–841. https://doi.org/10.1038/mt.2013.300

Capriotti, E., & Marti-Renom, M. A. (2008). *Computational RNA Structure Prediction*. *Current Bioinformatics* (Vol. 3).

Casares, D., Escribá, P. V., & Rosselló, C. A. (2019). Membrane lipid composition: Effect on membrane and organelle structure, function and compartmentalization and therapeutic avenues. *International Journal of Molecular Sciences*, *20*(9). https://doi.org/10.3390/ijms20092167

Cerchia, L., Esposito, C. L., Camorani, S., Rienzo, A., Stasio, L., Insabato, L., … De Franciscis, V. (2012). Targeting Axl with an high-affinity inhibitory aptamer. *Molecular Therapy*, *20*(12), 2291–2303. https://doi.org/10.1038/mt.2012.163

Chai, A. B., Leung, G. K. F., Callaghan, R., & Gelissen, I. C. (2020). P-glycoprotein: a role in the export of amyloid-β in Alzheimer's disease? *FEBS Journal*, *287*(4), 612–625. https://doi.org/10.1111/febs.15148

Chandola, C., & Neerathilingam, M. (2020). Aptamers for Targeted Delivery: Current Challenges and Future Opportunities. In *Role of Novel Drug Delivery Vehicles in Nanobiomedicine*. IntechOpen. https://doi.org/10.5772/intechopen.84217

Chauveau, F., Aissouni, Y., Hamm, J., Boutin, H., Libri, D., Ducongé, F., & Tavitian, B. (2007). Binding of an aptamer to the N-terminal fragment of VCAM-1. *Bioorganic and Medicinal Chemistry Letters*, *17*(22), 6119–6122. https://doi.org/10.1016/j.bmcl.2007.09.046

Chen, C. H. B., Chernis, G. A., Hoang, V. Q., & Landgraf, R. (2003). Inhibition of heregulin signaling by an aptamer that preferentially binds to the oligomeric form of human epidermal growth factor receptor-3. *Proceedings of the National Academy of Sciences of the United States of America*, *100*(16), 9226–9231. https://doi.org/10.1073/pnas.1332660100

Chen, F., Hu, Y., Li, D., Chen, H., & Zhang, X.-L. (2009). CS-SELEX Generates High-Affinity ssDNA Aptamers as Molecular Probes for Hepatitis C Virus Envelope Glycoprotein E2. *PLoS ONE*, *4*(12), e8142. https://doi.org/10.1371/journal.pone.0008142

Chen, I., & Lui, F. (2019). *Physiology, Active Transport*. *StatPearls*. StatPearls Publishing.

Chen, M., Yu, Y., Jiang, F., Zhou, J., Li, Y., Liang, C., … Zhang, G. (2016). Development of cell-SELEX technology and its application in cancer diagnosis and therapy. *International Journal of Molecular Sciences*. https://doi.org/10.3390/ijms17122079

Cho, I., Jackson, M. R., & Swift, J. (2016). Roles of Cross-Membrane Transport and Signaling in the Maintenance of Cellular Homeostasis. *Cellular and Molecular Bioengineering*, *9*(2), 234–246. https://doi.org/10.1007/s12195-016-0439-6

Cho, M., Xiao, Y., Nie, J., Stewart, R., Csordas, A. T., Oh, S. S., … Soh, H. T. (2010). Quantitative selection of DNA aptamers through microfluidic selection and high-throughput sequencing. *Proceedings of the National Academy of Sciences of the United States of America*, *107*(35), 15373–15378. https://doi.org/10.1073/pnas.1009331107

Chu, T. C., Marks, J. W., Lavery, L. A., Faulkner, S., Rosenblum, M. G., Ellington, A. D., & Levy, M. (2006). Aptamer:toxin conjugates that specifically target prostate tumor cells. *Cancer Research*, *66*(12), 5989–5992. https://doi.org/10.1158/0008-5472.CAN-05-4583

Cibiel, A., Dupont, D. M., & Ducongé, F. (2011). Methods To Identify Aptamers against Cell Surface Biomarkers. *Pharmaceuticals*, *4*, 1216–1235. https://doi.org/10.3390/ph4091216

Daniels, D. A., Sohal, A. K., Rees, S., & Grisshammer, R. (2002). Generation of RNA aptamers to the G-protein-coupled receptor for neurotensin, nts-1. *Analytical Biochemistry*, *305*(2), 214–226. https://doi.org/10.1006/abio.2002.5663

Dastjerdi, K., Tabar, G. H., Dehghani, H., & Haghparast, A. (2011). Generation of an enriched pool of DNA aptamers for an HER2-overexpressing cell line selected by Cell SELEX. *Biotechnology and Applied Biochemistry*, *58*(4), 226–230. https://doi.org/10.1002/bab.36

Dean, M. (2005). The genetics of ATP-binding cassette transporters. *Methods in Enzymology*. Academic Press Inc. https://doi.org/10.1016/S0076-6879(05)00024-8

Dollins, C. M., Nair, S., Boczkowski, D., Lee, J., Layzer, J. M., Gilboa, E., & Sullenger, B. A. (2008). Assembling OX40 Aptamers on a Molecular Scaffold to Create a Receptor-Activating Aptamer. *Chemistry and Biology*, *15*(7), 675–682. https://doi.org/10.1016/j.chembiol.2008.05.016

Dua, P., Kang, H. S., Hong, S. M., Tsao, M. S., Kim, S., & Lee, D. K. (2013). Alkaline phosphatase ALPPL-2 is a novel pancreatic carcinoma-associated protein. *Cancer Research*, *73*(6), 1934–1945. https://doi.org/10.1158/0008-5472.CAN-12-3682

Ellington, A. D., & Szostak, J. W. (1990). In vitro selection of RNA molecules that bind specific ligands. *Nature*. https://doi.org/10.1038/346818a0

Ellington, A. D., & Szostak, J. W. (1992). Selection in vitro of single-stranded DNA molecules that fold into specific ligand-binding structures. *Nature*, *355*(6363), 850–852. https://doi.org/10.1038/355850a0

Esposito, C. L., Passaro, D., Longobardo, I., Condorelli, G., Marotta, P., Affuso, A., … Cerchia, L. (2011). A neutralizing rna aptamer against egfr causes selective apoptotic cell death. *PLoS ONE*, *6*(9). https://doi.org/10.1371/journal.pone.0024071

Fairman, J. W., Noinaj, N., & Buchanan, S. K. (2012). The structural biology of β-barrel membrane proteins: a summary of recent reports. https://doi.org/10.1016/j.sbi.2011.05.005

Fang, X., & Tan, W. (2010). Aptamers generated from cell-SELEX for molecular medicine: A chemical biology approach. *Accounts of Chemical Research*, *43*(1), 48–57. https://doi.org/10.1021/ar900101s

Faryammanesh, R., Lange, T., Magbanua, E., Haas, S., Meyer, C., Wicklein, D., … Hahn, U. (2014). SDA, a DNA aptamer inhibiting E- And P-Selectin mediated adhesion of cancer and leukemia cells, the first and pivotal step in transendothelial migration during metastasis formation. *PLoS ONE*, *9*(4). https://doi.org/10.1371/journal.pone.0093173

Fernandes, C. F. C., Pereira, S. dos S., Luiz, M. B., Zuliani, J. P., Furtado, G. P., & Stabeli, R. G. (2017). Camelid single-domain antibodies as an alternative to overcome challenges related to the prevention, detection, and control of neglected tropical diseases. *Frontiers in Immunology*. Frontiers Media S.A. https://doi.org/10.3389/fimmu.2017.00653

Ferreira, C. S. M., Papamichael, K., Guilbault, G., Schwarzacher, T., Gariepy, J., & Missailidis, S. (2008). DNA aptamers against the MUC1 tumour marker:

Design of aptamer-antibody sandwich ELISA for the early diagnosis of epithelial tumours. *Analytical and Bioanalytical Chemistry*, *390*(4), 1039–1050. https://doi.org/10.1007/s00216-007-1470-1

Flint, M., Maidens, C., Loomis-Price, L. D., Shotton, C., Dubuisson, J., Monk, P., … McKeating, J. A. (1999). Characterization of Hepatitis C Virus E2 Glycoprotein Interaction with a Putative Cellular Receptor, CD81. *Journal of Virology*, *73*(8), 6235–6244. https://doi.org/10.1128/jvi.73.8.6235-6244.1999

Freyhult, E., Gustafsson, M. G., & Strömbergsson, H. (2015). A machine learning approach to explain drug selectivity to soluble and membrane protein targets. *Molecular Informatics*, *34*(1), 44–52. https://doi.org/10.1002/minf.201400121

Gong, Q., Wang, J., Ahmad, K. M., Csordas, A. T., Zhou, J., Nie, J., … Soh, H. T. (2012). Selection strategy to generate aptamer pairs that bind to distinct sites on protein targets. *Analytical Chemistry*, *84*(12), 5365–5371. https://doi.org/10.1021/ac300873p

Gottesman, M. M., & Ambudkar, S. V. (2001). Overview: ABC transporters and human disease. In *Journal of Bioenergetics and Biomembranes* (Vol. 33, pp. 453–458). https://doi.org/10.1023/A:1012866803188

Gouaux, E., & MacKinnon, R. (2005). Principles of selective ion transport in channels and pumps. *Science*. American Association for the Advancement of Science. https://doi.org/10.1126/science.1113666

Gwozdz, T., & Dorey, K. (2017). Western Blot. In *Basic Science Methods for Clinical Researchers* (pp. 99–117). Elsevier Inc. https://doi.org/10.1016/B978-0-12-803077-6.00006-0

Hartz, A. M. S., & Bauer, B. (2011). ABC Transporters in the CNS – An Inventory, 656–673.

He, F. (2011). Bradford Protein Assay. *BIO-PROTOCOL*, *1*(6). https://doi.org/10.21769/bioprotoc.45

He, Y., Wang, K., & Yan, N. (2014). The recombinant expression systems for structure determination of eukaryotic membrane proteins. *Protein & Cell*. Springer. https://doi.org/10.1007/s13238-014-0086-4

Hediger, M. A., Clémençon, B., Burrier, R. E., & Bruford, E. A. (2013). The ABCs of membrane transporters in health and disease (SLC series): Introduction. *Molecular Aspects of Medicine*. https://doi.org/10.1016/j.mam.2012.12.009

Heidi Ledford. (2011). Engineered antibodies cross blood-brain barrier, pp. 64–75. https://doi.org/doi:10.1038/news.2011.319

Hicke, B. J., Marion, C., Chang, Y. F., Gould, T., Lynott, C. K., Parma, D., … Warren, S. (2001). Tenascin-C Aptamers Are Generated Using Tumor Cells and Purified Protein. *Journal of Biological Chemistry*, *276*(52), 48644–48654. https://doi.org/10.1074/jbc.M104651200

Hicke, B. J., Watson, S. R., Koenig, A., Lynott, C. K., Bargatze, R. F., Chang, Y. F., … Parma, D. (1996). DNA aptamers block L-selectin function in vivo: Inhibition of human lymphocyte trafficking in SCID mice. *Journal of Clinical Investigation*, *98*(12), 2688–2692. https://doi.org/10.1172/JCI119092

Ho Lee, C., Lee, S.-H., Hyun Kim, J., Noh, Y.-H., Noh, G.-J., & Lee, S.-W. (2015). Pharmacokinetics of a Cholesterol-conjugated Aptamer Against the Hepatitis C Virus (HCV) NS5B Protein. https://doi.org/10.1038/mtna.2015.30

Hofacker, I. L. (2003). Vienna RNA secondary structure server. *Nucleic Acids Research*, *31*(13), 3429–3431. https://doi.org/10.1093/nar/gkg599

Homann, M., & Göringer, H. U. (2001). Uptake and intracellular transport of RNA aptamers in African trypanosomes suggest therapeutic "Piggy-Back" approach. In *Bioorganic and Medicinal Chemistry*. https://doi.org/10.1016/S0968-0896(01)00032-3

Hu, Y., Duan, J., Cao, B., Zhang, L., Lu, X., Wang, F., … Yang, X. D. (2015). Selection of a novel DNA thioaptamer against HER2 structure. *Clinical and Translational Oncology*, *17*(8), 647–656. https://doi.org/10.1007/s12094-015-1292-0

Huang, X., Zhong, J., Ren, J., Wen, D., Zhao, W., & Huan, Y. (2019). A DNA aptamer recognizing MMP14 for in vivo and in vitro imaging identified by cell-SELEX. *Oncology Letters*, *18*(1), 265–274. https://doi.org/10.3892/ol.2019.10282

Huang, Y. Z., Hernandez, F. J., Gu, B., Stockdale, K. R., Nanapaneni, K., Scheetz, T. E., … McNamara, J. O. (2012). RNA aptamer-based functional ligands of the neurotrophin receptor, TrkB. *Molecular Pharmacology*, *82*(4), 623–635. https://doi.org/10.1124/mol.112.078220

Hybarger, G., Bynum, J., Williams, R. F., Valdes, J. J., & Chambers, J. P. (2006). A microfluidic SELEX prototype. *Analytical and Bioanalytical Chemistry*. Springer. https://doi.org/10.1007/s00216-005-0089-3

Iaboni, M., Fontanella, R., Rienzo, A., Capuozzo, M., Nuzzo, S., Santamaria, G., … Esposito, C. L. (2016). Targeting Insulin Receptor with a Novel Internalizing Aptamer. *Molecular Therapy - Nucleic Acids*, *5*, e365. https://doi.org/10.1038/mtna.2016.73

Ii, J. O. M., Sullenger, B., Gilboa, E., Ii, J. O. M., Kolonias, D., Pastor, F., … Gilboa, E. (2008). Multivalent 4-1BB binding aptamers costimulate CD8 + T cells and inhibit tumor growth in mice Find the latest version : Technical advance Multivalent 4-1BB binding aptamers costimulate CD8 + T cells and inhibit tumor growth in mice. *Journal of Clinical Investigation*, *118*(1), 376–386. https://doi.org/10.1172/JCI33365.376

Ilgü, H., Jeckelmann, J. M., Gachet, M. S., Boggavarapu, R., Ucurum, Z., Gertsch, J., & Fotiadis, D. (2014). Variation of the detergent-binding capacity and phospholipid content of membrane proteins when purified in different detergents. *Biophysical Journal*, *106*(8), 1660–1670. https://doi.org/10.1016/j.bpj.2014.02.024

Ilgu, M., Fazlioglu, R., Ozturk, M., Ozsurekci, Y., & Nilsen-Hamilton, M. (2019). Aptamers for Diagnostics with Applications for Infectious Diseases. *Recent Advances in Analytical Chemistry*, (April). https://doi.org/10.5772/intechopen.84867

Iwagawa, T., Ohuchi, S. P., Watanabe, S., & Nakamura, Y. (2012). Selection of RNA aptamers against mouse embryonic stem cells. *Biochimie*, *94*(1), 250–257.

Iwasa, J. W. M. (2016). Cell and Molucular Biology Concepts and Experiments. https://doi.org/10.1017/CBO9781107415324.004

Jacobi, N., Seeboeck, R., Hofmann, E., & Eger, A. (2017). ErbB Family Signalling: A Paradigm for Oncogene Addiction and Personalized Oncology. *Cancers*, *9*(12), 33. https://doi.org/10.3390/cancers9040033

Jenison, R. D., Gill, S. C., Pardi, A., & Polisky, B. (1994). High-resolution molecular discrimination by RNA. *Science*, *263*(5152), 1425–1429. https://doi.org/10.1126/science.7510417

Jung, K., Fabiani, F., Hoyer, E., & Jung, K. (2018). Bacterial transmembrane signalling systems and their engineering for biosensing.

Kalina, T., Fišer, K., Pérez-Andrés, M., Kužílková, D., Cuenca, M., Bartol, S. J. W., … van Zelm, M. C. (2019). CD maps—dynamic profiling of CD1–CD100 surface expression on human leukocyte and lymphocyte subsets. *Frontiers in Immunology*, *10*(OCT), 2434. https://doi.org/10.3389/fimmu.2019.02434

Kalra, P., Dhiman, A., Cho, W. C., Bruno, J. G., & Sharma, T. K. (2018). Simple methods and rational design for enhancing aptamer sensitivity and specificity. *Frontiers in Molecular Biosciences*, *5*(MAY), 41. https://doi.org/10.3389/fmolb.2018.00041

Kang, H. S., Huh, Y. M., Kim, S., & Lee, D.-K. (2009). *HER-2-targeting*. *RNA Aptamers Bull. Korean Chem. Soc* (Vol. 30).

Kanjee, U., & Houry, W. A. (2013). Mechanisms of Acid Resistance in Escherichia coli. https://doi.org/10.1146/annurev-micro-092412-155708

Kim, B. H., & Gadd, G. M. (2019). Membrane transport – nutrient uptake and protein excretion. In *Prokaryotic Metabolism and Physiology* (pp. 31–57). Cambridge University Press. https://doi.org/10.1017/9781316761625.003

Kim, J. W., Kim, E. Y., Kim, S. Y., Byun, S. K., Lee, D., Oh, K. J., … Bae, K. H. (2014). Identification of DNA aptamers toward epithelial cell adhesion molecule via Cell-SELEX. *Molecules and Cells*, *37*(10), 742–746. https://doi.org/10.14348/molcells.2014.0208

Kim, M., Kim, D. M., Kim, K. S., Jung, W., & Kim, D. E. (2018). Applications of cancer cell-specific aptamers in targeted delivery of anticancer therapeutic agents. *Molecules*. MDPI AG. https://doi.org/10.3390/molecules23040830

Kim, M. Y., & Jeong, S. (2011). In vitro selection of RNA aptamer and specific targeting of ErbB2 in breast cancer cells. *Nucleic Acid Therapeutics*, *21*(3), 173–178. https://doi.org/10.1089/nat.2011.0283

Klussmann, S. (2006). *The Aptamer Handbook. Functional Oligonucleotides and Their Applications*. (S. Klussmann, Ed.). Berlin.

Kratschmer, C., & Levy, M. (2017). Effect of Chemical Modifications on Aptamer Stability in Serum. *Nucleic Acid Therapeutics*, *27*(6), 335–344. https://doi.org/10.1089/nat.2017.0680

Kwon, H.-M., Lee, K. H., Han, B. W., Han, M. R., Kim, D. H., & Kim, D.-E. (2014). An RNA Aptamer That Specifically Binds to the Glycosylated Hemagglutinin of Avian Influenza Virus and Suppresses Viral Infection in Cells. *PLoS ONE*, *9*(5), e97574. https://doi.org/10.1371/journal.pone.0097574

Kwon, J., Narayan, C., Kim, C., Han, M. J., Kim, M., & Jang, S. K. (2019). Development of a subtype-specific diagnostic system for influenza virus H3N2 using a novel virus-based systematic evolution of ligands by exponential enrichment (VIRO-SELEX). *Journal of Biomedical Nanotechnology*, *15*(7), 1609–1621. https://doi.org/10.1166/jbn.2019.2789

Lam, V. H., Lee, J. H., Silverio, A., Chan, H., Gomolplitinant, K. M., Povolotsky, T. L., … Saier, M. H. (2011). Pathways of transport protein evolution: Recent advances. *Biological Chemistry*, *392*(1–2), 5–12. https://doi.org/10.1515/BC.2011.018

Laterra, J., Keep, R., Betz, L. A., & Goldstein, G. W. (1999). Membrane Transport Processes.

Le, T. T., Chumphukam, O., & Cass, A. E. G. (2014). Determination of minimal sequence for binding of an aptamer. A comparison of truncation and hybridization inhibition methods. *RSC Advances*, *4*(88), 47227–47233. https://doi.org/10.1039/c4ra08243e

Lee, Y. J., Han, S. R., Kim, N. Y., Lee, S. H., Jeong, J. S., & Lee, S. W. (2012). An RNA aptamer that binds carcinoembryonic antigen inhibits hepatic metastasis of colon cancer cells in mice. *Gastroenterology*, *143*(1), 155-165.e8. https://doi.org/10.1053/j.gastro.2012.03.039

Lemech, C., & Arkenau, H.-T. (2011). Biomarkers in Advanced Colorectal Cancer: Challenges in Translating Clinical Research into Practice. *Cancers*, *3*(2), 1844–1860. https://doi.org/10.3390/cancers3021844

Li, C., Zhang, M., Zhang, Z., Tang, J., & Zhang, B. (2019). Microcantilever aptasensor for detecting epithelial tumor marker Mucin 1 and diagnosing human breast carcinoma MCF-7 cells. *Sensors and Actuators, B: Chemical*, *297*, 126759. https://doi.org/10.1016/j.snb.2019.126759

Li, N., Larson, T., Nguyen, H. H., Sokolov, K. V., & Ellington, A. D. (2010). Directed evolution of gold nanoparticle delivery to cells. *Chemical Communications*, *46*(3), 392–394. https://doi.org/10.1039/b920865h

Li, S., Xu, H., Ding, H., Huang, Y., Cao, X., Yang, G., … Shao, N. (2009). Identification of an aptamer targeting hnRNP A1 by tissue slide-based SELEX. *Journal of Pathology*, *218*(3), 327–336. https://doi.org/10.1002/path.2543

Lin, S. H., & Guidotti, G. (2009). Chapter 35 Purification of Membrane Proteins. In *Methods in Enzymology*. https://doi.org/10.1016/S0076-6879(09)63035-4

Liu, Y., Kuan, C. T., Mi, J., Zhang, X., Clary, B. M., Bigner, D. D., & Sullenger, B. A. (2009). Aptamers selected against the unglycosylated EGFRvIII ectodomain and delivered intracellularly reduce membrane-bound EGFRvIII and induce apoptosis. *Biological Chemistry*, *390*(2), 137–144. https://doi.org/10.1515/BC.2009.022

Liu, Z., Duan, J. H., Song, Y. M., Ma, J., Wang, F. D., Lu, X., & Yang, X. Da. (2012). Novel HER2 Aptamer Selectively Delivers Cytotoxic Drug to HER2-positive Breast Cancer Cells in Vitro. *Journal of Translational Medicine*, *10*(1). https://doi.org/10.1186/1479-5876-10-148

Lord, R. C. C. (1999). Osmosis, osmometry, and osmoregulation. *Postgraduate Medical Journal*, *75*(880), 67–73. https://doi.org/10.1136/pgmj.75.880.67

Lu, M., Zhou, L., Zheng, X., Quan, Y., Wang, X., Zhou, X., & Ren, J. (2015). A novel molecular marker of breast cancer stem cells identified by cell-SELEX method. *Cancer Biomarkers*, *15*(2), 169–176. https://doi.org/10.3233/CBM-140450

Lupold, S. E., Hicke, B. J., Lin, Y., & Coffey, D. S. (2002). Identification and characterization of nuclease-stabilized RNA molecules that bind human prostate cancer cells via the prostate-specific membrane antigen. *Cancer Research*, *62*(14), 4029–4033.

Lyu, Y., Chen, G., Shangguan, D., Zhang, L., Wan, S., Wu, Y., … Tan, W. (2016). Generating cell targeting aptamers for nanotheranostics using cell-SELEX. *Theranostics*. Ivyspring International Publisher. https://doi.org/10.7150/thno.15666

Magnus, M., Kappel, K., Das, R., & Bujnicki, J. M. (2019). RNA 3D structure prediction guided by independent folding of homologous sequences. *BMC Bioinformatics*, *20*(1), 512. https://doi.org/10.1186/s12859-019-3120-y

Mahlknecht, G., Maron, R., Mancini, M., Schechter, B., Sela, M., & Yarden, Y. (2013). Aptamer to ErbB-2/HER2 enhances degradation of the target and inhibits tumorigenic growth. *Proceedings of the National Academy of Sciences of the United States of America*, *110*(20), 8170–8175. https://doi.org/10.1073/pnas.1302594110

Mallikaratchy, P., Tang, Z., Kwame, S., Meng, L., Shangguan, D., & Tan, W. (2007). Aptamer directly evolved from live cells recognizes membrane bound immunoglobin heavy mu chain in Burkitt's lymphoma cells. *Molecular and Cellular Proteomics*, *6*(12), 2230–2238. https://doi.org/10.1074/mcp.M700026-MCP200

Marinko, J. T., Huang, H., Penn, W. D., Capra, J. A., Schlebach, J. P., & Sanders, C. R. (2019). Folding and Misfolding of Human Membrane Proteins in Health and Disease: From Single Molecules to Cellular Proteostasis. https://doi.org/10.1021/acs.chemrev.8b00532

Marshall, M. L., & Wagstaff, K. M. (2020). Internalized Functional DNA Aptamers as Alternative Cancer Therapies. *Frontiers in Pharmacology*. Frontiers Media S.A. https://doi.org/10.3389/fphar.2020.01115

Martínez-Espinosa, R. M. (2020). Heterologous and homologous expression of proteins from haloarchaea: Denitrification as case of study. *International Journal of Molecular Sciences*, *21*(1). https://doi.org/10.3390/ijms21010082

Mathieu, K., Javed, W., Vallet, S., Lesterlin, C., Candusso, M. P., Ding, F., … Orelle, C. (2019). Functionality of membrane proteins overexpressed and purified from E. coli is highly dependent upon the strain. *Scientific Reports*, *9*(1), 1–15. https://doi.org/10.1038/s41598-019-39382-0

Mayati, A., Moreau, A., Le Vée, M., Stieger, B., Denizot, C., Parmentier, Y., & Fardel, O. (2017). Protein kinases C-mediated regulations of drug transporter activity, localization and expression. *International Journal of Molecular Sciences*. https://doi.org/10.3390/ijms18040764

Mendonsa, S. D., & Bowser, M. T. (2004). In Vitro Evolution of Functional DNA Using Capillary Electrophoresis. *Journal of the American Chemical Society*, *126*(1), 20–21. https://doi.org/10.1021/ja037832s

Mercier, M.-C., Dontenwill, M., & Choulier, L. (2017). cancers Selection of Nucleic Acid Aptamers Targeting Tumor Cell-Surface Protein Biomarkers. https://doi.org/10.3390/cancers9060069

Mi, J., Liu, Y., Rabbani, Z. N., Yang, Z., Urban, J. H., Sullenger, B. A., & Clary, B. M. (2010). In vivo selection of tumor-targeting RNA motifs. *Nature Chemical Biology*, *6*(1), 22–24. https://doi.org/10.1038/nchembio.277

Mi, J., Zhang, X., Giangrande, P. H., McNamara, J. O., Nimjee, S. M., Sarraf-Yazdi, S., … Clary, B. M. (2005). Targeted inhibition of αvβ3 integrin with an RNA aptamer impairs endothelial cell growth and survival. *Biochemical and Biophysical Research Communications*, *338*(2), 956–963. https://doi.org/10.1016/j.bbrc.2005.10.043

Missailidis, S., Thomaidou, D., Borbas, K. E., & Price, M. R. (2005). Selection of aptamers with high affinity and high specificity against C595, an anti-MUC1 IgG3 monoclonal antibody, for antibody targeting. *Journal of Immunological Methods*, *296*(1–2), 45–62. https://doi.org/10.1016/j.jim.2004.10.011

Molefe, P. F., Masamba, P., Oyinloye, B. E., Mbatha, L. S., Meyer, M., & Kappo, A. P. (2018). Molecular application of aptamers in the diagnosis and treatment of cancer and communicable diseases. *Pharmaceuticals*, *11*(4). https://doi.org/10.3390/ph11040093

Mori, T., Oguro, A., Ohtsu, T., & Nakamura, Y. (2004). RNA aptamers selected against the receptor activator of NF-κB acquire general affinity to proteins of the tumor necrosis factor receptor family. *Nucleic Acids Research*, *32*(20), 6120–6128. https://doi.org/10.1093/nar/gkh949

Morris, K. N., Jensen, K. B., Julin, C. M., Weil, M., & Gold, L. (1998). *High affinity ligands from in vitro selection: Complex targets*. *Biochemistry* (Vol. 95).

Ni, S., Yao, H., Wang, L., Lu, J., Jiang, F., Lu, A., & Zhang, G. (2017). Chemical modifications of nucleic acid aptamers for therapeutic purposes. *International Journal of Molecular Sciences*, *18*(8). https://doi.org/10.3390/ijms18081683

Nilsen-hamilton, M., Miller, W. A., & Huiatt, T. W. (2012). Deciphering the details of RNA aminoglycoside interactions : from atomistic models to biotechnological applications To my daughter Devrim Ilgaz.

Nishikawa, F., Kakiuchi, N., Funaji, K., Fukuda, K., Sekiya, S., & Nishikawa, S. (2003). Inhibition of HCV NS3 protease by RNA aptamers in cells. *Nucleic Acids Research*. Nucleic Acids Res. https://doi.org/10.1093/nar/gkg291

O'Connell, D., Koenig, A., Jennings, S., Hicke, B., Han, H. L., Fitzwater, T., … Varki, A. (1996). Calcium-dependent oligonucleotide antagonists specific for L-selectin. *Proceedings of the National Academy of Sciences of the United States of America*, *93*(12), 5883–5887. https://doi.org/10.1073/pnas.93.12.5883

Ohuchi, S. (2012). Cell-SELEX Technology. https://doi.org/10.1089/biores.2012.0253

Ohuchi, S. P., Ohtsu, T., & Nakamura, Y. (2006). Selection of RNA aptamers against recombinant transforming growth factor-β type III receptor displayed on cell surface. *Biochimie*, *88*(7), 897–904. https://doi.org/10.1016/j.biochi.2006.02.004

Ospina-Villa, J. D., Zamorano-Carrillo, A., Castañón-Sánchez, C. A., Ramírez-Moreno, E., & Marchat, L. A. (2016). Aptamers as a promising approach for the control of parasitic diseases. *Brazilian Journal of Infectious Diseases*. Elsevier Editora Ltda. https://doi.org/10.1016/j.bjid.2016.08.011

Pandey, A., Shin, K., Patterson, R. E., Liu, X. Q., & Rainey, J. K. (2016). Current strategies for protein production and purification enabling membrane protein structural biology1. *Biochemistry and Cell Biology*. Canadian Science Publishing. https://doi.org/10.1139/bcb-2015-0143

Parashar, A. (2016a). Aptamer and its role in diagnostics. *International Journal of Bioassays*, *5*(02), 4799. https://doi.org/10.21746/ijbio.2016.02.007

Parashar, A. (2016b). Aptamers in therapeutics. *Journal of Clinical and Diagnostic Research*, *10*(6), BE01–BE06. https://doi.org/10.7860/JCDR/2016/18712.7922

Parekh, P., Kamble, S., Zhao, N., Zeng, Z., Portier, B. P., & Zu, Y. (2013). Immunotherapy of CD30-expressing lymphoma using a highly stable ssDNA aptamer. *Biomaterials*, *34*(35), 8909–8917. https://doi.org/10.1016/j.biomaterials.2013.07.099

Pastor, F., Soldevilla, M. M., Villanueva, H., Kolonias, D., Inoges, S., De Cerio, A. L., … Bendandi, M. (2013). CD28 aptamers as powerful immune response modulators. *Molecular Therapy - Nucleic Acids*, *2*, e98. https://doi.org/10.1038/mtna.2013.26

Pestourie, C., Cerchia, L., Gombert, K., Aissouni, Y., Boulay, J., De Franciscis, V., … Ducongé, F. (2006). Comparison of different strategies to select aptamers against a transmembrane protein target. *Oligonucleotides*, *16*(4), 323–335. https://doi.org/10.1089/oli.2006.16.323

Pfeiffer, F., & Mayer, G. (2016). Selection and Biosensor Application of Aptamers for Small Molecules. *Frontiers in Chemistry*, *4*(June), 1–21. https://doi.org/10.3389/fchem.2016.00025

Piater, B., Doerner, A., Guenther, R., Kolmar, H., & Hock, B. (2015). Aptamers Binding to c-Met Inhibiting Tumor Cell Migration. *PLoS ONE*, *10*(12). https://doi.org/10.1371/journal.pone.0142412

Pillai, G. (2019). *Chapter 9 - Nanotechnology Toward Treating Cancer: A Comprehensive Review*. *Applications of Targeted Nano Drugs and Delivery Systems*. Elsevier Inc. https://doi.org/10.1016/B978-0-12-814029-1.00009-0

Pignatello, R. (2013). Biological membranes and their role in physio-pathological conditions. In *Drug-Biomembrane Interaction Studies: The Application of Calorimetric Techniques* (pp. 1–46). Elsevier Inc. https://doi.org/10.1533/9781908818348.1

Poturnayová, A., Dzubinová, L., Buríková, M., Bízik, J., & Hianik, T. (2019). Detection of breast cancer cells using acoustics aptasensor specific to HER2 receptors. *Biosensors*, *9*(2). https://doi.org/10.3390/bios9020072

Pratico, E. D., Sullenger, B. A., & Nair, S. K. (2013). Identification and characterization of an agonistic aptamer against the T cell costimulatory receptor, OX40. *Nucleic Acid Therapeutics*, *23*(1), 35–43. https://doi.org/10.1089/nat.2012.0388

Qosa, H., Mohamed, L. A., Alqahtani, S., Abuasal, B. S., Hill, R. A., & Kaddoumi, A. (2016). Transporters as Drug Targets in Neurological Diseases, *100*(5), 441–453. https://doi.org/10.1002/cpt.435

Quang Vu, C., Tantirungrotechai, Y., Soontornworajit, B., & Rotkrua, P. (2016). Truncation of PDGF-BB Aptamer by Secondary Structural Analysis and Immunoassay. https://doi.org/10.18178/ijpmbs.5.1.1-6

Raddatz, M. S. L., Dolf, A., Endl, E., Knolle, P., Famulok, M., & Mayer, G. (2008). Enrichment of cell-targeting and population-specific aptamers by fluorescence-activated cell sorting. *Angewandte Chemie - International Edition*, *47*(28), 5190–5193. https://doi.org/10.1002/anie.200800216

Ravna, A. W., Sager, G., Dahl, S. G., & Sylte, I. (2008). Membrane Transporters : Structure , Function and Targets Membrane Transporters : Structure , Function and Targets for Drug Design, (March 2016). https://doi.org/10.1007/7355

Ray, P., Cheek, M. A., Sharaf, M. L., Li, N., Ellington, A. D., Sullenger, B. A., … White, R. R. (2012). Aptamer-mediated delivery of chemotherapy to pancreatic cancer cells. *Nucleic Acid Therapeutics*, *22*(5), 295–305. https://doi.org/10.1089/nat.2012.0353

Roberts, T. C., Langer, R., & Wood, M. J. A. (2020). Advances in oligonucleotide drug delivery. *Nature Reviews Drug Discovery*. Nature Research. https://doi.org/10.1038/s41573-020-0075-7

Robertson, D. L., & Joyce, G. F. (1990). Selection in vitro of an RNA enzyme that specifically cleaves single-stranded DNA. *Nature*. https://doi.org/10.1038/344467a0

Roth, F., De La Fuente, A. C., Vella, J. L., Zoso, A., Inverardi, L., & Serafini, P. (2012). Aptamer-mediated blockade of IL4Rα triggers apoptosis of MDSCs and limits tumor progression. *Cancer Research*, *72*(6), 1373–1383. https://doi.org/10.1158/0008-5472.CAN-11-2772

Rucevic, M., Hixson, D., & Josic, D. (2011). Mammalian plasma membrane proteins as potential biomarkers and drug targets. *Electrophoresis*, *32*(13), 1549–1564. https://doi.org/10.1002/elps.201100212

Saier, M. H. (2000). *A Functional-Phylogenetic Classification System for Transmembrane Solute Transporters*. *Microbiology and Molecular Biology Reviews* (Vol. 64).

Santulli-Marotto, S., Nair, S. K., Rusconi, C., Sullenger, B., & Gilboa, E. (2003). Multivalent RNA Aptamers That Inhibit CTLA-4 and Enhance Tumor Immunity. *Cancer Research*, *63*(21), 7483–7489.

Savir, Y., Martynov, A., & Springer, M. (2017). Achieving global perfect homeostasis through transporter regulation. *PLoS Computational Biology*, *13*(4). https://doi.org/10.1371/journal.pcbi.1005458

Schfneberg, T., Schulz, A., Biebermann, H., Hermsdorf, T., Rompler, H., & Sangkuhl, K. (2004). Mutant G-protein-coupled receptors as a cause of human diseases.

Sefah, K., Bae, K. M., Phillips, J. A., Siemann, D. W., Su, Z., McClellan, S., … Tan, W. (2013). Cell-based selection provides novel molecular probes for cancer stem cells. *International Journal of Cancer*, *132*(11), 2578–2588. https://doi.org/10.1002/ijc.27936

Sefah, K., Shangguan, D., Xiong, X., O'Donoghue, M. B., & Tan, W. (2010). Development of DNA aptamers using cell-selex. *Nature Protocols*, *5*(6), 1169–1185. https://doi.org/10.1038/nprot.2010.66

Sett, A., Borthakur, B. B., & Bora, U. (2017). Selection of DNA aptamers for extra cellular domain of human epidermal growth factor receptor 2 to detect HER2 positive carcinomas. *Clinical and Translational Oncology*, *19*(8), 976–988. https://doi.org/10.1007/s12094-017-1629-y

Shangguan, D., Tang, Z., Mallikaratchy, P., Xiao, Z., & Tan, W. (2007). Optimization and modifications of aptamers selected from live cancer cell lines. *ChemBioChem*, *8*(6), 603–606. https://doi.org/10.1002/cbic.200600532

Shen, M., Rusling, J. F., & Dixit, C. K. (2017). Site-selective orientated immobilization of antibodies and conjugates for immunodiagnostics development. *Methods*. Academic Press Inc. https://doi.org/10.1016/j.ymeth.2016.11.010

Shi, Y. Z., Wu, Y. Y., Wang, F. H., & Tan, Z. J. (2014). RNA structure prediction: Progress and perspective. *Chinese Physics B*. https://doi.org/10.1088/1674-1056/23/7/078701

Shigdar, S., Lin, J., Yu, Y., Pastuovic, M., Wei, M., & Duan, W. (2011). RNA aptamer against a cancer stem cell marker epithelial cell adhesion molecule. *Cancer Science*, *102*(5), 991–998. https://doi.org/10.1111/j.1349-7006.2011.01897.x

Shigdar, S., Macdonald, J., O'Connor, M., Wang, T., Xiang, D., Shamaileh, H. Al, … Duan, W. (2013). Aptamers as theranostic agents: Modifications, serum stability and functionalisation. *Sensors (Switzerland)*, *13*(10), 13624–13637. https://doi.org/10.3390/s131013624

Shigdar, S., Qiao, L., Zhou, S. F., Xiang, D., Wang, T., Li, Y., … Duan, W. (2013). RNA aptamers targeting cancer stem cell marker CD133. *Cancer Letters*, *330*(1), 84–95. https://doi.org/10.1016/j.canlet.2012.11.032

Singer, S. J., & Nicolson, G. L. (1972). The fluid mosaic model of the structure of cell membranes. *Science*, *175*(4023), 720–731. https://doi.org/10.1126/science.175.4023.720

Siontorou, C. G., Nikoleli, G. P., Nikolelis, D. P., & Karapetis, S. K. (2017). Artificial lipid membranes: Past, present, and future. *Membranes*. MDPI AG. https://doi.org/10.3390/membranes7030038

Slack, J. M. W. (2020). Cell: Additional Information | Britannica. In *Britannica*.

Smith, S. M. (2017). Strategies for the purification of membrane proteins. In *Methods in Molecular Biology* (Vol. 1485, pp. 389–400). Humana Press Inc. https://doi.org/10.1007/978-1-4939-6412-3_21

Soksawatmaekhin, W., Kuraishi, A., Sakata, K., Kashiwagi, K., & Igarashi, K. (2004). Excretion and uptake of cadaverine by CadB and its physiological functions in Escherichia coli. *Molecular Microbiology*, *51*(5), 1401–1412. https://doi.org/10.1046/j.1365-2958.2003.03913.x

Soldevilla, M. M., Villanueva, H., Casares, N., Lasarte, J. J., Bendandi, M., Inoges, S., … Pastor, F. (2016). MRP1-CD28 bi-specific oligonucleotide aptamers: Target costimulation to drug-resistant melanoma cancer stem cells. *Oncotarget*, *7*(17), 23182–23196. https://doi.org/10.18632/oncotarget.8095

Somasunderam, A., Thiviyanathan, V., Tanaka, T., Li, X., Neerathilingam, M., Lokesh, G. L. R., … Gorenstein, D. G. (2010). Combinatorial selection of DNA thioaptamers targeted to the HA binding domain of human CD44. *Biochemistry*, *49*(42), 9106–9112. https://doi.org/10.1021/bi1009503

Song, S., Wang, L., Li, J., Zhao, J., & Fan, C. (2008). Aptamer-based biosensors, *27*(2). https://doi.org/10.1016/j.trac.2007.12.004

Song, Y., Zhu, Z., An, Y., Zhang, W., Zhang, H., Liu, D., … Yang, C. J. (2013). Selection of DNA aptamers against epithelial cell adhesion molecule for cancer cell imaging and circulating tumor cell capture. *Analytical Chemistry*, *85*(8), 4141–4149. https://doi.org/10.1021/ac400366b

Souf, S. (2016). BioscienceHorizons Recent advances in diagnostic testing for viral infections. https://doi.org/10.1093/biohorizons/hzw010

Soundararajan, S., Chen, W., Spicer, E. K., Courtenay-Luck, N., & Fernandes, D. J. (2008). The nucleolin targeting aptamer AS1411 destabilizes Bcl-2 messenger RNA in human breast cancer cells. *Cancer Research*, *68*(7), 2358–2365. https://doi.org/10.1158/0008-5472.CAN-07-5723

Soundararajan, S., Wang, L., Sridharan, V., Chen, W., Courtenay-Luck, N., Jones, D., … Fernandes, D. J. (2009). Plasma membrane nucleolin is a receptor for the anticancer aptamer AS1411 in MV4-11 leukemia cells. *Molecular Pharmacology*, *76*(5), 984–991. https://doi.org/10.1124/mol.109.055947

Souza, A. G., Marangoni, K., Fujimura, P. T., Alves, P. T., Silva, M. J., Bastos, V. A. F., … Goulart, V. A. (2016). 3D Cell-SELEX: Development of RNA aptamers as molecular probes for PC-3 tumor cell line. *Experimental Cell Research*, *341*(2), 147–156. https://doi.org/10.1016/j.yexcr.2016.01.015

Szeitner, Z., András, J., Gyurcsányi, R. E., & Mészáros, T. (2014). Is less more? Lessons from aptamer selection strategies. *Journal of Pharmaceutical and Biomedical Analysis*. https://doi.org/10.1016/j.jpba.2014.04.018

Takahashi, M. (2018). Aptamers targeting cell surface proteins. *Biochimie*, *145*, 63–72. https://doi.org/10.1016/j.biochi.2017.11.019

Takahashi, M., Sakota, E., & Nakamura, Y. (2016). The efficient cell-SELEX strategy, Icell-SELEX, using isogenic cell lines for selection and counter-selection to generate RNA aptamers to cell surface proteins. *Biochimie*, *131*, 77–84. https://doi.org/10.1016/j.biochi.2016.09.018

Tan, Y., Shi, Y. S., Wu, X. D., Liang, H. Y., Gao, Y. B., Li, S. J., … Gao, T. M. (2013). DNA aptamers that target human glioblastoma multiforme cells overexpressing epidermal growth factor receptor variant III In vitro. *Acta Pharmacologica Sinica*, *34*(12), 1491–1498. https://doi.org/10.1038/aps.2013.137

Tanaka, K. J., Song, S., Mason, K., & Pinkett, H. W. (2018). Selective substrate uptake: The role of ATP-binding cassette (ABC) importers in pathogenesis. *Biochimica et Biophysica Acta - Biomembranes*. Elsevier B.V. https://doi.org/10.1016/j.bbamem.2017.08.011

Tang, Zhiwen; Parekh, Parag; Turner, Pete; Moyer, Richard P.; Tan, W. (2009). Generating aptamers for recognition of virus-infected cells. *Clinical Chemistry*, *55:3*.

Thiel, K. W., Hernandez, L. I., Dassie, J. P., Thiel, W. H., Liu, X., Stockdale, K. R., … Giangrande, P. H. (2012). Delivery of chemo-sensitizing siRNAs to HER2+-breast cancer cells using RNA aptamers. *Nucleic Acids Research*, *40*(13), 6319–6337. https://doi.org/10.1093/nar/gks294

Thiel, W. H., Thiel, K. W., Flenker, K. S., Bair, T., Dupuy, A. J., Mc namara, J. O., … H. Giangrande, P. (2015). Cell-internalization SELEX: method for identifying cell- internalizing RNA aptamers for delivering siRNAs to target cells. *Methods in Molecular Biology*, *1218*, 187–199. https://doi.org/10.1007/978-1-4939-1538-5_11

Traxler, P. (2003). Tyrosine kinases as targets in cancer therapy - Successes and failures. *Expert Opinion on Therapeutic Targets*. https://doi.org/10.1517/14728222.7.2.215

Tuerk, C., & Gold, L. (1990). Systematic evolution of ligands by exponential enrichment: RNA ligands to bacteriophage T4 DNA polymerase. *Science*, *249*(4968), 505–510. https://doi.org/10.1126/science.2200121

Várady, G., Cserepes, J., Németh, A., Szabó, E., & Sarkadi, B. (2013). Cell surface membrane proteins as personalized biomarkers: Where we stand and where we are headed. *Biomarkers in Medicine*, *7*(5), 803–819. https://doi.org/10.2217/bmm.13.90

Vashist, S. K., & Luong, J. H. T. (2018). Enzyme-linked immunoassays. In *Handbook of Immunoassay Technologies: Approaches, Performances, and Applications* (pp. 97–127). Elsevier. https://doi.org/10.1016/B978-0-12-811762-0.00005-0

Vivekananda, J., & Kiel, J. L. (2006). Anti-Francisella tularensis DNA aptamers detect tularemia antigen from different subspecies by Aptamer-Linked Immobilized Sorbent Assay. *Laboratory Investigation*, *86*(6), 610–618. https://doi.org/10.1038/labinvest.3700417

Voet, Donald; Voet, J. (2011). Biochemistry, 4th edition. In *Biochemistry, 4th edition*.

Wan, L. Y., Yuan, W. F., Ai, W. B., Ai, Y. W., Wang, J. J., Chu, L. Y., … Wu, J. F. (2019). An exploration of aptamer internalization mechanisms and their applications in drug delivery. *Expert Opinion on Drug Delivery*. Taylor and Francis Ltd. https://doi.org/10.1080/17425247.2019.1575808

Wang, D. L., Song, Y. L., Zhu, Z., Li, X. L., Zou, Y., Yang, H. T., … Kang, D. Z. (2014). Selection of DNA aptamers against epidermal growth factor receptor with high affinity and specificity. *Biochemical and Biophysical Research Communications*, *453*(4), 681–685. https://doi.org/10.1016/j.bbrc.2014.09.023

Wang, J., Jiang, H., & Liu, F. (2000). In vitro selection of novel RNA ligands that bind human cytomegalovirus and block viral infection. *RNA*, *6*(4), 571–583. https://doi.org/10.1017/S1355838200992215

Wang, R., Zhu, G., Mei, L., Xie, Y., Ma, H., Ye, M., … Tan, W. (2014). Automated modular synthesis of Aptamer-drug conjugates for targeted drug delivery. *Journal of the American Chemical Society*, *136*(7), 2731–2734. https://doi.org/10.1021/ja4117395

Watanabe, T., Ito, K., Matsumoto, M., Seya, T., Nishikawa, S., Hasegawa, T., & Fukuda, K. (2006). Isolation of RNA aptamers against human Toll-like receptor 3 ectodomain. *Nucleic Acids Symposium Series (2004)*, (50), 251–252. https://doi.org/10.1093/nass/nrl125

White, R. R., Roy, J. A., Viles, K. D., Sullenger, B. A., & Kontos, C. D. (2008). A nuclease-resistant RNA aptamer specifically inhibits angiopoietin-1- mediated Tie2 activation and function. *Angiogenesis*, *11*(4), 395–401. https://doi.org/10.1007/s10456-008-9122-4

White, R. R., Shan, S., Rusconi, C. P., Shetty, G., Dewhirst, M. W., Kontos, C. D., & Sullenger, B. A. (2003). Inhibition of rat corneal angiogenesis by a nuclease-resistant RNA aptamer specific for angiopoietin-2. *Proceedings of the National Academy of Sciences of the United States of America*, *100*(9), 5028–5033. https://doi.org/10.1073/pnas.0831159100

Wilner, S. E., Wengerter, B., Maier, K., Borba Magalhães, M. D. L., Del Amo, D. S., Pai, S., … Levy, M. (2012). An RNA alternative to human transferrin: A new tool for targeting human cells. *Molecular Therapy - Nucleic Acids*, *1*(5), e21. https://doi.org/10.1038/mtna.2012.14

Wright, E. M., Hirayama, B. A., & Loo, D. F. (2007). Active sugar transport in health and disease. In *Journal of Internal Medicine* (Vol. 261, pp. 32–43). John Wiley & Sons, Ltd. https://doi.org/10.1111/j.1365-2796.2006.01746.x

Wu, C. C. N., Castro, J. E., Motta, M., Cottam, H. B., Kyburz, D., Kipps, T. J., … Carson, D. A. (2003). Selection of oligonucleotide aptamers with enhanced uptake and activation of human leukemia B cells. *Human Gene Therapy*, *14*(9), 849–860. https://doi.org/10.1089/104303403765701141

Wu, S., Duan, N., Qiu, Y., Li, J., & Wang, Z. (2017). Colorimetric aptasensor for the detection of Salmonella enterica serovar typhimurium using ZnFe2O4-reduced graphene oxide nanostructures as an effective peroxidase mimetics. *International Journal of Food Microbiology*, *261*, 42–48. https://doi.org/10.1016/j.ijfoodmicro.2017.09.002

Wu, X., Liang, H., Tan, Y., Yuan, C., Li, S., Li, X., … Zhang, X. (2014). Cell-SELEX aptamer for highly specific radionuclide molecular imaging of glioblastoma in vivo. *PLoS ONE*, *9*(3). https://doi.org/10.1371/journal.pone.0090752

Xayaphoummine, A., Bucher, T., & Isambert, H. (2005). Kinefold web server for RNA/DNA folding path and structure prediction including pseudoknots and knots. *Nucleic Acids Research*, *33*(SUPPL. 2). https://doi.org/10.1093/nar/gki447

Xiao, Z., Shangguan, D., Cao, Z., Fang, X., & Tan, W. (2008). Cell-specific internalization study of an aptamer from whole cell selection. *Chemistry - A European Journal*, *14*(6), 1769–1775. https://doi.org/10.1002/chem.200701330

Yan, A., & Levy, M. (2014). Cell internalization SELEX: In vitro selection for molecules that internalize into cells. *Methods in Molecular Biology*, *1103*, 241–265. https://doi.org/10.1007/978-1-62703-730-3_18

Yang, N. J., & Hinner, M. J. (2015). Getting across the cell membrane: an overview for small molecules, peptides, and proteins. *Methods in Molecular Biology (Clifton, N.J.)*. NIH Public Access. https://doi.org/10.1007/978-1-4939-2272-7_3

Yazdian-Robati, R., Ramezani, M., Khedri, M., Ansari, N., Abnous, K., & Taghdisi, S. M. (2017). An aptamer for recognizing the transmembrane protein PDL-1 (programmed death-ligand 1), and its application to fluorometric single cell detection of human ovarian carcinoma cells. *Microchimica Acta*, *184*(10), 4029–4035. https://doi.org/10.1007/s00604-017-2436-4

Yeagle, P. L. (2016). *Chapter 10 – Membrane Proteins*. *The Membranes of Cells*. https://doi.org/10.1016/B978-0-12-800047-2.00010-3

Yin, H., & Flynn, A. D. (2016). Drugging Membrane Protein Interactions. *Annual Review of Biomedical Engineering*, *18*(1), 51–76. https://doi.org/10.1146/annurev-bioeng-092115-025322

Yu, Y., Zhao, J., & Bayly, A. E. (2008). Development of Surfactants and Builders in Detergent Formulations. *Chinese Journal of Chemical Engineering*, *16*(4), 517–527. https://doi.org/10.1016/S1004-9541(08)60115-9

Zhang, H., Zhang, C., Li, Z., Li, C., Wei, X., Zhang, B., & Liu, Y. (2019). A new method of RNA secondary structure prediction based on convolutional neural network and dynamic programming. *Frontiers in Genetics*, *10*(MAY), 467. https://doi.org/10.3389/fgene.2019.00467

Zhang, J., Li, S., Liu, F., Zhou, L., Shao, N., & Zhao, X. (2015). SELEX aptamer used as a probe to detect circulating tumor cells in peripheral blood of pancreatic cancer patients. *PLoS ONE*, *10*(3), 1–9. https://doi.org/10.1371/journal.pone.0121920

Zhang, Y., Lai, B. S., & Juhas, M. (2019). Recent advances in aptamer discovery and applications. *Molecules*, *24*(5). https://doi.org/10.3390/molecules24050941

Zhao, R. N., Feng, Z., Zhao, Y. N., Jia, L. P., Ma, R. N., Zhang, W., … Wang, H. S. (2019). A sensitive electrochemical aptasensor for Mucin 1 detection based on catalytic hairpin assembly coupled with PtPdNPs peroxidase-like activity. *Talanta*, *200*, 503–510. https://doi.org/10.1016/j.talanta.2019.03.012

Zhou, J., & Rossi, J. (2017). Aptamers as targeted therapeutics: Current potential and challenges. *Nature Reviews Drug Discovery*, *16*(3), 181–202. https://doi.org/10.1038/nrd.2016.199

Zhou, J., Tiemann, K., Chomchan, P., Alluin, J., Swiderski, P., Burnett, J., … Rossi, J. (2013). Dual functional BAFF receptor aptamers inhibit ligand-induced proliferation and deliver siRNAs to NHL cells. *Nucleic Acids Research*, *41*(7), 4266–4283. https://doi.org/10.1093/nar/gkt125

Zhou, Q., Rahimian, A., Son, K., Shin, D., Patel, T., & Revzin, A. (2016). Development of an aptasensor for electrochemical detection of exosomes. *Methods*, *97*, 88–93. https://doi.org/10.1016/j.ymeth.2015.10.012

Zhou, W., Jimmy Huang, P. J., Ding, J., & Liu, J. (2014). Aptamer-based biosensors for biomedical diagnostics. *Analyst*, *139*(11), 2627–2640. https://doi.org/10.1039/c4an00132j

Zhu, G., Niu, G., & Chen, X. (2015). Aptamer–Drug Conjugates. *Bioconjugate Chemistry*, *26*(11), 2186–2197. https://doi.org/10.1021/acs.bioconjchem.5b00291

Zhu, G., Zhang, H., Jacobson, O., Wang, Z., Chen, H., Yang, X., … Chen, X. (2017). Combinatorial Screening of DNA Aptamers for Molecular Imaging of HER2 in Cancer. *Bioconjugate Chemistry*, *28*(4), 1068–1075. https://doi.org/10.1021/acs.bioconjchem.6b00746

Zhuo, Z., Yu, Y., Wang, M., Li, J., Zhang, Z., Liu, J., … Zhang, B. (2017). Molecular Sciences Recent Advances in SELEX Technology and Aptamer Applications in Biomedicine. https://doi.org/10.3390/ijms18102142

APPENDICES

A. Appendix A

Aptamers to MPs and their potent applications

Aptamer Name	Membrane Protein as Target	Backbone	Application of Aptamer	References
Apt5	PD-L1	DNA	Cancer cell imaging, CTC enrichment	(Yazdian-Robati et al., 2017)
M17	MMP14	DNA	Tumor imaging, cancer therapy	(X. Huang et al., 2019)
S1.3/S2.2	MUC1	DNA	Early diagnosis and therapy of breast and pancreatic cancers	(Missailidis, Thomaidou, Borbas, & Price, 2005)
MUC1-5TR-1, 2, 3, 4	His-tagged unglycosylated form of the MUC1 protein containing five tandem repeats of the VTR (*E. coli* system) DNA	DNA	Potential application: diagnosis assays for early or metastatic diseases	(Ferreira et al., 2008)
EpCAM	Epithelial cell adhesion molecule-EpCAM (CD326)	2'F-RNA	Target stem cell marker. Potential applications: development of targeted cancer nanomedicine and molecular imaging	(Shigdar et al., 2011)

SYL3C	EpCAM	DNA	Novel targeted cancer therapy, cancer cell imaging, and CTC enrichment	(Song et al., 2013)
YJ-1	Carcinoembryonic antigen- CEA (CD66e)	2'F-RNA	Inhibition of cell migration/invasion *in vivo*. Promotion of cell anoikis resistance	(Lee et al., 2012)
Apt-αvβ3	Integrin αvβ3	2'F-RNA	Increases endothelial cell apoptosis Recognizes distinct binding sites on a single target (αV or β3) with minimal cross-reactivity	(Mi et al., 2005)
αV-1 and β3-1	Integrin αvβ3	2'F-RNA		(Gong et al., 2012)
SDA	E-and P-Selectin	DNA	Inhibition of cancer cell adhesion Potential applications in therapies during metastasis formation	(Faryammanesh et al., 2014)
14.12	L-Selectin	2'-NH_2-RNA	Potential applications in therapies during metastasis formation	(O'Connell et al., 1996)
LD201, LD174, and LD196	L-Selectin	DNA	Inhibition of lymphocyte rolling on endothelial cells	(Hicke et al., 1996)
J18	EGFR	RNA	Drug delivery (internalization of gold nanoparticles) Potential application: delivery of siRNA and cancer detection	(Li, Larson, Nguyen, Sokolov, & Ellington, 2010)

E07 Internalized	EGFR	2'F-RNA	Prevention of proliferation of tumor cells (blocks receptor autophosphorylation) Drug delivery (Gemcitabine) and induces cell death	(Li et al., 2010; Ray et al., 2012)
Tutu-22	EGFR	DNA	Potential applications: development of novel targeted cancer detection, imaging, and therapy	(Wang et al., 2014)
E21	EGFRVIII histidine-tagged EGFRvIII ectodomain (*E. coli.* system) recombinant glutathione S-transferase	2'F-RNA	Disruption of post-translational modifications of immature EGFRvIII Induction of apoptosis	(Y. Liu et al., 2009)
SE15-8	HER-2	2'F-RNA	High specificity to ErbB2 and not to other members of the ErbB family Potential applications: drug delivery and imaging for *in vivo* diagnosis	(M. Y. Kim & Jeong, 2011)
HB5	HER-2 peptide from the juxtamembrane region of HER2 extracellular domain	DNA	Drug delivery (Doxorubicin)	(Z. Liu et al., 2012)

HY6	extracellular domain 20-amino acid HER2 peptide	Thio-DNA	Potential application: targeted therapy Potential	(Hu et al., 2015)
ECD_Apt1	His-tagged Her2–extracellular domain (*E. coli* system)	DNA	Potential applications: theranostic (non-invasive cancer diagnosis), therapeutics and monitoring patient compliance	(Sett, Borthakur, & Bora, 2017)
A30	extracellular domains of HER3 produced in S2 insect cells	RNA	Inhibition of HER3 activation and growth of tumor cells Potential application: anticancer drug	(Chen, Chernis, Hoang, & Landgraf, 2003)
CLN3 and CLN4	c-MET	DNA	Recruits NK cells to the tumor and induce ADCC	(Boltz et al., 2011)
CLN64	c-MET	2'F-RNA	Inhibition of tumor cell migration. Potential application: therapeutics and diagnosis	(Piater, Doerner, Guenther, Kolmar, & Hock, 2015)
A9, A10, A10-3	Prostate-specific membrane antigen-PSMA	2'F-RNA	Promotion of tumor regression Delivery of siRNA Potential application: diagnosis and therapies	(Lupold, Hicke, Lin, & Coffey, 2002)

9C7, 11F11	T-cell receptor OX40 T-cell	2'F-RNA	The increasing proliferation of T lymphocytes and the production of IFN-γ. Potential application: therapeutics in association with dendritic cell-based vaccines (adoptive cellular therapy	(Pratico, Sullenger, & Nair, 2013)
9.8	The murine extracellular domain of OX40-Fc fusion protein	2'F-RNA	Induces nuclear localization of NFκB, cytokine production, and cell proliferation. Increases dendritic cell-based tumor vaccine effects	(Dollins et al., 2008)
M12-23 (multimeric aptamer) affinity	The murine extracellular domain of 4-1BB-Fc fusion protein	2'F-RNA	Inhibition of tumor growth *in vivo*. Potential application: therapeutic manipulation of the immune system	(Ii et al., 2008)
apt1, apt2, and apt3	RANK/IgG1Fc chimera	RNA	Potential application: therapeutics against osteoclastogenesis	(Mori, Oguro, Ohtsu, & Nakamura, 2004)
CD28Apt2 20and CD28Apt7	murine recombinant CD28-Fc fusion protein	2'F-RNA	Reduction of tumor progression and increased overall survival (*in vivo*) Potential application: enhancing vaccine-induced immune responses	(Pastor et al., 2013)

R-1, R-2, and R-4	Human recombinant BAFF-R protein	2'F-RNA	Delivery of siRNA. Potential application: combinatorial therapeutics	(Zhou et al., 2013)
M9-9	Cytotoxic T cell Antigen-4-CTLA-4 B-cell-activating factor	2'F-RNA	Increases tumor immunity (*in vivo*) Potential application: Immunotherapy	(Santulli-Marotto, Nair, Rusconi, Sullenger, & Gilboa, 2003)
cL42	CD124 (IL-4Rα) recombinant ILR4α protein enzymatically cleaved	2'F-RNA	Reduction of tumor progression *in vivo*	(Roth et al., 2012)
12.11	N-terminal fragment of VCAM-1	2'F-RNA	Potential application: imaging	(Chauveau et al., 2007)
Family-I and Family-II	Toll-like receptor 3 ectodomain with N-terminal FLAG and C-terminal His	RNA	Aptamer without agonist and antagonist effects	(Watanabe et al., 2006)
TA1-TA6	HA-binding domain of human CD44 (cell-free expression system)	Thio-DNA	Potential applications targeted therapy and imaging	(Somasunderam et al., 2010)
Apt1	GST-tagged human recombinant full-length CD44 protein	2'F-RNA	Potential applications therapeutic (targeted delivery against stem cells) and diagnosis	(Ababneh et al., 2013)
ANG9-4	recombinant human Angiopoietin-1	2'F-RNA	Inhibition of cell endothelial cell survival	(White, Roy, Viles, Sullenger, & Kontos, 2008)

11-1 and truncated 1.41	Angiopoietin-2	2'F-RNA	Inhibition of angiogenesis (*in vivo*)	(White et al., 2003)
Aptamer 32	EGFRvIII	DNA	Potential applications: delivery of chemical drug and diagnosis	(Tan et al., 2013)
U2	EGFRvIII	DNA	Imaging (radiolabeled 188Re, *in vivo*) Potential applications: diagnosis in stratifying patient and monitoring treatment	(Wu et al., 2014)
S6	HER-2	RNA	Potential application: therapy	(Kang, Huh, Kim, & Lee, 2009)
E1, B1, and C1	N202.1A mammary carcinoma clonal cell lines expressing high levels of surface HER-2/neu	2'F-RNA	Drug delivery (Bcl-2 siRNA) Induces chemo sensibilization and reduces drug resistance	(Thiel et al., 2012)
aptamer 2-2(t)	HER-2 cleared extract of ErbB-2-overexpressing N87 cells	DNA	Acceleration of ErbB-2 degradation in lysosomes Inhibition of growth of tumor cell *in vitro* and tumor mass *in vivo* PET	(Mahlknecht et al., 2013)
Heraptamer 1 and Heraptamer 2	HER-2 overexpressed in SKOV3 ovarian cancer cells	DNA	PET imaging (radiolabeled, *in vivo*	(Zhu et al., 2017)

Enriched aptamers	HER-2 overexpressing breast cancer cell line, SK-BR3	DNA	Development of a new method to monitor the enrichment of aptamers in a given round of cell-SELEX	(Dastjerdi, Tabar, Dehghani, & Haghparast, 2011)
S1, S2, S3, S4, S5	Receptor tyrosine kinase-RET^{C634Y}	2'F-RNA	Potential applications: diagnosis, imaging, and therapy Neuroprotective	(Pestourie et al., 2006)
C4-3	Neurotrophin receptor TrkB	2'F-RNA	Neuroprotective effects Potential in therapy for neurodegenerative disease Potential	(Y. Z. Huang et al., 2012)
Aptamer A07	TGFβ III receptor	2'F-RNA	Potential application: therapy through inhibition of TGFβIII receptor	(Ohuchi, Ohtsu, & Nakamura, 2006)
C2 aptamer	CD71	2'F-RNA	Delivery of siRNA Targets cell in liposomes	(Wilner et al., 2012)
MRP1-CD28 bivalent aptamer	Multidrug resistant-associated protein 1-MRP1	2'F-RNA	Reduction of cell growth in vitro and improved survival in vivo	(Soldevilla et al., 2016)
EP166	Epithelial cell adhesion molecule-EpCAM (CD326)	DNA	Potential application: stem cell marker	(J. W. Kim et al., 2014)
Integrin α6β4-specific DNA Aptamer (IDA)	Integrin α6β4	DNA	Imaging (confocal) Potential application: drug delivery	(Berg, Lange, Mittelberger, Schumacher, & Hahn, 2016)

Apt02, Apt09, Apt10	Integrin αv	RNA	Potential application: targeting channels, transporters	(Takahashi, Sakota, & Nakamura, 2016)
bsA17, bsA22	CD16α	DNA	ADCC (tumor cell lysis)	(Boltz et al., 2011)
CD133-A, CD-133-A58, CD133-A35, CD133A21, CD-133-A15, CD133-B19	CD133	2'F-RNA	Potential application: target cancer stem cells and molecular imaging	(Shigdar et al., 2013)
C2NP	CD30 TNFRSF8	DNA	Potential application: therapy	(Parekh et al., 2013)
CL4	EGFR	2'F-RNA	Induces EGFR-mediated signal pathways causing selective cell death Inhibits tumor growth *in vivo* Combined cetuximab-aptamer treatment shows clear synergy in inducing apoptosis *in vitro* and *in vivo.* Potential application: translational therapy	(Esposito et al., 2011)
Gint4.T	PDGFR β	2'F-RNA	Inhibition of receptor signaling and glioblastoma-derived tumor growth Inhibition of cell migration and proliferation Induction of differentiation	(Camorani et al., 2014)

SQ-2	Alkaline phosphatase placental-like 2-ALPPL-2	2'F-RNA	Targets ALPPL-2 in both forms of membrane-bound and secretary. Potential applications: diagnosis, imaging, and therapy	(Dua et al., 2013)
Sgc-3b and Sgc-4e	selectin L and integrin α4	DNA	Potential application: therapeutic intervention	(Bing, Shangguan, & Wang, 2015)
MS03	CD44/CD24	DNA	Potential applications: disruption of therapeutic resistance, invasion, and angiogenesis	(Lu et al., 2015)
CSC13	CD44	DNA	Potential applications: cancer detection, imaging, and drug delivery	(Sefah et al., 2013)
sgc8	Protein Tyrosine Kinase 7-PTK7	DNA	Potential application: drug delivery Inhibition	(Xiao, Shangguan, Cao, Fang, & Tan, 2008)
GL56	Insulin Receptor	2'F-RNA	Inhibition of IR signaling Reduction of cell viability Potential applications: targeted therapies Interferes	(Iaboni et al., 2016)

GL21.T	Axl	2'F-RNA	Interferes with cell migration and invasion Inhibition of spheroid formation and cell transformation Inhibition of tumor growth	(Cerchia et al., 2012)
AS1411	Nucleolin	DNA	Interferes with multiple biological activities in tumor cells Induction of apoptosis via down-regulation of bcl-2 proteins	(Bates, Laber, Miller, Thomas, & Trent, 2009; Bates et al., 2017; Soundararajan, Chen, Spicer, Courtenay-Luck, & Fernandes, 2008; Soundararajan et al., 2009)
TD05	Axl Nucleolin Immunoglobulin heavy mu chain	DNA	Role in identification of cell membrane receptor with increased expression levels Potential applications: early diagnosis, targeted therapy and mechanistic studies	(Mallikaratchy et al., 2007)

B. Appendix B

Protein Purification

Reagent	Supplier
TRIS-hydrochloride pH 8.0	Sigma-Aldrich, USA
Sodium Chloride	Merck, Germany
1.5 % (w/v) DDM	Affymetrix Inc (AFFX), USA
dH_2O	Milli-Q® Synthesis A10®, France
10% (v/v) glycerol	Aklar Kimya, Turkey
L-histidine	Merck, Germany
PBS (pH 7.4)	nzytech, Portugal
Ethanol	Sigma Aldrich, Germany
Imidazole	Sigma-Aldrich, Germany

Protein Quantification

Reagent	Supplier
Bovine Serum Albumin	Sigma-Aldrich, USA
Coomassie® Brilliant Blue G 250 dye	Sigma-Aldrich, USA

SELEX

Reagent	Supplier
WizPure™ DNA Polymerase Kit*	Wizbiosolutions, South Korea
WizPure™ PCR 2X Master**	Wizbiosolutions, South Korea
WizScript™ cDNA Synthesis Kit***	Wizbiosolutions, South Korea
Apt-Get 2'-F T7 Transkription Kit******	Roboklon, Germany
dH_2O	Milli-Q® Synthesis A10®, France
DNase I	Gene All, Korea
Sodium Acetate	Merck, Germany
Isopropanol	Riedel-de Haën, Germany
Urea	Sigma-Aldrich, Germany

*10X PCR buffer, Taq DNA polymerase, dNTPs.

**dNTPs, RTase, Taq DNA polymerase, $MgCl_2$, enhancer and stabilizer.

***10X Reaction Buffer, 20X dNTP mix, RNase inhibitor, RNase free water.

**** T7 Reaction Buffer, 2'F Py NTP mix, Apt-Get 2'F T7 RNA polymerase, RNase-free water.

SDS-PAGE

Reagent	Supplier
PageRuler™ Plus Prestained Protein Ladder	Thermo Scientific™, USA
Acrylamide	Nzytech, Portugal
dH_2O	Milli-Q® Synthesis A10®, France
TRIS-base	Sigma-Aldrich, Germany
TRIS- hydrochloride	Sigma-Aldrich, USA
SDS Solution	nzytech, Portugal
APS	Bio-Rad, USA
TEMED	Bio-Rad, USA
Glycine	Merc, Germany
Glacial acetic acid	Emir Kimya, Turkey
Methanol	Sigma-Aldrich, Germany
Coomassie® Brilliant Blue R 250 dye	Sigma-Aldrich, Germany
β-mercaptoethanol	Merck, Germany
Bromophenol Blue	Merk, Germany

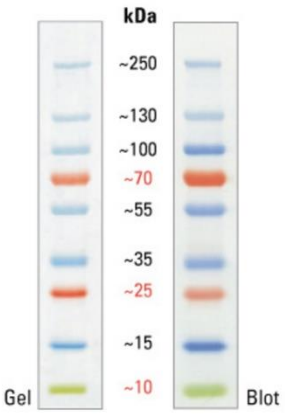

Figure B.1. SDS-PAGE Band Profile of PageRuler™ Plus Prestained Protein Ladder

Agarose Gel

Reagent	Supplier
Ethidium Bromide	AppliChem GmbH, Germany
100bp Plus DNA Ladder	TransGen Biotech, China
6X Loading Dye	Wizbiosolutions, South Korea

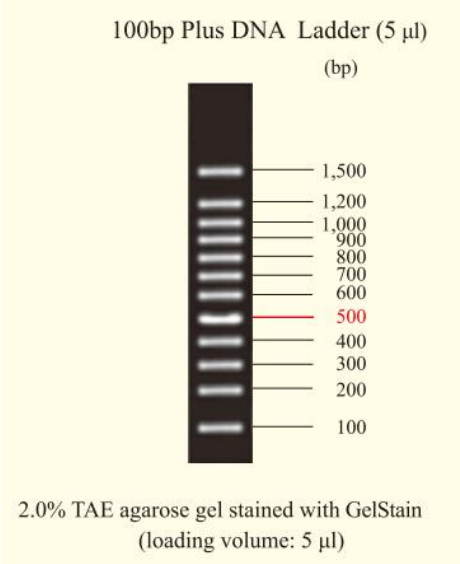

Figure B.2. Agarose Gel Band Profile of Transgen100bp Plus DNA Ladder

Preparation *E. Coli* BL21 Components

Reagent	Supplier
Luria Bertani	Conda, Spain
Glycerol	Aklar Kimya, Turkey
Calcium Chloride	Merck, Germany
Potassium Acetate	AppliChem GmbH, Germany
Potassium Hydroxide	Merck, Germany
Acetic Acid	Emir Kimya, Turkey
Ruthenium Chloride	Merck, Germany
MOPS	Merck, Germany

C. Appendix C

SDS-PAGE Separation

12 % Separating (10 mL for 2 Gel)	**mL or µL**
30% Polyacrylamide	4 mL
3 M Tris-base (pH: 8.8)	1.25 mL
dH_2O	4.5 mL
20% SDS	50 µL
10% APS	200 µL
TEMED	8 µL
5% Stacking (5 mL for 2 Gel)	**mL or µL**
30% Polyacrylamide	850 µL
1 M Tris HCl (pH: 6.8)	625 µL
dH_2O	3.395 mL
20% SDS	25 µL
10% APS	100 µL
TEMED	5 µL

5X Sample Loading Buffer Preparation

Reagent
250 mM Tris-HCl, pH 6.8
10% SDS
50% Glycerol
0.25% Bromophenol Blue
5% β-mercaptoethanol (β-ME) or 500 mM dithiothreitol (DTT)

1 Liter of Staining Solution Preparation

100 mL of glacial acetic acid is added to 500 mL of dH_2O.

400 mL of 100% methanol is added then mixed.

1 g of Coomassie® Brilliant Blue R 250 dye is added and mixed by rotational shaking.

In case of any insoluble particles, the buffer can be filtered, and then it is kept at room temperature.

1 Liter of De-staining Solution Preparation

100 mL of glacial acetic acid is added to 700 mL of dH_2O.

200 mL of methanol is added and then mixed rotationally.

The solution is stored at room temperature.

D. Appendix D

The PCR cycle number for each round of SELEX

PCR	
Rounds	**Number of Cycles**
1	16
2	15
3	15
4	15
5	15
6	15
7	15
8	13

Each round of SELEX calculation of volumes for incubation of CadB with RNA pool (Reaction volume is 50 µL and CadB concentration is 7.71 µM).

Rounds	RNA pool (µM)	RNA volume (µL)	CadB Volume (µL)	2X PBS Volume (µL)	H_2O volume (µL)
1	80.00	6.25	13.00	18.50	12.30
2	74.85	6.00	11.00	19.50	13.50
3	65.45	6.20	9.40	20.00	14.10
4	63.33	5.75	8.00	21.00	15.30
5	43.64	7.55	6.80	21.60	14.00
6	52.42	5.65	5.80	22.11	16.50
7	41.21	6.45	4.95	22.55	16.10
8	52.42	4.60	4.20	23.00	18.20

Amount of components for agarose gel preparation

Agarose Gel Electrophoresis

Rounds	Gel%	1%EtBr (µL)	Ladder (µL)	Dye (µL)	Sample amount (µL)
1	1	4	5	2(6X wizbiosolutions)	10
2	1	4	5	2	10
3	1	4	5	2	10
4	1	4	5	2	10
5	1	4	5	2	10
6	1	4	5	2	10
7	1	4	5	2	10
8	1	4	5	2	10

1% of Agarose gel preparation in 40 mL of Tris-acetate EDTA (TAE)

0.4 g of agarose is put into the flask.

40 mL of TAE is added into the flask, and then it is shaken slowly.

The flask is placed into the microwave for 1 minute; after that, the solution is ensured to be homogeneous. If agarose is not dissolved completely, it is put back into the microwave.

4 µL of EtBr is added into the flask, and it is shaken.

The solution is poured into the gel tray quickly and air bubbles if any are removed.

A comb is put onto the gel station and kept for 15 minutes.

12% of Non-Denaturing RNA PAGE Preparation

40 mL of 30% acrylamide/bisacrylamide is added to a flask.

20 mL of 5X TBE is added into the flask.

Volume is completed up to 100 mL by adding dH_2O.

For the preparation of 6 mL of gel, 40 µL of 10% APS and 4 µL of TEMED are added.

After gel running, the gel is put into a gel box, and then TBE and 4 µL of EtBr are added and shaken gently. Then, the box is placed at room temperature for 10 minutes to visualize by machine.

E. Appendix E

The result of multiple alignment of 29 different aptamer candidate sequences by Clustal Omega

```
CLUSTAL O(1.2.4) multiple sequence alignment


CadB28      GGGAGACAAGAAUAAACGCUCAAACCGUUAUUGU--UCUCCUUCCUUCUUGUU----CUU    54
CadB41      GGGAGACAAGAAUAAACGCUCAAUUUCUUCUUCU-UU---------UCUAUUC----CUA    46
CadB73      GGGAGACAAGAAUAAACGCUCAAUUUCGAUUCAU-UU---------UCU---------UA    41
CadB68      GGGAGACAAGAAUAAACGCUCAAUCUCGAUUUAA-GCCUCCAACUAUUUAUUG----CUU    55
CadB8       GGGAGACAAGAAUAAACGCUCAAUUCCUGUUCUU-UCC-------UUUUAU---------    43
CadB44      GGGAGACAAGAAUAAACGCUCAAUUAUC--UCUU--UCU------UCUUAU---------    41
CadB60      GGGAGACAAGAAUAAACGCUCAAUUUAU--UCAU-UUUU------UAUAAU---------    42
CadB84      GGGAGACAAGAAUAAACGCUCAAACUAUUUGUUGAGCCUCACACAUUAUAAUUUACAUUU    60
CadB37      GGGAGACAAGAAUAAACGCUCAACCUCAUAU-CAACAAUUAUUAACACUUUUUUAA----    55
CadB17      GGGAGACAAGAAUAAACGCUCAACGUUUGUGAUGCCUCUUGUUUAUUUUAUUU-GUGUUU    59
CadB99      GGGAGACAAGAAUAAACGCUCAACGAUUGUGAUGCCUCUUUUUUAUUUUAUUU-GUGUUG    59
CadB31      GGGAGACAAGAAUAAACGCUCAAUCUUUAUU-CUAUUUCUCUUUUUCCC-------UCUU    52
CadB22      GGGAGACAAGAAUAAACGCUCAACCUUAAUUGUUCU-----------CU-------ACUU    42
CadB88      GGGAGACAAGAAUAAACGCUCAAUUCCUGCUUCC-UUAUUUUAAAUAUUAGUGCGAGCUU    59
CadB85      GGGAGACAAGAAUAAACGCUCAAUUCUUCUCUUUCUUUUUCU------------------    42
CadB78      GGGAGACAAGAAUAAACGCUCAAUUUUGUCAUUAUUUU---UUCGGUCUAUCCUGUCUUU    57
CadB36      GGGAGACAAGAAUAAACGCUCAACUCCUCU-UCCAUUUCUUUUCUUACCAUUC---UUAU    56
CadB7       GGGAGACAAGAAUAAACGCUCAACUU-UCU-UCCAUUUCUUUUCUUACCACUC---UUAU    55
CadB35      GGGAGACAAGAAUAAACGCUCAACUU-UCU-UCCAUUUCUUUUCUUACCAUUC---UUAU    55
CadB20      GGGAGACAAGAAUAAACGCUCAAUCUUUUCUUUCCCU-UUAUUAGUUGCACUC---ACCA    56
CadB54      GGGAGACAAGAAUAAACGCUCAACUCUUGUUUUCGUUG---UUAUCCACAUUU---U--C    52
CadB72      GGGAGACAAGAAUAAACGCUCAAUAUUCUUUC------------AUUCGAUGU---UCUU    45
CadB30      GGGAGACAAGAAUAAACGCUCAAUUUUCUAAUCUUC---------------UU-----UU    40
CadB32      GGGAGACAAGAAUAAACGCUCAAUUUUUCCUUCCUU---------------UU-----UU    40
CadB43      GGGAGACAAGAAUAAACGCUCAACCUUGAUUU--------------UCCAAUU---CAUC    43
CadB2       GGGAGACAAGAAUAAACGCUCAAUUUCCUUUUCUCUU--------UUCCAUUU---UCUU    49
CadB39      GGGAGACAAGAAUAAACGCUCAAAUUCCUACUUUAUUACUCUUAAUACCAUUU---AUUU    57
CadB59      GGGAGACAAGAAUAAACGCUCAACUAAUCUUUU-------------------------UU    35
CadB97      GGGAGACAAGAAUAAACGCUCAACUUCCUUUUU-------------------------UC    35
            **********************

CadB28      UGU-----AUUCCU---UGCCUUGUGUUUCUUCGACAGGAGGCUCACAACAGGC          100
CadB41      UCUACCAUAAUCCUUCUUUCUAACCUUCUUUUUCGACAGGAGGCUCACAACAGGC          100
CadB73      U------------UUUCUUUUACCCUUCUAUUCGACAGGAGGCUCACAACAGGC           83
CadB68      UGC---A------ACUUCGUUCUUGUUGCUUUCGACAGGAGGCUCACAACAGGC          100
CadB8       -------------UUUUUGUUUUUGUGAUUUUCGACAGGAGGCUCACAACAGGC           84
CadB44      -------------UUUUCUUUAUUUUUUCCUUCGACAGGAGGCUCACAACAGGC           82
CadB60      -------------UUUU----AUUUAAUAUUUCGACAGGAGGCUCACAACAGGC           79
CadB84      UUU---U-----------GAAUGCCUUGCAUUCGACAGGAGGCUCACAACAGGC          100
CadB37      ------UUA-UACU--UUAUAACAUAUUUAUUCGACAGGAGGCUCACAACAGGC          100
CadB17      UUU---A---------U-AUUGGGAUUUUAUUCGACAGGAGGCUCACAACAGGC          100
CadB99      UUU---A---------U-AUUGGGAUUUUAUUCGACAGGAGGCUCACAACAGGC          100
CadB31      UU----UUCAUGU---UUCCUUGUGGUGCUUUCGACAGGAGGCUCACAACAGGC           99
CadB22      ------UUA---CA-AC----UUUUGGCUUUUCGACAGGAGGCUCACAACAGGC           82
CadB88      -UU---U-----G----AUCCUGUUCAGUUUUCGACAGGAGGCUCACAACAGGC          100
CadB85      -UU---UUAACCUA-UUUCUCUCUAACUCAUUCGACAGGAGGCUCACAACAGGC           91
CadB78      UUU---UUAUCGCA--UUU----UAUCCUCUUCGACAGGAGGCUCACAACAGGC          102
CadB36      UUU---C-----CA-ACACCUUUGUGCUUCUUCGACAGGAGGCUCACAACAGGC          101
CadB7       UUU---C-----CA-ACACCUUUGUGCUUCUUCGACAGGAGGCUCACAACAGGC          100
CadB35      UUU---C-----CA-ACACCUUUGUGCUUCUUCGACAGGAGGCUCACAACAGGC          100
CadB20      UUU---U-----CU-AU-UUCCCUUGUGACUUCGACAGGAGGCUCACAACAGGC          100
CadB54      -AU---CUAGCGUU---CUUUUUAUGUUUAUUCGACAGGAGGCUCACAACAGGC           99
CadB72      UC----------------CCUUCUUUUUUUUUUCGACAGGAGGCUCACAACAGGC           83
CadB30      UU----------C---UUUCA--GGCUUGUUUCGACAGGAGGCUCACAACAGGC           79
CadB32      UC----------U---UAUCA--UUUUUCUUUCGACAGGAGGCUCACAACAGGC           79
CadB43      -----------------AUUUUUUCUAUUUUUCGACAGGAGGCUCACAACAGGC           80
CadB2       UCC---UUUGUGGC-AUUUUAGUACUUUUAUUCGACAGGAGGCUCACAACAGGC           99
CadB39      UCU---U-----CU-CUUUUAUCUCUUUUUUUCGACAGGAGGCUCACAACAGGC          102
CadB59      CUC---U-----CU-UUUCUUUUCCUUUUUUUCGACAGGAGGCUCACAACAGGC           80
CadB97      AUU---U-----CU-CUUAGAUUUUUUAUUUUCGACAGGAGGCUCACAACAGGC           80
                                             ************************
```

The thermodynamic ensemble results for aptamer candidates

Aptamer Candidate	Thermodynamic Ensemble Results
CadB30	**The free energy of the thermodynamic ensemble is -13.36 kcal/mol. The frequency of the MFE structure in the ensemble is 17.99 %. The ensemble diversity is 11.94 .**
CadB35	**The free energy of the thermodynamic ensemble is -20.54 kcal/mol. The frequency of the MFE structure in the ensemble is 17.64 %. The ensemble diversity is 18.18 .**
CadB39	**The free energy of the thermodynamic ensemble is -11.26 kcal/mol. The frequency of the MFE structure in the ensemble is 2.06 %. The ensemble diversity is 10.91 .**
CadB41	**The free energy of the thermodynamic ensemble is -5.17 kcal/mol. The frequency of the MFE structure in the ensemble is 3.60 %. The ensemble diversity is 18.72 .**

CadB85	**The free energy of the thermodynamic ensemble is -13.28 kcal/mol.** **The frequency of the MFE structure in the ensemble is 5.61 %.** **The ensemble diversity is 12.46 .**

The MFE values prediction for randomly chosen sequences from the phylogenetic tree

Name	RNAfold (kcal/mol)	KineFold (kcal/mol)
CadB41	-3.12	-10.6
CadB85	-11.50	-12.1

F. Appendix F

Preparation *E. Coli* BL21 Competent Cells

BL21 cells are inoculated to 3 mL of LB and then incubated o/n at 37˚C.

This seed then is inoculated to 200 mL of LB until OD_{600} reaches up between 0.4-0.6.

The culture is incubated on the ice at 4˚C for 15 minutes.

The pellet is resuspended in 20 mL of ice-cold Buffer I for 15 minutes.

The cells are centrifuged at 3,500 rpm at 4˚C for 5 minutes.

The pellet then is resuspended gently in 8 mL of ice-cold Buffer II.

100 µL of aliquots are incubated on ice for 15-30 minutes. The cells are made frozen in liquid nitrogen and stored at -80˚C.

- Buffer I contains 100 mM $RuCl_3$, 30 mM KAc, 10 mM $CaCl_2$, 15% glycerol and pH is arranged to 5.8 using dilute acetic acid and filter sterilized.
- Buffer II contains 75 mM $CaCl_2$, 10 mM $RuCl_3$, 10 mM MOPS, 15% glycerol and pH is arranged to 6.5 using 0.2 KOH and filter sterilization.